



<https://theses.gla.ac.uk/>

Theses Digitisation:

<https://www.gla.ac.uk/myglasgow/research/enlighten/theses/digitisation/>

This is a digitised version of the original print thesis.

Copyright and moral rights for this work are retained by the author

A copy can be downloaded for personal non-commercial research or study,
without prior permission or charge

This work cannot be reproduced or quoted extensively from without first
obtaining permission in writing from the author

The content must not be changed in any way or sold commercially in any
format or medium without the formal permission of the author

When referring to this work, full bibliographic details including the author,
title, awarding institution and date of the thesis must be given

Enlighten: Theses

<https://theses.gla.ac.uk/>
research-enlighten@glasgow.ac.uk

IMMUNOHISTOCHEMISTRY, LIGHT AND
ELECTRON MICROSCOPY OF THE
TESTIS FROM THE ALBINO SWISS RAT
FOLLOWING VASECTOMY

Craig Charles Dobson
M.B. Ch.B. B.Sc. (hons)

PhD Thesis

Faculty of Medicine
University of Glasgow

Laboratory of Human Anatomy
University of Glasgow

April 2000

ProQuest Number: 10645949

All rights reserved

INFORMATION TO ALL USERS

The quality of this reproduction is dependent upon the quality of the copy submitted.

In the unlikely event that the author did not send a complete manuscript and there are missing pages, these will be noted. Also, if material had to be removed, a note will indicate the deletion.



ProQuest 10645949

Published by ProQuest LLC (2017). Copyright of the Dissertation is held by the Author.

All rights reserved.

This work is protected against unauthorized copying under Title 17, United States Code
Microform Edition © ProQuest LLC.

ProQuest LLC.
789 East Eisenhower Parkway
P.O. Box 1346
Ann Arbor, MI 48106 – 1346



12336
COPY 2

ABSTRACT

Previous work in our laboratory has reported degeneration of the testes following left unilateral vasectomy in the Albino Swiss rat. This degeneration can be ipsilateral to the side of vasectomy or bilateral. We paid particular attention to the ultrastructure of the seminiferous tubules nine months or more following vasectomy in an attempt to elucidate the aetiology of the degeneration. There were marked differences between degenerated tubules following vasectomy and healthy tubules from sham operated controls or following vasectomy. The seminiferous epithelium in degenerated tubules rarely contained any recognisable sperm precursors. It consisted of Sertoli cells with few vacuoli and nuclei with deep intranuclear clefts displaying peripheral clumps of heterochromatin which were often found more central in the tubule than those from controls. The boundary zones from degenerated tubules were also greatly different from controls. The Sertoli cell basal laminae were thrown into marked folds as were those of the myoepithelial cell. The latter often had nuclei with triangular profiles as did the outer lymphatic endothelium. The basal lamina of these cells also appeared detached in places from the soma. There was no ultrastructural difference observed between unilateral and bilateral degeneration. The degenerated tubules were found to be smaller, often containing more Sertoli cells than controls. The similarity of these findings to those reported following other insults suggested that the findings may not be specific for vasectomy. The similarity observed between degeneration following vasectomy and that following maternal in *utero* flutamide administration supported the notion of these changes being due to shrinkage of the tubule. The only difference being the presence of immunocompetent cells in the boundary zone of degenerated tubules following vasectomy.

Despite the gross change in Sertoli cell appearance, we were able to demonstrate that both healthy and degenerated tubules following vasectomy retained typical Sertoli-Sertoli cell tight junctions as were found in sham operated controls. We used lanthanum as an intercellular tracer to test the function of these junctions. Both healthy and degenerated tubules following vasectomy were able to exclude lanthanum from the lumen as in controls. It would appear that the blood-testis barrier remains intact in rats nine to fifteen months following vasectomy or sham

procedure, even in degenerated tubules. There was no difference demonstrated between bilateral and ipsilateral degeneration.

Immunohistochemical investigation of testis three weeks, three months, six months and one year following vasectomy compared with sham operated controls revealed the presence of low numbers of immunocompetent cells in the testis of healthy control testes. We were also able to describe the pattern of MHC I and II distribution in healthy testis. Degenerated testes following vasectomy contained focal areas of immunocompetent cells which expressed T-suppressor, T-Helper and macrophage markers. Such accumulations could be centred on degenerated tubules or on blood vessels. They were also found in the grossly healthy right testis of one animal with unilateral degeneration. There also appeared to be an increased number of immunocompetent cells in sections from degenerated testis, however, this may be partly accounted for by shrinkage of the testis.

MHC I expression was markedly different in degenerated testis following vasectomy compared with healthy tubules from sham operated controls or following vasectomy. In degenerated tubules the intratubular and interstitial cells were labelled whereas healthy tubules had only limited staining of intratubular late spermatids as well as in the interstitium. This suggests that degenerated tubules contained Sertoli cells which expressed MHC I and may therefore play a role in the activation of the immune response demonstrated by the focal accumulations of immunocompetent cells. In contrast, there was no observed change in MHC II bearing cells. Taken together, our results suggest that the morphological changes to the boundary zone and Sertoli cells following unilateral vasectomy are the same for unilateral and bilateral degeneration and probably represent a non specific effect from tubal shrinkage. The aetiology of these degenerations remains unclear but the blood-testes barrier remains intact. There may be a role for the immune system as evidenced by the appearance of focal accumulations of immunocompetent cells and expression of MHC I by Sertoli cells in degenerated testis. The role of these MHC I bearing Sertoli cells is unclear but they are capable of phagocytosis and possibly therefore antigen presentation.

CONTENTS

Abstract		2
List of figures and tables		7
Acknowledgements		16
Authors Declaration		17
Chapter 1	General Introduction.	18
	Complications of vasectomy in man.	19
	Early complications of vasectomy.	20
	Late complications of vasectomy.	22
	The effect of experimental vasectomy on the testis in animal models.	28
	The effect of experimental vasectomy on the testis in the rat.	29
Chapter 2	Electron and light microscopic observations on the boundary zone of the seminiferous epithelium and Sertoli cell following vasectomy in the rat.	32
	Introduction.	32
	Material and Methods.	34
	Sertoli cell numbers and seminiferous tubule areas.	37
	Results.	38
	Gross observations.	38
	Light microscopy.	40
	Electron microscopy.	43
	Flutamide.	45

	Analysis of counts.	46
	Discussion.	48
Chapter 3	Examination of the Blood-testis barrier following vasectomy.	51
	Introduction.	51
	Material and Methods.	52
	Results.	55
	Gross appearance and light microscopy.	55
	Electron microscopy.	56
	Permeability to lanthanum.	56
	Discussion.	57
Chapter 4	Immunohistochemistry of the testis following vasectomy in the Albino Swiss rat.	60
	Introduction.	60
	Materials and Methods.	61
	Immunohistochemistry.	63
	Pilot study.	65
	Results.	68
	Gross appearance.	68
	Immunohistochemistry.	70
	Discussion.	73
Chapter 5	Conclusions.	76
Illustrations		82
Appendices	Publications:	
1	The effect of vasectomy on the seminiferous tubule boundary zone in the Albino Swiss rat. Clinical Anatomy in press.	128

Presentations with Abstract publications:

- 2 Boundary changes in the seminiferous tubules of the rat following vasectomy. 147
- 3 Comparison of boundary zone changes in atrophic rat testes following vasectomy and flutamide administration. 148
- 4 Structural alterations to Sertoli cells following vasectomy in the Albino Swiss rat. 149
- 5 Changes in Sertoli cells and seminiferous tubular boundary zone following vasectomy in the rat. 150
- 6 Morphological integrity of Sertoli-Sertoli cell tight junctions following vasectomy in the rat. 151
- 7 Distribution of class I and II MHC antigens in the testis following vasectomy in the Albino Swiss rat. 152

References 153

List of tables and figures

Table 1.	Complications of vasectomy up to five years.	19
Table 2.	Complications of vasectomy in the long term.	23
Table 3.	Protocol for osmication and embedding.	36
Table 4.	Protocol for staining resin sections with toluidine blue.	36
Table 5.	Protocol for contrast staining for electron microscopy.	37
Table 6.	The appearance of testis with time after vasectomy.	39
Table 7.	Mass of testis with time following vasectomy.	39
Table 8.	The mean area, perimeter, Sertoli cell count and leukocyte count.	46
Table 9.	Pilot study for lanthanum profusion.	53
Table 10.	Protocol for lanthanum perfusion via the heart.	54
Table 11.	Protocol for Immunohistochemical staining.	64
Table 12.	Primary antibody dilutions.	65
Table 13.	Procedure for counter-staining.	65
Table 14.	Gross appearance prior to immunohistochemistry.	69
Figure 1.	Diagram illustrating the division of the testis in to 8 blocks for processing.	83
Figure 2.	An example of part of an initial camera lucida drawing from a healthy left testis following vasectomy.	83
Figure 3.	An example of a high powered camera lucida drawing of a section through a single seminiferous tubule from a healthy left testis following vasectomy	84
Figure 4.	The typical appearance of a seminiferous tubule from a healthy left testis of a sham operated animal stained with toluidine blue	84
Figure 5.	The typical appearance of a seminiferous tubule from a healthy right testis of a sham operated animal stained with toluidine blue	85

- Figure 6. An example of the presence of a leukocyte in the boundary zone of a tubule from a healthy right testis of a sham operated animal stained with toluidine blue. 85
- Figure 7. The typical appearance of a tubule from a healthy right testis of a sham operated animal stained with toluidine blue 86
- Figure 8. The typical appearance of a healthy tubule from a left testis following vasectomy stained with toluidine blue. 86
- Figure 9. The typical appearance of a seminiferous tubule from a healthy right testis following vasectomy stained with toluidine blue. 87
- Figure 10. The typical appearance of a healthy right testis from an animal with ipsilateral (left sided) degeneration following vasectomy stained with toluidine blue. 87
- Figure 11. The typical appearance of a tubule in a healthy right testis from an animal with ipsilateral (left sided) degeneration following vasectomy stained with toluidine blue. 88
- Figure 12. The typical appearance of an ipsilaterally degenerated left testis stained with toluidine blue 88
- Figure 13. The typical appearance of a seminiferous tubule from a degenerated left testis of an animal with bilateral degeneration following vasectomy stained with toluidine blue 89
- Figure 14. The typical appearance of a degenerated tubule from a right testis of an animal with bilateral degeneration following vasectomy stained with toluidine blue 89
- Figure 15. The typical appearance of a degenerated seminiferous tubule from a right testis of an animal with bilateral degeneration following vasectomy stained with toluidine blue. 90
- Figure 16. An electron micrograph demonstrating the appearance of a grossly degenerated testis from a Swiss Albino rat following in *utero* maternal flutamide administration. 90

- Figure 17. An electron micrograph showing a Sertoli cell nucleus from a healthy sham operated left testis. 91
- Figure 18. An electron micrograph showing typical boundary zones lying between two adjacent seminiferous tubules from a healthy sham operated right testis. 91
- Figure 19. An electron micrograph showing a Sertoli cell nucleus and two adjacent boundary zones from seminiferous tubules of a healthy right testis following vasectomy. 92
- Figure 20. An electron micrograph showing a typical Sertoli cell nucleus from a left testis following vasectomy. 92
- Figure 21. An electron micrograph showing typical boundary zones lying between two adjacent seminiferous tubules from a healthy right testis of an animal with ipsilateral degeneration following vasectomy. 93
- Figure 22. An electron micrograph showing the boundary zone of a seminiferous tubule from a left testis of an animal exhibiting bilateral degeneration following vasectomy. 93
- Figure 23. An electron micrograph showing the typical boundary zone of a seminiferous tubule from a right testis of an animal with bilateral degeneration following vasectomy. 94
- Figure 24. An electron micrograph showing typical boundary zones of two adjacent seminiferous tubules from a left testis of an animal with ipsilateral degeneration following vasectomy. 94
- Figure 25. An electron micrograph showing the boundary zone of a seminiferous tubule from a left testis from an animal exhibiting bilateral degeneration following vasectomy. 95
- Figure 26. An electron micrograph showing a right testis of an animal with bilateral degeneration of the testis following vasectomy. 95
- Figure 27. An electron micrograph showing the boundary zone of a seminiferous tubule from a left testis of an animal with ipsilateral degeneration of the testis following vasectomy. 96

- Figure 28. An electron micrograph showing the seminiferous epithelium from a left testis of an animal exhibiting bilateral degeneration following vasectomy. 96
- Figure 29. An electron micrograph showing the typical appearance of the boundary zone from seminiferous tubules from a degenerated right testis of an animal exposed to flutamide in *utero*. 97
- Figure 30. An electron micrograph showing a Sertoli-Sertoli cell junctional complex from a healthy sham operated left testis. 97
- Figure 31. An electron micrograph showing a typical healthy Sertoli-Sertoli cell junctional complex from a healthy sham operated right testis. 98
- Figure 32. An electron micrograph showing a Sertoli-Sertoli cell junctional complex from a healthy left testis following vasectomy. 98
- Figure 33. An electron micrograph showing a typical Sertoli cell junctional complex from a healthy right testis following vasectomy. 99
- Figure 34. An electron micrograph showing a Sertoli-Sertoli cell junctional complex the healthy right testis of a rat exhibiting ipsilateral degeneration following vasectomy. 99
- Figure 35. An electron micrograph showing a Sertoli- Sertoli cell junctional complex from an degenerated left testis of a rat exhibiting ipsilateral degeneration following vasectomy. 100
- Figure 36. An electron micrograph showing a typical Sertoli-Sertoli cell junctional complex from an degenerated left testis of a rat exhibiting bilateral degeneration following vasectomy. 100
- Figure 37. An electron micrograph showing a Sertoli-Sertoli cell junctional complex from an degenerated right testis of a rat exhibiting bilateral degeneration following vasectomy. 101

Figure 38.	An electron micrograph showing lanthanum confined to the outer compartment of the seminiferous tubule from a healthy sham operated left testis.	101
Figure 39.	An electron micrograph from a healthy sham operated right testis.	102
Figure 40.	An electron micrograph from a healthy left testis following vasectomy.	102
Figure 41.	An electron micrograph showing lanthanum confined to the outer compartment of the seminiferous tubule from healthy right testis following vasectomy.	103
Figure 42.	A high powered electron micrograph of Figure 41.	103
Figure 43.	An electron micrograph showing the luminal aspect of the seminiferous tubule from a healthy right testis of an animal with ipsilateral degeneration following vasectomy.	104
Figure 44.	An electron micrograph showing lanthanum confined to the outer compartment of the seminiferous tubule from an ipsilateral degenerated left testis following vasectomy.	104
Figure 45.	An electron micrograph from the left testis of an animal with bilateral degeneration following vasectomy.	105
Figure 46.	An electron micrograph from the right testis of an animal with bilateral degeneration following vasectomy.	105
Figure 47.	The appearance of OX18 labelling of the seminiferous tubules of a healthy left testis from a sham operated animal 12 months after the procedure.	106
Figure 48.	The appearance of OX18 labelling of the seminiferous tubules of a healthy left testis 3 months following vasectomy.	106
Figure 49.	The appearance of OX18 labelling of the seminiferous tubules of an degenerated right testis from an animal with bilateral degeneration 12 months following vasectomy.	107

Figure 50.	The appearance of testes labelled no primary antibody as a control.	107
Figure 51.	An example of a table recording the number of cells counted on a section.	108
Figure 52.	The appearance of OX19 labelling of the spleen from a sham operated animal 12 months after the procedure.	109
Figure 53.	The appearance of W3/25 labelling of the spleen from a sham operated animal 12 months following the procedure.	109
Figure 54.	The appearance of OX8 labelling of the spleen from a sham operated animal 12 months after the procedure.	110
Figure 55.	The appearance of OX33 labelling of the spleen from a sham operated animal 12 months following the procedure.	110
Figure 56.	The appearance of OX18 labelling of the spleen from a sham operated animal 12 months after the procedure.	111
Figure 57.	The appearance of OX18 labelling of the spleen from a sham operated animal 12 months after the procedure.	111
Figure 58.	The appearance of OX6 labelling of the spleen from a sham operated animal 12 months after the procedure.	112
Figure 59.	The appearance of OX42 labelling of the spleen from a sham operated animal 12 months following the procedure.	112
Figure 60.	The appearance of OX33 labelling of a healthy left testis of a sham operated animal 6 months following the operation.	113
Figure 61.	The appearance of OX19 labelling of a healthy left testis of a sham operated animal 6 months following the procedure.	113
Figure 62.	The appearance of OX8 labelling of a healthy left testis of a sham operated animal 12 months following the procedure.	114
Figure 63.	The appearance of W3/25 labelling of a healthy right testis of a sham operated animal 3 weeks following the procedure.	114
Figure 64.	The appearance of W3/25 labelling of a healthy left testis of a sham operated animal 6 months following the procedure.	115

Figure 65.	The appearance of OX42 labelling of a healthy right testis of a sham operated animal 6 months following the procedure.	115
Figure 66.	The appearance of OX 6 labelling of a healthy left testis of a sham operated animal 6 months following the procedure.	116
Figure 67.	The appearance of OX18 labelling of a healthy right testis of a sham operated animal 6 months following the procedure.	116
Figure 68.	The appearance of OX 33 labelling of a healthy left testis 3 months following vasectomy.	117
Figure 69.	The appearance of OX 33 labelling of a healthy right testis 12 months following vasectomy.	117
Figure 70.	The appearance of OX 19 labelling of a healthy left testis 3 months following vasectomy.	118
Figure 71.	The appearance of OX 8 labelling of a healthy right testis 12 months following vasectomy.	118
Figure 72.	The appearance of W3/25 labelling of a healthy right testis 12 months following vasectomy.	119
Figure 73.	The appearance of OX 42 labelling of a healthy left testis 3 months following vasectomy.	119
Figure 74.	The appearance of OX 6 labelling of a healthy left testis 3 months following vasectomy.	120
Figure 75.	The appearance of OX 6 labelling of a healthy right testis from an animal with ipsilateral degeneration 12 months following vasectomy.	120
Figure 76.	The appearance of OX 18 labelling of a healthy right testis 12 months following vasectomy.	121
Figure 77.	The appearance of OX 33 labelling of a degenerated left testis from an animal with bilateral degeneration 12 months following vasectomy.	121

Figure 78.	The appearance of OX 19 labelling of a degenerated left testis from an animal with ipsilateral degeneration 12 months following vasectomy.	122
Figure 79.	The appearance of OX 8 labelling of a degenerated left testis from an animal with bilateral degeneration 12 months following vasectomy	122
Figure 80.	The appearance of W3/25 labelling of a degenerated left testis from an animal with ipsilateral degeneration 12 months following vasectomy.	123
Figure 81.	The appearance of OX 42 labelling of a seminiferous tubule from a degenerated right testis from an animal with bilateral degeneration 12 months following vasectomy.	123
Figure 82.	The appearance of OX 6 labelling of a degenerated right testis from an animal with bilateral degeneration 12 months following vasectomy.	124
Figure 83.	The appearance of OX 18 labelling of a seminiferous tubule from a degenerated left testis from an animal with bilateral degeneration 12 months following vasectomy.	124
Figure 84.	The appearance of OX 33 labelling of a degenerated left testis from an animal with bilateral degeneration 12 months following vasectomy.	125
Figure 85.	The appearance of OX 42 labelling of a seminiferous tubule from a degenerated left testis from an animal with bilateral degeneration 12 months following vasectomy.	125
Figure 86.	The appearance of OX 6 labelling of a degenerated left testis from an animal with bilateral degeneration 12 months following vasectomy.	126
Figure 87.	The appearance of W3/25 labelling of a seminiferous tubule from a degenerated left testis from an animal with bilateral degeneration 12 months following vasectomy.	126

- Fig 88. The appearance of OX 42 labelling of a 127
degenerated left testis from an animal with ipsilateral
degeneration 12 months following vasectomy.
- Figure 89. The appearance of W3/25 labelling in a 127
degenerated right testis from an animal with bilateral
degeneration 12 months following vasectomy.

ACKNOWLEDGEMENTS

Thanks are due to my supervisor Dr Stuart McDonald for his advice, support and encouragement. To Dr John Shaw Dunn and Professor Tony Payne for inspiration. To Neil Bennett for performing the operations. To Owen Reid and Robert Kerr for teaching me how to process and section for electron microscopy. To Jimmy McGadie, David Russell and Andy Lockhart for teaching me how to carry out immunohistochemistry. To my wife and four children for granting me time to complete this work. To my mother and greatly mourned father who made all things possible.

DECLARATION

I declare that unless specifically stated otherwise in the text, this is all my own original work.

Craig Charles Dobson.

GENERAL INTRODUCTION

Vasectomy is a very popular method of birth control in many countries (1). Surveys in countries such as New Zealand suggest that it is the single most popular method of birth control (2). In the United States, figures from 1991 suggest that there were 10.3 vasectomies per 1000 men aged 25-49 (3) whilst in 1995 there were approximately 494000 procedures carried out (4). In China alone, over 30 million individuals have undergone this procedure (5). The vast numbers of individuals undergoing this procedure mean that even small risks of complications are likely to materialise as large numbers of cases. These large numbers make it of the utmost importance to ensure the safety of the procedure particularly in the long term. In this work we investigate the long term consequences of vasectomy in an experimental rat model.

Vasectomy is performed on essentially healthy individuals (6). The procedure is not designed to benefit the patient's health directly, although, some epidemiological studies have suggested that vasectomy is associated with a lower over all mortality rate compared with controls (7). This may be via maintenance or improvement of economic conditions of the individual or may reflect patient selection (8). From a practical point of view, in the increasingly litigious environment of clinical practice, any complications arising from this procedure could have severe medico-legal repercussions (9). In reaching a decision to undergo this voluntary operation the equation becomes, in health terms, no proven direct health benefit against the risk of any complications. An investigation into how this decision was reached concluded that both partners were involved, using their knowledge of other peoples' experience (10). Complications should be identified so that patients can be allowed to make an informed choice as to their method of contraception and to allow for the development of measures to reduce their occurrence.

Complications of Vasectomy in Man

Approximately 10 per cent of men who have had vasectomy develop some form of complication (11, 12). This may be slightly reduced with modern minimally invasive no scalpel techniques requiring less exposure (13). The complications can be divided into early, occurring within five years after procedure and late, occurring after that time. The former have been extensively studied and have been divided into 12 categories (table 1) (12).

Table 1. Complications of vasectomy up to five years with incidence per 100 cases (12).

A/ General

1	Failure of Procedure	Early (0.25)
2		Late (0)
3		Technical (0.49)
4	Haemorrhage	Minor (0.33)
5		Major (0)
6	Infection	Minor (3.8)
7		Major (0.16)
8	Regret (0.9)	

B/ Confined to GU Tract

9	Epididymitis (1.9)	
10	Orchitis (0.16)	
11	Sperm Granuloma (1.3)	
12	Miscellaneous (1.5)	Intra-scrotal pain Others

Early Complications of Vasectomy (table 1).

Early complications following vasectomy can be divided into two groups. The first general group consists of those which have features in common with any surgical intervention including the failure of the procedure, haemorrhage and infection. The second relates to the site of the procedure, the male reproductive tract in the case of vasectomy.

A: General Complications: Vasectomy is a procedure aimed at reducing fertility. In this sense the most important complication is the failure rate. It can be divided into three types (table 1), the first consisting of early failure. This would usually be measured in terms of motile sperm as the finding of immotile sperm present in the semen is a common finding early after vasectomy (14). The early failure rate varies with surgical technique but usually lies between 0.2% (12) and 7.8% (15). With increasing experience and careful technique, the failure rate should be nearer 0.2% (11). The pregnancy rate following vasectomy is likely to be considerably lower still but enough to cause considerable medico-legal trouble (9). The results can be considerably improved if correct seminal monitoring procedures are carried out following the operation. Patient compliance remains a problem with this (11,16).

Other failures of vasectomy occur after an apparently successful operation and constitute late failures (table 1). This is thought to result from recanalation of the vas as part of healing or else to failure to find the vas deferens (11) and has led to fatherhood in a small number of cases (11, 17). In some individuals, sperm are detected in the ejaculate three months or more following vasectomy but the sperm are immotile. This constitutes the group of technical failures (table 1) in which the operation may have resulted in incomplete blockage to the vas but, the practical consequences are the desired ones of infertility due, for example, to immotile sperm.

Wound haemorrhage and infection (table 1) are complications of any form of surgery (18). They usually arise early and resolve with minimal intervention (12). Their incidence can be minimised by experienced surgical technique and sterile procedures.

The use of antibiotics allows resolution of minor infections whilst more than one course is required to resolve a major one.

There is an emerging trend for some individuals who have been vasectomized to request reversal of the procedure (19). The reason for this change of mind frequently involves a change in the relationship and is often the partner's initiative (20). The success of microsurgical reversal of vasectomy in one study of 1,247 first time procedures was 86% in terms of sperm presence in the semen (21). This figure presupposes the presence of a patent ductus deference and the production of sperm in the testes and decreases to 71% 15 years and more following vasectomy. The subsequent pregnancy rate was only 30% at this interval after vasectomy. Clearly, the chances of a successful vasectomy reversal decreases considerably with time after the initial procedure. The incomplete reversibility of the procedure has lead some to conclude that vasectomy is not an ideal form of contraception (1). It also suggests the possibility of factors other than tubal blockage in infertility following vasectomy reversal. In one study of reasons for donor insemination, irreversible vasectomy represented 10.5% of 200 cases (22). This provides a further reason for studying vasectomy to determine the cause of this.

B: Complications of Vasectomy in the Male reproductive tract: Infections localised to the male reproductive tract are found following vasectomy (table 1). Epididymitis which presents as inflammation localised to the epididymis is rarely thought to be infective in origin and is treated conservatively usually leading to rapid resolution (12) although, there may be recurrences (23). Orchitis can also follow vasectomy, is assumed to be infective in nature and usually settles with antibiotics (12). This contrast with the possible autoimmune nature of sperm granulomata which are found following vasectomy in some animal models (24). They consist of sperm, epithelioid cells and lymphocytes (25). Granulomata are thought to be frequent findings after vasectomy (26) being more common after open ended techniques (27) although, they rarely cause the patient to return to the clinic for treatment. They often resolving with simple anti-inflammatory analgesia (12).

Other recognised problems following vasectomy include intra-scrotal pain and haematuria. These were classified as miscellaneous abnormalities as they tend to resolve spontaneously requiring minimal or no treatment. They occur in around 1.5 per cent of patients following vasectomy (12) although this may be a considerable under estimate. Other questionnaire based studies have put the number of patients suffering from Chronic Testicular pain as high as 33 per cent of those vasectomized (28) although, only 15 per cent found this troublesome and only a third sought medical advice. Another study found that 108 of 396 men surveyed had experienced pain following vasectomy but this had settled either spontaneously or with simple analgesia (29). They identified a residuum of 17 patients who had pain for more than 3 months requiring surgical deinnervation to relieve the pain. In both symptomatic and asymptomatic patients, epididymal cysts were a common finding on ultrasound examination (30). This might go along with the possibility that the pain is due to increased pressure proximal to the sight of ligation with subsequent rupture and granuloma or cyst formation (31).

Late Complications of Vasectomy (table 2).

Recently, interest has focused on the long term consequences of vasectomy, as larger numbers of vasectomized men are reaching 30 or more years following operation and various epidemiological studies have suggested that vasectomy is a risk factor for heart disease and some forms of cancer. Despite these concerns, vasectomy seems to remain a popular form of fertility control (32).

Table 2. Complications of vasectomy in the long term.

13	Late Post Vasectomy Syndrome
14	Irreversibility
15	Associated Conditions
16	Prostate Cancer
17	Testicular Cancer
18	Cardiovascular Disease
19	Other Cancers
20	Renal stones
21	Osteoporosis
21	Immunological Abnormalities
22	Anti sperm antibodies
22	Others
22	Histological Abnormalities

The late post vasectomy syndrome consists of chronic epididymal pain lasting typically five to seven years following vasectomy (33). It often requires surgical intervention, being cured by unilateral or bilateral epididymectomy which constitutes its major difference from post vasectomy orchalgia (26), congestive epididymitis (34), post vasectomy pain syndrome (31) and chronic testicular pain (28). All of the later also either resolve or are cured earlier than the five to seven year period of late post-vasectomy syndrome. They do, however, share many features in common leading some to suggest a common identity (28). In the prolonged cases of late post-vasectomy syndrome, the pathology is that of obstruction which is also thought to contribute in the other forms of intrascrotal pain (31). Congestive epididymitis is three times more frequent in closed as opposed to open ended vasectomy (35) which possibly supports the role of obstruction and pressure build up in the aetiology of the various forms of intrascrotal pain.

The apparent irreversibility of some vasectomies is an increasing problem encountered in a proportion of men who wish to start a new family (21). This can be considered to be the late development of the regret phenomenon (table 1). As discussed above, reversal, even using microsurgical techniques, has a worse prognosis as the time span following vasectomy increases. The fertility rate shows a

particularly marked decline ten years or more following vasectomy (36). The best achievable pregnancy rate following vasectomy reversal has been estimated to be 67 per cent (37). This does not allow for an estimated 12 per cent due to partner infertility (37). Clearly, in a large proportion of men, vasectomy is not a readily reversible procedure. This is becoming a major problem as the numbers of men requesting reversal increases (38).

There is ongoing controversy over the relationship, if any, between vasectomy and prostate cancer. The potential mechanism of this is unclear although, there have been reports of elevated levels of dihydrotestosterone in men vasectomized for 10-19 years compared with age matched controls (39). This could possibly be due to a decreased level of sex hormone binding globulin (40) although, the evidence is not overwhelming. Several groups have found vasectomy to be a risk factor for prostate cancer (41, 42, 43, 44, 45). Other workers have found vasectomy not to increase the risk of prostate cancer (8, 40, 46, 47, 48). Some authors have reversed previous findings (41) producing new results that provide little support for vasectomy as a risk factor for prostate cancer (49). This emphasises the need for careful statistical analysis to rule out confounding variables (41). Such factors might include diet which has been suggested to play a role in the development of prostate cancer (50,51). On balance, more recent evidence (52) suggests that there is no increased risk of prostate cancer following vasectomy (53). Vasectomy does not appear to effect prostatic volume or the occurrence of benign prostatic hyperplasia (54).

Vasectomy has also been linked with testicular cancer (55, 56). In one study, recent vasectomy was one of a number of risk factors identified for testicular cancer (55). In another, an excess of observed over predicted cases in those having had vasectomy was found (56). Since then several large epidemiological studies have found no association between vasectomy and testicular cancer (46, 57, 58). The balance of evidence therefore seems to suggest that there is probably no increase in risk of testicular cancer following vasectomy except possibly, in certain discreet areas, Ireland and Scotland. This may have an underlying genetic basis as an unidentified confounding variable. This debate has lead some, including ourselves, to investigate just what the long term effects of vasectomy are on the testis.

Concerns that vasectomy may lead to an increased risk of cardiovascular disease stemmed largely from the experimental models of vasectomy in the Rhesus Monkey (59). Large epidemiological surveys in man, however, have largely not identified this increased risk (60, 61) indeed, and have often found vasectomized individuals healthier or of lower mortality than controls (7, 46, 62). Additionally, there has been no independent confirmation of the results in experimental animals (63, 64).

Some workers have suggested that there is link between vasectomy and mortality from cancer in those having had the operation more than twenty years earlier and was primarily due to lung cancer (7) although, this has not been detected elsewhere (8). Some authors have suggested a link between vasectomy and urolithiasis (65, 66) although, this has not been widely found and specifically not identified in terms of hospital admissions by others (46). Other groups have expressed concern over a possible increased risk of osteoporosis but this appears not to be the case (67).

Vasectomy has been known to have immunological consequences for some time. The most well recognised is the formation of antibodies to sperm antigens which occurs in around 55 per cent of patients following vasectomy (68, 69). Such antibodies do occur in a proportion of men before vasectomy (68) but their significance is uncertain. They also occur in around eight per cent of infertile men (69). The antibodies formed have been linked to infertility following vasectomy by numerous possible mechanisms including, decreasing the number of motile sperm (70) and interference with pre implantation embryos in experimental models (71). Conversely, some reports have suggested no link with infertility following vasovasostomy (72). These apparent discrepancies may be resolved once the specificity of the antisperm antibodies are known. It is not difficult to imagine that some of these antibodies to sperm will bind to sites which are not essential for fertility whilst others may effect sperm motility or ovum binding. Thus, the titre of antibody may be less important than the nature of the target antigen (69). The antigenic proteins are now being identified which should shed more light on this problem and on the initiation of such autoimmune responses (73).

The formation of antisperm antibodies has led some investigators to suggest that vasectomized men may be exposed to a variety of autoimmune hypersensitivity reactions including immune complex formation and delayed type hypersensitivity (74). Despite the theoretical concern there is little evidence for this in man in the short term (6). Testicular biopsies in man have failed to identify immune complex deposition in the basement membrane of the seminiferous tubules following vasectomy (75) although, they have been reported in some other species, notably, the rabbit (24).

The antibodies are interesting as they are directed towards self antigens and represent a breakdown of the normal immune privilege in the testis (76). Such a breakdown and concomitant immune response, taking the form of sperm specific antibodies and local granuloma, are common features after vasectomy in man (26, 77). Both humoral (78) and cell mediated immunity (79) to human sperm have been shown to increase with time after operation. Thus, autoimmune orchitis might be expected to follow vasectomy as foreign antigens are recognised in the testis. There is, however, little evidence to support the occurrence of autoimmune orchitis in man following vasectomy, despite the great theoretical concern (80). Immune complex deposition does occur in the testes in a proportion of patients with infertility (81). Such deposition has been associated with variable degrees of tubular degeneration (82). The inference being that an immune complex mediated orchitis can lead to tubular degeneration similar to glomerulonephritis (83). With the possible exception of the testis and epididymis, however, there is little evidence for immune mediated disease in man following vasectomy (8) and no differences in circulating immune complexes between vasectomized and control subjects have been found by investigators (78).

There is some evidence for the occurrence of infiltrative autoimmune orchitis in infertile men (84). Focal mononuclear infiltration of seminiferous tubules being the characteristic finding on histology of biopsy specimens (77). Interestingly, normalisation of sperm counts can be achieved using oral prednisolone over six

months (77). Lymphocyte infiltration has also been found in oligospermic and azoospermic infertile men (85). This provides evidence for involvement of the immune system in the pathology of infertility although, it does not confirm self antigens to be the only target. The focal nature of the orchitis has been invoked by some as a possible explanation as to why orchitis has not been reported previously in infertile or in vasectomized men (80).

There are reports that spermatids showed degenerative features and that there was increased vacuolation of Sertoli cells following vasectomy in man (86, 87). Other workers have suggested even more severe alterations to the seminiferous tubules in a proportion of cases, including the finding of minimal spermatogenesis and aspermatogenesis on follow up (88). The changes were largely confined to the tubules of the testis with a largely normal interstitium. The seminiferous tubules have been described as hypocellular (89) with an increased thickness of the boundary zone (88). Other workers have reported spermatogenic arrest, boundary zone thickening and interstitial fibrosis (90). Alterations in the histological appearances were not associated with high titres of antisperm antibodies (91). The finding of altered boundary zones alone after vasectomy may have significance for fertility following vasovasostomy. The majority view, however, seems to be that spermatogenesis continues after vasectomy (64, 75, 87) with some minor impairment (92, 93), in the majority of cases. This is consistent with the ability to obtain normal sperm counts following vasovasostomy in a percentage of men (21). Alterations to the boundary zone of the seminiferous tubules are a common feature in infertile patients (83, 94, 95), although they may be of many different causes (82). The inability to obtain sperm in the ejaculate of all men following vasovasostomy leaves open the possibility of a more detrimental effect in a small percentage of cases.

The Effects of Experimental Vasectomy on the Testis in Animal Models

The difficulty of obtaining specimens of human material requiring an invasive procedure, combined with the poor fixation of cadaveric material for use in ultrastructural analysis, has led to the development of animal models of vasectomy. The work which has been done on vasectomy in the human, using biopsies, only gives a limited picture of what is happening in the organs as a whole. This is of particular concern when considering conditions which are known to be focal in nature as appears to be the case with certain forms of orchitis (80).

The principle problem with animal models is that there is considerable variation in the effects of vasectomy on the male reproductive tract in different species (96). This may reflect different morphological features some of which may be significant for their response to vasectomy. Disrupted spermatogenic activity has been reported in the guinea pig (97), hamster (98), mouse (99), rabbit (100) and rat (101, 102). Apparently conflicting reports of normal spermatogenesis following vasectomy have been made in the gerbil (103), monkey (104), mouse (105), rabbit (106) and rat (107). These contradictions may be partially resolved by allowing for variation between different strains of the same species. Thus in the case of the rat, Albino rats may undergo spermatogenic arrest (101) whilst Wistar rats may not (107). Other factors such as time after vasectomy may play a role in this variation (96), for example, Flickinger (102) examined rat material seven months following operation, whilst the others waited approximately one month (101, 107). In some species the differing effects of vasectomy with time after operation suggest that initial inhibition of spermatogenesis is followed by a return to normal. Such effects are well documented in the dog (108) and Rhesus monkey (109) but have also been found in some strains of mice (110) and Albino rats (111). This stresses further the importance of observing long term consequences of the procedure as is the intention of this work.

Orchitis has been found following vasectomy in a number of animal models but is best documented in the rabbit (24, 112, 113) although, monocytic infiltration has

also been found in the Guinea pig (97, 114). There is good evidence in the rabbit that an autoimmune process is occurring as circulating antibody can be detected in the blood and immune complexes can be demonstrated in the boundary zone of the seminiferous tubule (24). In the Guinea pig, direct comparison of the effects of vasectomy with experimentally induced allergic orchitis found some difference between the two suggesting other possible aetiologies (115). Monocytic orchitis has been documented in the rhesus macaque following vasectomy, although, some controls were also affected which raises the possibility of infection as an underlying aetiology (116). Frank orchitis has not been found to follow vasectomy in the rat although, sperm autoantibodies have been documented in vasectomized Lewis rats (117) and in pre-pubertal rats with experimental vasal obstruction (118). There have also been reports of anti-sperm antibodies associated with histological abnormality in Lewis rats (119) although, it is not certain that this link is causal.

The Effects of Experimental Vasectomy on the Testis in the Rat

The effects of vasectomy on the testis of the rat are still controversial (120). Several authors have reported that the testes remain unchanged following vasectomy (121, 122, 123). Other authors have reported a variety of structural changes in the testis ranging from gross degeneration (124, 125) to impaired spermatogenesis (126) and ultrastructural changes in the boundary zone (102, 127). The changes reported following vasectomy in the rat reflect, to an extent, the mode of investigation chosen. Some have performed only gross observation or mass measurement (123, 124) whilst, others report accompanying histological degeneration of the seminiferous tubules (128, 129). The majority of reports now suggest that some degree of structural alteration of the testis occurs in at least a proportion of certain strains of vasectomized rat.

The explanation for the variability in the presence or absence of post vasectomy degeneration of the testis in the rat is unknown although, several suggestions have been made. It may be because of the difference in the strain of rat used (96, 130). Different strains of rats might have differing susceptibility to degeneration which

might be due to differing immune responses. The number of rats with circulating antisperm antibodies following vasectomy has been shown to vary with the strain (131). Even amongst responders, some strains of rat seem to produce a bigger response than others (132). The latter presupposes an autoimmune aetiology of the degeneration. This is by no means certain although, higher titres of antibody to sperm have been linked with more severe degeneration of the testis (133). The pattern of antigen recognition as manifested by the antibody immune response in vasectomy is similar to that of immunisation with spermatozoa (134), giving further support to the notion of vasectomy producing an autoimmune response. This cannot provide the entire explanation as not all animals of a given strain will develop degeneration and when unilateral vasectomy is performed only a fraction of animals develop bilateral degeneration (135). Differences in the procedure have also been suggested as a cause for this variability (96). Open and closed vasectomy have been compared with both groups having grossly normal testes (123). Efferent duct ligation has been compared with partial epididymectomy with both producing some tubular degeneration which was more severe in the case of the latter (136). Non-sterile technique has also been implicated as a cause of altered testicular morphology following vasectomy in the rat (137).

This study was intended to further investigate both the ipsilateral and bilateral degeneration of the testis observed following unilateral vasectomy in the Albino Swiss rat (138). In previous studies (139), ipsilateral degeneration of the testis was found in only two out of sixty-three rats sacrificed up to six months following procedure and not in controls from these time spans. Bilateral degeneration was not observed before six months following vasectomy. In contrast, six months or more following vasectomy, seventeen out of fifty-eight demonstrated ipsilateral degeneration whilst eleven out of fifty-eight demonstrated bilateral degeneration of the testis. Of controls sacrificed six months or more following vasectomy, two out of sixty showed bilateral degeneration. These animals were eighteen months after the operation having reached an age of twenty-one months. Ipsilateral degeneration of the testis following vasectomy in the Albino Swiss rat in our experience seems to be linked with the formation of granuloma in the caput epididymis on the vasectomized side and is likely to result from pressure phenomena (139). The cause of the bilateral

degeneration remains unclear but it does not appear to result from vascular compression (139). Autoimmune phenomena have been suggested (140) but no concrete evidence for this exists at present.

This study intended to further investigate the model of degeneration of the testis following vasectomy along three main avenues. The first was to look for ultrastructural changes in the testis of rats six months and more following vasectomy to see if any subtle electron microscopic changes could be observed in both the grossly normal testes where ipsilateral degeneration had occurred and in those where both sides appeared normal. Light microscopic examination of the apparently healthy testes of rats six months following vasectomy had previously detected no abnormality (141). The second avenue of investigation was to examine the integrity of the blood testis barrier both morphologically and functionally, using lanthanum as a junction permeability marker. The final avenue of exploration was to look for evidence of immunocompetent cells in the testis following unilateral vasectomy using immunohistochemical techniques.

ELECTRON AND LIGHT MICROSCOPIC OBSERVATIONS ON THE BOUNDARY ZONE OF THE SEMINIFEROUS EPITHELIUM AND SERTOLI CELLS FOLLOWING VASECTOMY IN THE RAT

INTRODUCTION

Previous work in this laboratory has examined the effect of vasectomy on the gross and light microscopical appearances of the testis in the Albino Swiss rat and in particular on the germ cells (135, 139, 140). In this first chapter, we focused particularly on two areas not previously examined by our group. These areas would be examined and compared in healthy sham operated control testes, healthy testes following vasectomy and those undergoing both unilateral and bilateral degeneration. In addition, we would compare the ultrastructure of degenerated testes following vasectomy with those following maternal in *utero* flutamide administration.

The first area of interest was the boundary zone of the seminiferous tubule which, forms the interface between the seminiferous epithelium and the interstitium. It consists of the Sertoli cell basal lamina, the myoepithelial cell and its surrounding basal laminae (142, 143, 144). The latter lies on either side of the single layer of myoepithelial cells. Lymphatic spaces, lined by endothelium, frequently lie adjacent to this (142). Lymphocytes are never found beyond the myoepithelial cell in health but can rarely be found immediately on its interstitial aspect (145). The basal lamina of the Sertoli cell is produced by both the Sertoli cell and the myoepithelial cell in vitro (146) and is now thought to play a role in the development and expression of Sertoli cell structure and function (147). Any structural alterations in this region may have a deleterious result on the function of the entire seminiferous epithelium.

Previous work suggests that up to eight weeks following vasectomy there is no alteration in Sertoli cell function as assessed by the level of androgen binding protein in Sprague-Dawley rats (148). In this chapter we look at the long term effects of vasectomy on boundary zone structure.

The second area of particular interest was the Sertoli cell which forms part of the seminiferous epithelium. This is a complex highly specialised, stratified epithelium (149) that lines the seminiferous tubules of the testis. It normally has two populations of cells; a non dividing supporting portion consisting of Sertoli cells and a proliferative population of germ cells which mature and migrate towards the centre of the lumen. The nuclei of these cells can be readily identified at light microscopy by their irregular shaped nucleus found in the peripheral regions of the seminiferous epithelium (150). The cell is thought to support the developing sperm precursors and produces a wide variety of proteins including those destined to be part of the boundary zone (151). It also divides the epithelium into distinct physiological compartments via special junction complexes (152).

Altered morphology of Sertoli cells has been associated with degeneration of the testis resulting from a variety of insults in a number of species (153). In man, the morphology of the Sertoli cell nucleus has been used to provide information on both aetiology and prognosis for return of fertility (154). Cytoplasmic involvement usually takes the form of an increased number of cytoplasmic vacuoles often containing lipid as in man (86), the monkey (109) rabbit (100) and rat (102). Lysosomes have also been described as increasing following vasectomy in man (88), the rabbit (112) and rat (102). In the case of experimental cryptorchidism, the Sertoli cell nuclear morphology was also modified (155). In this chapter, we examine for such changes in a model of degeneration of the testes following vasectomy.

Degeneration of the seminiferous epithelium of the rat can follow numerous insults including vasectomy (128, 133, 138) and the use of anti-androgenic drugs (156). Following vasectomy, detailed studies have suggested that changes can occur in the boundary zones of the seminiferous tubules as well as in Sertoli cell cytoplasm. In particular, thickening of the Sertoli cell basement membrane has been reported following vasectomy (157) associated on occasion with increased vacuolation of Sertoli cell cytoplasm (129). Anti-androgenic drugs, which include flutamide, cause maldescent and degeneration of the testis when administered in *utero* (158, 159). We intend to examine all the layers of the boundary zones of seminiferous epithelium

from healthy tubules following vasectomy and sham procedure and compare them with degenerated tubules following vasectomy and with those following flutamide administration *in utero*.

MATERIALS AND METHODS

Animals: Fifteen Albino Swiss rats from a departmental inbred colony, maintained at the Laboratory of Human Anatomy at the University of Glasgow, were divided into two groups at three months of age. Twelve underwent unilateral left sided vasectomy. Surgery was carried out by trained technicians, to avoid training time and learning curve problems, under sterile conditions with pentobarbitone sodium anaesthesia supplemented with halothane by face mask. The ductus deferens was occluded by two silk ligatures, approximately 4mm apart, placed within 2cm of the origin of the ductus deferens from the epididymis. The portion of the ductus between the ligatures was then excised. A further three animals underwent a similar left sided sham procedure using the same anaesthetic. Two silk ligatures were only loosely tied around the ductus which was not transected. The animals were then maintained under standard conditions until sacrificed at between nine and fifteen months post operation. A greater number of vasectomized animals were included because the effect of vasectomy on the testis is unpredictable with only about thirty percent of testes from long-term vasectomized rats undergo degeneration (134). It has not proved possible to predict which animals would undergo degeneration and those that would retain healthy testis. Nor was it possible to predict which would undergo unilateral rather than bilateral degeneration. The animals were kept in standard conditions and sacrificed between nine and fifteen months following operation and prepared for light and electron microscopy.

Flutamide: Three Albino Swiss rats whose mothers had been treated with 10mg per day of flutamide in 0.1ml propylene glycol by subcutaneous injection from day ten following time mating until birth were sacrificed at twelve months of age. Flutamide, an anti-androgenic agent, can produce both maldescent and degeneration of the testis

(158, 159). In this study, only grossly degenerated testes were collected to provide a comparison with degenerated testes following vasectomy. The resin embedded blocks were donated by Professor A.P. Payne. They had undergone the same preparation as for the material in this study but the testicular weights were not available. All three testes were from animals with unilateral degeneration, one left and two right.

Electron Microscopy: Twelve unilateral vasectomized and three sham operated control animals were sacrificed between nine and fifteen months after operation. Each rat was anaesthetised with an overdose of sodium pentobarbitone and its abdomen was opened by a midline incision. This was extended first into the thorax which gave access to the heart. The right atrium was opened and a cannula was inserted into the left ventricle and immediately perfused with 200ml of Ringer's solution containing one percent lignocaine over five minutes at a pressure of 130cm of water. This was to remove blood from the vasculature and the lignocaine was to help maintain patency of the vessels. The incision was then carried down into the scrotum and the testes visualised. During this, perfusion continued with 200 mls of fixative consisting of 1% paraformaldehyde and 3% glutaraldehyde in cacodylate buffer (ph 7.8) for twenty minutes at 130cm of water pentobarbitone anaesthesia.

Fixation was continued overnight by immersion in 100mls of 1% paraformaldehyde and 3% glutaraldehyde in cacodylate buffer. After rinsing in three changes of cacodylate buffer, the testes were weighed and divided into eight according to the reference diagram (Fig. 1) with a razor blade and placed into labelled bottles. The contents of each bottle was further divided in two to allow for easier handling. The specimens were then osmicated and embedded in araldite resin (Table 3) (160). Sections were taken from 4 blocks of each testis at 6 micrometers thickness using glass knives and an ultramicrotome (Porter Blum MT-2). They were stained with toluidine blue (Table 4) and examined under light microscopy (Wild. Heerbrugg Switzerland).

Table 3. Protocol for osmication and embedding of specimens for electron microscopy.

1. Rinse in phosphate buffer twice.
2. Immerse in 0.1M Osmium Tetroxide for one and a half hours.
3. Rinse in Phosphate buffer for twenty minutes three times.
4. Immerse in 70 per cent alcohol overnight.
5. Immerse in 90 per cent alcohol for one hour.
6. Immerse in 100 per cent alcohol for one hour.
7. Immerse in pure alcohol for one and a half hours three times.
8. Immerse in propylene oxide for one hour twice.
9. Immerse in propylene oxide and araldite resin 1:1 overnight.
10. Immerse in propylene oxide and araldite resin 1:2 for eight hours.
11. Immerse in pure araldite resin overnight.
12. Immerse in pure araldite resin overnight*.
13. Embed in pure araldite resin until fully polymerised (forty-eight hours) at 60 degrees Centigrade.

*Steps 1-12 were carried out at room temperature with the use of shakers between steps.

Table 4. Protocol for staining resin sections with toluidine blue.

1. Place section on drop of distilled water on clean microscope slide.
2. Dry on hot plate for five minutes at 60 degrees Centigrade.
3. Cover specimen with toluidine blue and place on hot plate for two minutes at 60 degrees Centigrade.
4. Wash in running distilled water to remove excess stain.
5. Allow to dry for at least one hour.
6. Place in Xylene for five minutes.
7. Cover with glass coverslip using Histomount as adhesive.

Areas containing circular profiles of tubules were identified at light microscopy and the resin blocks were trimmed to include these before being hardened overnight in an oven at 60 degrees Centigrade. Sections were then cut at 60-90 nanometres using an ultramicrotome (Porter-Blum MT-2) and glass knives . These sections were placed on copper grids and stained with standard lead citrate and uranyl acetate (Table 5) to further enhance contrast. They were then examined under the electron microscope (Jeol; JEM100s).

Table 5. Protocol for contrast staining for electron microscopy.

1. Place grid specimen side down onto drop of a saturated solution of uranyl acetate in 40 percent ethanol for two minutes on dental wax in a covered petri dish.
2. Immerse in covered petri dish of distilled water for two minutes.
3. Dry on filter paper in covered petri dish for two minutes, specimen side up.
4. Place grid specimen side down onto drop of a saturated solution of lead citrate for two minutes on dental wax in a covered petri dish.
5. Immerse in covered petri dish of distilled water for two minutes.
6. Dry on filter paper in covered petri dish for two minutes, specimen side up.

SERTOLI CELL NUMBERS AND SEMINIFEROUS TUBULAR AREAS

Sertoli cell nuclei have characteristic features which allow them to be readily identified at light microscopic level (150). The mean number of Sertoli cell nuclei per seminiferous tubular profile was obtained as follows. One toluidine blue section from each testis of three sham operated animals were selected at random from a collection of masked slides. Similarly, one section from each testis of three animals with bilateral degeneration of the testes and three animals with healthy testis following vasectomy were selected.

Each of the sections had their labels masked and were drawn using a camera lucida (Fig 2). Starting at either the top or bottom of the specimen, decided on the toss of a

coin and left or right, decided in the same manner, tubules were selected. For each, the form factor (161) was ascertained by drawing around the profile on the camera lucida map using a Kontron MOP-AM02. The form factor is a measure of circularity and is equivalent to four Pi multiplied by the area of the tubule divided by the square of the perimeter. If the form factor was greater than 0.8, the tubule was included in the count as the closer this figure is to unity then the more circular the profile. Ten tubules were thus identified from each section from control and healthy testis following vasectomy. In the case of degenerated testis, ten degenerated tubules were selected in the same fashion. Circular profiles of tubules were preferentially examined to avoid the complications of oblique sections effecting the shape of the components of the boundary zone and Sertoli cell nuclear number.

For each tubule thus identified, the perimeter and surface area were also measured (using a Kontron MOP-AM02). The number of Sertoli nuclei was then counted for each section of sham operated and healthy tubule following vasectomy and its location noted on a second camera lucida drawing (Wild. Heerbrugg Switzerland) (Fig. 3). Each tubule was then re-examined and the number of leukocytes and their relative location, if determinable, in the boundary zone was noted onto the camera lucida drawing. During the count, the sections were not identified to avoid this as a source of observer bias. In the case of degenerated tubules, all nuclei present in the tubule were noted onto a camera lucida drawing. Such tubules were readily identified as being from vasectomized individuals because of their appearance and would thus present an unavoidable source of bias. The relative position of any leukocytes in the boundary zone was also marked onto the camera lucida drawing and counted.

RESULTS

Gross Observations The gross appearance of the testis following sacrifice could be divided into three groups by their naked eye appearance and the procedure undergone (table 6) (139). The first consisted of healthy testis from sham operated controls. These were pink in colour with the epididymis retaining a healthy glistening appearance although, the site of sham ligation could be identified on the vas. The

second group were grossly healthy testes following vasectomy which had a similar appearance to those of the sham operated control group. They had a similar mass to those of controls and came from either animals with both sides healthy or from the contralateral side in animals with ipsilateral atrophy (Table 7). The only difference lay in the epididymis in which some showed creamy granulomatous masses in the cauda in addition to that found at the site of ligation.

Table 6. The appearance of testis with time after vasectomy.

TIME POST OP (months)	NUMBER WITH APPEARANCE		
	NORMAL	ATROPHY UNI (L=Left, R=Right)	ATROPHY BI
V A S 9	5	1L	3
S H A 15	2	1L	0
S H A 9	1	0	0
A 14	2	0	0
F L U 12	0	2R+1L	0

Vas = Vasectomy Sham = Sham Flu = Flutamide

Table 7. Mass of testis with time following vasectomy.

SPECIMEN	TIME (months)	MASS(g)		APPEARANCE
		Left	Right	
VT1	9	1.01	1.61	I
VT5	12	1.44	1.44	H
VT14	12	1.34	1.44	H
VT20	15	0.65	1.37	I
VT24	15	1.36	1.30	H
V30	9	0.72	0.54	B
V32	9	0.53	0.48	B
V35	9	1.36	1.32	H
V36	9	1.16	1.26	H
V37	9	1.11	1.30	H
V38	9	1.20	1.20	H
V39	9	0.60	0.57	B
ST1	9	1.65	1.69	H
S22	14	1.21	1.26	H
S23	12	1.36	1.34	H

S = Sham V = Vasectomized H = Healthy I = Ipsilaterally Atrophied B = Bilaterally Atrophied

The third group consisted of those testes which were darker, often visibly smaller and appearing like a watery bag. These were termed degenerated testis. One or both sides could be affected, being termed unilateral or bilateral degeneration, respectively. Unilateral degeneration was only observed on the same side as the vasectomy, leading to the use of ipsilateral to describe them. The contralateral testis and epididymis had a healthy gross appearance. The mass of degenerated testes was considerably lighter compared with either controls or healthy specimens after vasectomy (Table 7). The epididymis often had a similar appearance to those of healthy testes following vasectomy but sometimes, additional granulomas in the caput of the epididymis were found.

Light Microscopy

Healthy testes from sham operated controls: Both the left and right testes from the three sham unilaterally operated control animals had similar healthy gross and microscopic appearances. Typical sections contained both seminiferous tubules and interstitial spaces (Fig. 4). In the latter, islands of Leydig cells could be found often in relation to blood vessels. Frequent lymphatic spaces could be identified separating tubules and are typically lined by squamous endothelial cells. Leukocytes were frequently observed in these vessels.

The boundary zone of the seminiferous tubules separates the interstitial spaces from the seminiferous epithelium. In the rat it consists of a single layer of contractile, squamous myoepithelial cells which circumferentially surround the tubule. These cells have flattened nuclei with long cytoplasmic processes extending part way around the perimeter of the tubule. These cells could be clearly resolved from the lymphatic endothelium where the elongated nuclei of the latter were stained with toluidine blue (Fig. 5). In such cases, a pale band constituting the outer layer of the basement membrane of the myoepithelial cell, could be seen to separate the myoepithelial and endothelial cells. Infrequently, leukocytes could be seen in relation to this outer layer of basement membrane (Fig. 6). The inner layer of the myoepithelial cell basal lamina, lying on its luminal aspect, is indistinct with toluidine blue as it apparently

merges with the Sertoli cell basement membrane. The later is very difficult to resolve with toluidine blue but is best seen as a pale region lying between the Sertoli cell nuclei and the outer myoepithelial cell (Fig. 7).

The seminiferous tubules contained a diverse compliment of spermatogenic precursors as well as Sertoli cells. These cells could be readily identified, near the periphery of seminiferous tubules, by their pale staining irregular nucleus frequently displaying slight intranuclear clefts and a prominent nucleolus (Figs 5, 6 and 7). In typical circular profiles, most of these nuclei were orientated with their long axis parallel to the perimeter although, occasional nuclei could be seen arranged perpendicular to the perimeter (Fig. 6).

A variety of spermatogenic precursors could be identified in the seminiferous epithelium (Figs 6 and 7). In the basal regions adjacent to the boundary zone, spermatogonia could be identified by their round or oval nuclei and characteristic pattern of nucleoplasm staining; fine granular for the type A peripheral heterochromatin for the type B (Fig. 6). Pachytene primary spermatocytes could also be identified further into the tubular lumen by their intense chromatin staining (Fig. 6). Early and late spermatids were also identified, the later by their elongated nuclei the former by pale staining round nuclear profiles.

Healthy testes following vasectomy: The seven animals whose testes remained grossly healthy after vasectomy had both left and right testes with histological appearances similar to those of the control group (Figs 8, 9 and 10). Interstitial spaces contained Leydig cells frequently in relation to blood vessels. Endothelial lined lymphatic spaces containing occasional leukocytes were also found. The boundary zone was characterised by flattened myoepithelial cells but contained occasional leukocytes adjacent to the outer layer of the basement membrane (Fig. 8). The Sertoli and myoepithelial cell basement membranes were not undulated. The seminiferous epithelium retained the typical complement of spermatogenic precursors and contained Sertoli cells with typical morphology.

The two animals undergoing ipsilateral degeneration had contralateral (right) testes with appearances like those of controls (Fig. 11). Interstitial spaces contained Leydig cells and blood vessels. The boundary zone maintained its flattened layer of myoepithelial cells. Sertoli cell nuclei could be readily identified, retaining their typical features, in the periphery of the seminiferous epithelium which contained a wide variety of sperm precursors (Fig. 11).

Degenerated testes following vasectomy: The five ipsilaterally and three contralaterally degenerated testes had markedly different histology from that of the healthy testes (compare Figs 10 and 12). The degenerated tubules appeared smaller whilst the lymphatic spaces seemed much enlarged. The seminiferous epithelium was reduced to a population of cells whose nuclei were mainly found in the periphery. Their nuclei had features of those of Sertoli cells but in an exaggerated form. They exhibited large intranuclear clefts and many had prominent nucleoli whilst some had peripheral clumps of heterochromatin (Figs 14 and 15). The cytoplasm showed areas containing large vacuoles. Leydig cells were still present frequently in association with blood vessels. In places, the endothelial nuclei were no longer elongated but adopted a more oval appearance, occasionally appearing almost triangular in section (Fig. 14).

The myoepithelial cells remained a single layer but had a triangular profile in many sections (Fig. 15). Thin cytoplasmic processes could be seen to extend part way around the perimeter of the tubule as in the controls. Occasionally, leukocytes were seen in this zone adjacent to myoepithelial nuclei (Figs 14 and 15). The myoepithelial and endothelial cells could be seen to be separated by a much thickened paler zone representing the outer layer of the myoepithelial basement membrane (Figs 14 and 15). On the luminal aspect of the myoepithelial cell, the pale layer representing the inner layer of the myoepithelial cell basement membrane and that of the Sertoli cell appeared thickened compared to controls. It was also thrown into folds which projected into the lumen (Fig. 14).

Flutamide administration: The three grossly degenerated testes following in *utero* flutamide administration showed an appearance similar to the vasectomy induced degenerated group but only very occasional immunocompetent cells could be seen (Fig. 16).

Electron Microscopy

Healthy testes from sham operated controls: Both left and right testes from the three sham operated animals had seminiferous tubules containing a wide variety of sperm precursors. The boundary zones were of similar appearance to that described in the literature (Figs 17 and 18) (143). Flattened lymphatic endothelium was frequently found to separate the interstitial regions from the tubules. Immunocompetent cells were rarely found adjacent to the lymphatic endothelium lumen (Fig. 17) but never closer to the tubular lumen.

The outer component of the myoepithelial basal lamina could be found adjacent to the luminal aspect of endothelium. It consisted of an amorphous electron dense region immediately in relation to the myoepithelial cytoplasm and a sparse fibrillar layer outside (Fig. 17). A single layer of electron dense myoepithelial cells with elongated nuclei could be seen (Fig 18). Inside this were two electron dense layers separated by a layer containing fibrils. The outer layer forms part of the myoepithelial cell basal lamina which surrounds the cell on both aspects. The inner electron dense layer is the Sertoli cell basal lamina which was, occasionally, thrown into slight undulations towards the lumen (Fig.17). Beneath these undulations the fibrils were more numerous but the dense layers apparently retained a similar thickness throughout the circumference of the tubule. Most fibrils were cut in transverse sections when examining circular tubules suggesting that their main orientation was parallel to the longitudinal axis of the tubule. The seminiferous epithelium consisted of a wide range of spermatogenic precursors as well as Sertoli cells. The irregular nuclei of the latter could be readily identified by their basal

position adjacent to their basal lamina. When sectioned appropriately, prominent nucleoli and intra nuclear clefts could also be observed (Fig. 17).

Healthy testes following vasectomy: The seven animals with testes which were grossly normal following vasectomy had seminiferous tubules and boundary zones with similar appearances to the control group (compare Figs.17 and 19). Sertoli cells retained their typical basal position, marked nucleolus and intranuclear clefts. The boundary zone consisted of an inner layer constituting the Sertoli cell basal lamina adjacent to which was the myoepithelial cell basal lamina (Fig 20). The elongated myoepithelial cell lay on its outer basal lamina outside of which, the endothelial cell cytoplasm could be identified (Fig. 19). The two contralateral grossly healthy testes from the ipsilaterally degenerated animals also had seminiferous tubules and boundary zones with similar appearances to controls (compare Figs 18 and 21).

Degenerated testes following vasectomy: The five ipsilaterally and three contralaterally degenerated testes had similar appearances which were very different from control or healthy testes following vasectomy. The boundary zones were markedly different from those of controls (compare Figs 17 and 22). The inner electron dense layer of the Sertoli cell basal lamina projected towards the germ cells giving a undulated appearance in some areas producing the appearances of multiple layers (Figs. 21 and 23). The myoepithelial cells still consisted of a single layer but in many tubules appeared triangular rather than elongated in outline (Fig. 22). The apex of which, frequently projected into the tubules as a fine cytoplasmic extension (Fig. 24). The luminal layer of the myoepithelial basal lamina had become folded as well and was, in places, clearly separated from the cytoplasm (Fig. 22). The fibrils appeared more numerous and more random in arrangement, with many no longer parallel to the longitudinal axis of the tubule when compared with healthy tubules (Fig. 22). The outer layer of the myoepithelial cell basal lamina was, in some tubules, much thicker than in the controls although, this may have been due to extensive folding (Figs 22 and 23).

The lymphatic spaces were greatly enlarged but were still lined by a squamous layer of endothelium. Pseudopodia of leukocytes were frequently observed on the interstitial aspect of the endothelium (Fig 22). Occasional lymphocytes and macrophages were seen adjacent to the myoepithelial cell layer (Fig. 25). They were most numerous immediately deep to the outer part of the myoepithelial cell basal lamina and were more common in degenerated testes following vasectomy than in those after flutamide administration. They were also occasionally found on the tubular aspect of the myoepithelial cell (Fig 26). These cells were readily found in seminiferous tubules from both bilaterally and ipsilaterally degenerated testes following vasectomy (Figs 26 and 27).

The Sertoli cells from degenerated tubules were also markedly different from controls (compare Figs 17, 25 and 28). Their nuclei had deep intranuclear clefts with peripheral clumps of heterochromatin. The cytoplasm did not contain many vacuoles nor visible remnants of sperm precursors.

Flutamide administration: In the three testes which were grossly degenerated following in *utero* flutamide administration, the appearance of the boundary zones of seminiferous tubules was similar to that following vasectomy induced degeneration (compare Figs 22 and 29). Extensive folding of the Sertoli cell basal lamina and the adoption of triangular profiles by the myoepithelial cells were seen (Fig. 29). The only difference being that immunocompetent cells seemed to be confined to the extratubular aspect of the lymphatic endothelium. The seminiferous epithelium again demonstrated an absence of sperm precursors with Sertoli cell nuclei displaying large intranuclear clefts and peripheral clumps of heterochromatin (Fig 29).

Analysis of Counts: The mean number of Sertoli cells per tubule for each testis was calculated (Table 8) and subjected to a one way analysis of variance and multiple range test via Statgraphics program to compare side, histology and procedure. These indicated that there were significantly more ($p < 0.0005$, confidence interval 95 per cent) Sertoli cells in degenerated tubules following vasectomy than in control animals or in healthy tubules following vasectomy. No significant difference was

detected between the sides or between control and healthy testes following vasectomy.

Table 8. The mean area, perimeter, Sertoli cell count and leukocyte count for each group in the study per tubule in 1/360 mm squared, 1/360mm, number of cells per tubule and number of cells per tubule.

Group	Area	Perimeter	Sertoli	Leukocyte
Sham Left				
1	724.7	100.1	19.9	0.1
2	751.5	103.3	20.3	0.0
3	697.2	96.5	19.8	0.1
Mean	724.5	100.0	20.0	0.07
Sham Right				
1	858.8	108.3	20.3	0.1
2	959.3	114.2	20.8	0.2
3	770.1	102.3	20.4	0.2
Mean	862.7	108.2	20.5	0.17
H Vas Left				
1	636.2	94.2	20.4	0.2
2	821.3	107.0	19.2	0.4
3	657.7	94.0	19.3	0.4
Mean	705.1	98.4	19.6	0.33
H Vas Right				
1	737.2	100.0	20.4	0.6
2	616.4	91.7	18.8	0.4
3	682.4	97.3	19.4	0.7
Mean	678.6	96.3	19.5	0.57
D Vas Left				
1	193.2	50.5	21.8	1.0
2	243.2	56.6	22.6	1.1
3	292.2	63.9	21.4	0.8
Mean	242.9	57.0	21.9	0.97
D Vas Right				
1	241.7	57.0	24.1	0.9
2	179.2	49.2	22.6	1.2
3	189.0	49.8	22	0.4
Mean	203.3	52.0	22.9	0.83

Significance for Degenerated versus Healthy:

p<0.0005 p<0.0005 p<0.0005 p<0.0005

H=Healthy

D=Degenerated

The mean number of leukocytes in the boundary zone per tubule for each testis was calculated (Table 8). A one way analysis of variance and multiple range test was then performed using Statgraphics program to compare side, histology and procedure. This indicated that there were significantly more ($p < 0.0005$, confidence interval 95 per cent) leukocytes detected in the boundary zone of the degenerated tubules than in controls. No difference was detected between the sides. Healthy tubules from the right testes following vasectomy had significantly more cells in the boundary zone than controls but not more than the corresponding healthy left side following vasectomy.

The mean perimeter of the ten tubules from each testis was calculated (Table 8). A one way analysis of variance and multiple range test was performed using the Statgraphics program to compare side, histology and procedure. The results indicated that the degenerated tubules had significantly smaller perimeters ($p < 0.0005$, confidence interval 95 per cent) than either healthy tubules following vasectomy or controls. No significant difference was detected between the sides or between healthy tubules following vasectomy and controls.

The mean area of the ten tubules from each testis was calculated (Table 8). A one way analysis of variance and multiple range test was performed using the Statgraphics program to compared side, histology and procedure. The results indicated that the degenerated tubules had significantly smaller areas ($p < 0.0005$, confidence interval 95 per cent) than either healthy tubules following vasectomy or in controls. The right testis from controls had tubules with significantly greater areas than those from healthy tubules following vasectomy. There was no significant difference between the tubular areas from the sides alone or between control and healthy testes following vasectomy.

DISCUSSION

Degenerated tubules from atrophic testes following vasectomy were significantly smaller in cross-sectional area than those from either healthy testes following vasectomy or healthy sham operated testes (Appendix 1). They contained significantly more Sertoli cells per cross-sectional profile than healthy counterparts. There was no evidence, on morphological grounds for this increase in number of cells to have been due to the presence of additional cells, such as migratory lymphocytes, within the epithelium as all the cells had similar appearances. It seemed more likely to be due to a shrinkage in both length and width of the tubules. There also appeared to be an increase in the absolute numbers of leukocytes in the boundary zone following vasectomy although, the numbers of testes assessed was relatively small and may have been influenced by shrinkage of the tubule.

Our observations at both light and electron microscopy suggest that there is considerable morphological difference between the boundary zone of healthy tubules following vasectomy or sham procedure and degenerated tubules following vasectomy in the Albino Swiss rat (Appendix 2). Healthy tubules from sham operated controls or following vasectomy had a boundary zone structure as described in the literature (143). The Sertoli cell basal lamina was extensively folded with thickening of the fibres forming part of the basement membrane. These fibres also appeared increased in number with a more irregular orientation. There was no gross evidence of deposition of immune complexes but rather, the findings suggested a simple geometric explanation for the appearances of the basal laminae consistent with loss of tubular diameter and perhaps length.

The myoepithelial cells remained a single layer with the cytoplasm of many adopting a triangular profile around their respective nuclei. The myoepithelial basal lamina was also folded with its inner aspect becoming clearly separated from the cell body in places. Leukocytes, often lymphocytes with some macrophages, were also readily observed adjacent to the outer aspect of the myoepithelial basal lamina. Some of these cells were seen to send pseudopodia around the outer aspect of the

endothelium. A few leukocytes were observed to have penetrated beyond the myoepithelial cells. Leukocytes are thought not to be present beyond the myoepithelial cell in healthy testis (145). The changes in the boundary zone of degenerated tubules following vasectomy are not limited just to the Sertoli cell basal lamina as has been reported in Lewis rats (129) but involve all layers of the boundary zone. The finding of some immuno-competent cells in the boundary zone raised the possibility of a role for the cell mediated immune system in the mechanism underlying degeneration following vasectomy and lead us to the immunohistochemical study performed in Chapter 4 (page 60).

We were unable to demonstrate any structural differences between the boundary zones from ipsilateral or bilaterally degenerated testes following vasectomy. We found no evidence for alterations of the boundary zone preceding degeneration and altered boundary zones were only found in degenerated tubules. We directly compared degenerated tubules from rats following anti-androgen treatment (flutamide) in *utero* and those following vasectomy (Appendix 3). Both showed very similar changes in both the seminiferous epithelium and in the boundary zones. This supports the notion that the changes in the boundary zone of degenerated tubules following vasectomy are not specific to the mechanism of insult. This is further strengthened by the striking similarity of the boundary zone changes reported here to those reported following X-ray irradiation in the rat (142).

The seminiferous epithelium of degenerated tubules was also markedly different from that of healthy tubules following vasectomy or sham procedure. The epithelium was reduced to Sertoli cells only which themselves had altered morphology (Appendix 4). Many adopted a more central position within the tubule. Most had developed one or more deep intranuclear clefts. Peripheral clumps of heterochromatin were readily identified in many nuclei (Appendix 5). The almost complete absence of vacuoles in the Sertoli cell cytoplasm of severely degenerated tubules probably reflects the complete absence of sperm precursors in such tubules. The changes to Sertoli cells described here are very similar to those previously reported by some groups following experimental cryptorchidism (155). Attempts have been made to specify

the changes in a range of conditions with some authors suggesting that they are non-specific (162) and others suggesting the pattern may be used to give clues as to the underlying aetiology (154). Our finding of similar changes between ipsilateral and bilateral atrophy following vasectomy and flutamide administration in *utero* again support the notion of non specific affects.

It seems possible that the boundary zone changes reported here occurred in association with decreased tubular diameter. Our observations, along with those of several others, associate decreased tubular diameters with some boundary zone changes (129, 136, 163). Some authors, however, have associated thickening of the Sertoli cell basement membrane with increased tubular diameter in man (90). This difference may be due to species variability in complexity of the boundary zone (143).

EXAMINATION OF THE BLOOD-TESTIS BARRIER FOLLOWING VASECTOMY

INTRODUCTION

The testes are separated from the other body compartments by a barrier termed, although not universally, the blood-testis barrier (164). The anatomical site of this barrier probably lies within the seminiferous epithelium at the level of Sertoli-Sertoli cell tight junctions (152) although, a partial barrier is thought to exist at the level of the myoepithelial cells (152, 165) and possibly at the lymphatic endothelium (166). Several functions have been attributed to this barrier including the maintenance of a selective hormonal and ionic environment within the tubules and sequestration of the immunogenic spermatozoa (167). This barrier seems to be very important for the function of the testis as its integrity may well be required for normal spermatogenesis. Disruption of the blood testes with chemical toxins (168) and vitamin A deficiency (169) has been linked with degeneration of the seminiferous epithelium.

Previous work in this laboratory has shown that degeneration of the testis occurs in combination with granulomas of the caput epididymis (139) in a proportion of Albino Swiss rats six months or more following unilateral vasectomy. Other animals retain histologically normal testis. The degeneration can be ipsilateral, occurring only on the side of vasectomy, or bilateral. The mechanisms underlying both forms of degeneration are unknown although, disruption of the blood-testis barrier could play a role in either or both. It has been previously demonstrated that severely degenerated tubules three months after bilateral vasectomy, in the Lewis rat, had an increased permeability to lanthanum (128). Our study investigates the integrity of the blood-testis barrier following unilateral vasectomy by examining the morphological appearance of Sertoli-Sertoli tight junctions and their permeability to lanthanum used as an electron dense tracer.

MATERIALS AND METHODS

Animals: Twenty-six Albino Swiss rats from a departmental inbred colony were assigned to one of two groups at three months of age. The first, consisting of nineteen animals, underwent left sided unilateral vasectomy as described in the first chapter (Page 34). Seven controls underwent a similar unilateral sham operation. The animals were kept in standard conditions, sacrificed between nine and fifteen months following operation and perfusion fixed via the heart as detailed below.

Pilot Study: In order to obtain optimum fixation of the testis and perfusion of lanthanum, a series of trial procedures were attempted using varying concentrations of fixatives and lanthanum based on the experience of previous workers (152, 169, 170). Fourteen animals, ten vasectomized and four sham, were used in this part of the study at the end of which, a standardised protocol was used for the remaining study. The specimens were processed for light and electron microscopy as detailed below. Tracer presence and fixation were then assessed. The buffer was chosen to allow for dissolution of the lanthanum. Attempts were made to introduce lanthanum after the initial Ringer's perfusion but these tended to reduce perfusion to such an extent that fixation of the testis was grossly impaired. The explanation for this is unclear, however lanthanum is thought to bind to various calcium binding sites including inside cardiac muscle cells (171). It is possible that a similar event is occurring in vascular smooth muscle causing contraction and reducing perfusion considerably. All solutions of lanthanum were maintained at room temperature, to reduce precipitation and were filtered before use. The final concentration of lanthanum in the fixative was two per cent. The procedure and concentrations which gave optimum results is detailed in table 9.

Table 9. Pilot study for lanthanum perfusion.

PROCEDURE	TIME	APPEARANCE	LANTHANUM	FIXATION
V	9	I	1%	2%G
V	10	H	1%	2%G
S	9	H	1%	2%G
V	10	H	1%	2%G
V	15	B	1%	3%G
S	9	H	1%	2%G
V	12	H	1%	Pr2%G
S	9	H	1%	2%G
V	13	H	1%	Pr3%G
V	12	H	1%	Pr1%P3%G
S	11	H	1%	Pr2%G
V	12	H	2%	Pr1%P3%G
V	12	H	2%	Pr3%G
V	13	B	2%	Pr1%P3%G

Key:

S = Sham operated V = Vasectomized H = Healthy

I = Ipsilateral Degeneration B = Bilateral Degeneration

G = Glutaraldehyde P = Paraformaldehyde Pr = Prefixed

Time was in months following procedure

Lanthanum Perfusion: Lanthanum is an electron dense heavy metal with an atomic size of 0.114nm which can be used to assess the permeability of the blood testis barrier following vasectomy (171) . We used a technique which was modified from that used by Dym and Fawcett (153) and Cavicchia (170) on nine vasectomized and three sham operated control rat. Each animal was terminally anaesthetised with an over dose of sodium pentobarbitone and its abdomen was opened by a midline incision. This was extended first into the thorax which gave access to the heart. The right atrium was opened and a cannula was inserted into the left ventricle and immediately perfused with 200ml of Ringer`s solution containing 1% lignocaine over five minutes at a pressure of 130cm of water. This was to remove blood from the vasculature and to maintain patency of the vessels. The incision was then carried down into the scrotum and the testes were visualised. During this, perfusion continued with 200 mls of the fixative consisting of 1% paraformaldehyde and 3% glutaraldehyde in cacodylate buffer (pH 7.8) for five minutes at 130cm of water to prevent lanthanum from penetrating cells as opposed to the extracellular space (165).

Lanthanum was then introduced at a final concentration of 2% into 400ml of the same initial fixative, filtered and perfused for 30-40 minutes at 130cm of water (Table 10)

Table 10. Protocol for lanthanum perfusion via the heart.

1. Perfuse 200ml Ringer's solution containing 1 per cent lignocaine over five minutes at 130cm water pressure.
2. Perfuse 200ml fixative containing 1 per cent paraformaldehyde and 3 per cent glutaraldehyde in cacodylate buffer at pH 7.8, room temperature and 130 cm of water for five minutes.
3. Perfuse 400ml of filtered 2 per cent lanthanum solution in fixative (as above) and same conditions over 30-40 minutes.
4. Remove tissue and store overnight in fixative (1 per cent paraformaldehyde and 3 per cent glutaraldehyde in cacodylate buffer at pH 7.8) without lanthanum.

The progress of fixation was monitored initially by observation of tissue blanching as blood was purged from the vessels and later by the development of a waxy coloration of the organs. Handling of the testes was kept to a minimum with the firmness of other tissues, such as the liver, as a gauge to the completeness of fixation. Each testis and epididymis was removed en bloc and placed in a labelled container of fixative excluding lanthanum overnight. The lanthanum was also excluded from all subsequent stages of preparation

Preparation for Electron Microscopy: The testes were then rinsed in cacodylate buffer and placed in buffer for four hours to remove fixative for handling. Each testis was divided into eight and each piece labelled according to a standard reference (Fig 1). The testis was divided using a razor blade and placed in separate labelled containers. Further preparation involved osmication and embedding in araldite resin (Table 3). Osmication fixes and enhances contrast whilst araldite provides sufficient

support to allow sectioning for electron microscopy. Random sections were taken from four of the blocks of each testis at 1 micrometer using an ultramicrotome (Porter Blum MT-2) and stained with toluidine blue (Table 4) and examined with light microscopy. Areas containing circular profiles of tubules were identified and the blocks were trimmed to include these and hardened overnight in the oven at 60 degrees Centigrade. Sections were then cut at 60-90 nanometres using an ultramicrotome (Porter-Blum MT-2) and glass knives. These sections were placed on copper grids and stained with lead citrate and uranyl acetate (Table 5) to further enhance contrast. They were then examined under the electron microscope (Jeol; JEM100s). Sections from the eight vasectomized and three sham operated control animals used in the previous study were also examined under electron microscopy.

RESULTS

Gross appearance and Light Microscopy: As previously observed, the gross appearance of the testis following sacrifice could be divided into three groups by their naked eye appearance and the procedure undergone (page 38) (139). The first consisted of six healthy testes from three sham operated controls. The second, of ten healthy testes from six animals following vasectomy. Four of these animals had healthy testes on both sides, whilst two had undergone ipsilateral degeneration with grossly healthy right testes. Both of these groups had similar gross appearances and contained a wide variety of sperm precursors on light microscopy. The third group, consisting of eight degenerated testes following vasectomy, were markedly different from healthy testes both in gross appearance and in their paucity of sperm precursors on light microscopy. The eight degenerated testes were from five animals, three with bilateral degeneration and two with ipsilateral (left sided) degeneration.

Electron microscopy

Healthy testes from sham operated controls: The testes from sham operated control animals contained seminiferous tubules containing a wide variety of sperm precursors as well as Sertoli cells. The Sertoli cells were inter-connected in their basal portions by typical tight junctional complexes (Figs 30 and 31). These have been well described in the literature and consist of areas of Sertoli cell membrane fusion with subjacent electron dense fibrillar deposits often in approximation to endoplasmic reticulum (152, 166, 167).

Healthy testes following vasectomy: The grossly healthy testes from animals following vasectomy shared similar appearances to those of the sham animals. Typical Sertoli-Sertoli tight junctional complexes consisting of areas of apparent Sertoli cell membrane fusion with subjacent electron dense deposits and endoplasmic reticulum (Figs 32 and 33). They were readily seen in the basal portions of the tubules. They were also seen in healthy right testes of animals with ipsilateral degeneration (Fig. 34).

Degenerated testes following vasectomy: The grossly degenerated testes following vasectomy shared a common appearance regardless of whether they belonged to the ipsilateral (Fig 35) or bilateral group and in the later instance, whether they were from the left or right side (Figs 36 and 37). Most tubules contained only Sertoli cells with no recognisable sperm precursors as has been previously described. Typical Sertoli-Sertoli junctional complexes were identified in the basal regions of the tubule consisting of areas of Sertoli cell membrane fusion with subjacent electron dense fibrillar deposits often in approximation to endoplasmic reticulum (Fig. 36).

Permeability to Lanthanum

Healthy testes from sham operated controls: Lanthanum was not found beyond the basal compartment of the seminiferous tubules in any section examined and no

tracer was identified in the lumen of the seminiferous tubule. The tracer was seen to stop at or before the level of the Sertoli-Sertoli cell tight junctions (Figs 38). In some cases it seemed not to have travelled far beyond the vasculature (Fig. 39).

Healthy testes following vasectomy: animals with healthy testes following vasectomy were seen to exclude lanthanum from their luminal aspects (Fig. 40). It was rarely seen as far as the Sertoli-Sertoli cell junctional complexes (Fig. 41). It did not penetrate far into these in agreement with reports by others (152) (Fig. 42). Even in grossly healthy testes from animals with ipsilateral atrophy, no lanthanum was identified in the lumen (Fig. 43).

Degenerated testes following vasectomy: animals with ipsilateral degeneration of the testes following vasectomy showed no evidence of lanthanum in the lumen. The tracer was seen to stop in the basal portions of the seminiferous tubules (Fig. 44). A similar picture was observed in both left and right testes following bilateral degeneration. Tracer was confined to the basal portions of the seminiferous tubule (Figs 45 and 46) with no lanthanum seen in the lumen.

DISCUSSION

Our results suggested that Sertoli-Sertoli tight junctions remain morphologically intact nine to fifteen months following vasectomy in the rat (Appendix 6). We were able to identify typical Sertoli-Sertoli cell tight junctional complexes in healthy testes from sham operated controls and those following vasectomy. This was even true of healthy testes from animals with ipsilateral degeneration. Degenerated testes themselves, whether from animals bilateral or ipsilateral degeneration, also contained typical junctional complexes as described in the literature (167).

The results of the Lanthanum permeability have to be interpreted in the light of an understanding of the nature of the blood-testes barrier. It includes more than just the Sertoli-Sertoli cell tight junction in the rat but also varying contributions from the

lymphatic endothelium (166) and the myoepithelial cell (152, 172) in maintaining a gradient of material at low concentration in the seminiferous tubule (166). It is therefore not surprising that we were rarely able to clearly identify lanthanum stopped discretely by a junctional complex as described by some (152) (Fig. 42). This is probably due to a combination of factors including the presence of partial barriers to the passage of tracers into the seminiferous epithelium at several levels prior to the junctional complex itself. This is supported by the findings of others who have noted Lanthanum only rarely to reach as far as the Sertoli-Sertoli cell junctional complexes in the rat (173). The important finding as far as the blood-testes barrier permeability is concerned is that lanthanum was not found beyond the basal compartment of the seminiferous tubules in any section examined regardless of the histology of the testis and no lanthanum was seen in the tubular lumen.

The results suggest that the morphologically intact Sertoli-Sertoli cell junctions also appeared to retain their ability to exclude lanthanum from all but the very basal portions of the seminiferous tubule. This applied in healthy testis following vasectomy and sham operation as well as in ipsilaterally and bilaterally degenerated testes. Previous work on the permeability of the blood testis barrier following vasectomy is limited. Vasoligation has been shown to produce no change in permeability to lanthanum up to one month following the procedure, where as, efferent duct ligation produces an increased permeability over the same time span (172). Other workers in the mouse (174) and rat (173) have found no increased permeability to lanthanum following efferent duct ligation. This is possibly because the later were examining effects in the short term, only up to two days. Bilateral vasectomy has been shown to produce increased permeability to lanthanum after three months in the Lewis rat (128) but only in degenerated tubules.

The permeability of the seminiferous tubules to lanthanum has been investigated in several other causes of degeneration of the testis, including vitamin A deficiency (175) and cryptorchidism in the rat (176), post-pubertal pituitary failure in man (177) and experimental allergic orchitis or vasectomy in the Guinea pig (178). All of these suggest that the blood-testis barrier remains intact following the respective insult in agreement with our findings after vasectomy in the rat. Other methods of

investigation including dye penetration and fluid sampling have also generally shown that the blood-testis barrier remains intact following a variety of insults in several species (166). In short term studies of vitamin A deficiency in the rat, however, the barrier had increased permeability to lanthanum at ten days (169). This raises the possibility that the barrier had recovered by seven weeks accounting for the findings of other workers (175).

Most of the previously published literature support our findings. It has been shown that up to four months following vasoligation, in the Holtzman rat, grossly normal tubules retain their impermeability to lanthanum (172). The same author examined degenerated tubules of Lewis rats three months following vasectomy and concluded that in the most severely degenerated tubules, lanthanum was able to penetrate through the Sertoli-Sertoli cell tight junctions (128). Our findings on Albino Swiss rats are that the barrier is impermeable to lanthanum between nine and fifteen months after vasectomy. This raise the possibility that the blood-testis barrier remains initially intact following vasectomy followed by a transient leaky phase around three months before regaining its integrity by nine months. Other explanations may be sought in the fact that different strains of rat were used, it being possible that these strains respond differently to vasectomy. It should be remembered, however, that both Lewis (129) and Albino Swiss (139) rats have been shown to undergo a similar response to vasectomy. It therefore seem unlikely that strain variability provides the explanation for this. A similar rationale may explain the findings following efferent duct ligation and vitamin A deficiency discussed above.

IMMUNOHISTOCHEMISTRY OF THE TESTIS FOLLOWING VASECTOMY IN THE ALBINO SWISS RAT

INTRODUCTION

Previous work in this laboratory (135, 139) (Appendix 1) has investigated testicular degeneration in the rat following left unilateral vasectomy. This degeneration seemed to occur in combination with granulomas of the caput epididymis. It was found to be both ipsilateral to the side of vasectomy but also, frequently bilateral (139). The latter form of degeneration was of particular interest to us as it raised the possibility of the action of systemic factors because, the right side was untouched at operation. Both vascular and autoimmune causes have been postulated as the underlying aetiology of the bilateral degeneration although, the former seemed not to be the cause (139). During our electron microscopic investigations, we more frequently observed leukocytes in the boundary zone of degenerated testis following vasectomy when compared with healthy testes following vasectomy or sham operated controls (page 48). This apparent increase in leukocytes numbers in degenerated tubules may also be true of other areas of the testis as, the simple histology performed could not reliably exclude small numbers of white cells within the tubules. These observations raised the possibility of an autoimmune mechanism for the bilateral degeneration of testes following vasectomy being comparable to experimentally induced autoimmune orchitis (179). A mechanical obstructive mechanism may still apply to the ipsilateral side (139).

There is little literature looking specifically for a cell mediated response to vasectomy in the testis of rats although, there is good evidence for orchitis following vasectomy in the rabbit (24, 112, 113) and of monocytic infiltration of seminiferous tubules in the Guinea pig (97, 114). Monocytic orchitis has been documented in the rhesus macaque following vasectomy, although, some controls were also affected which raises the possibility of infection as an underlying aetiology (116). Frank orchitis has not been found to follow vasectomy in the rat although, sperm autoantibodies have been documented in vasectomized Lewis rats (117) and in pre-pubertal rats with experimental vasal obstruction (118). There have also been

reports of anti-sperm antibodies associated with histological abnormality in Lewis rats (119) although, it is not certain that this link is causal. T-lymphocytes and macrophages have been identified in the interstitial space surrounding the *rete* testes of healthy human testes by immunohistochemistry (180).

In this chapter, we intended to identify the sub-populations of leukocytes present in healthy testes from sham operated control rats as well as in healthy and degenerated testes following vasectomy. It was also hoped to explore a temporal relationship between the lymphocyte subpopulations and the degeneration and in particular to examine the possibility that leukocyte infiltration may precede degeneration. Four time periods were chosen based on the previous work which suggested that gross degeneration did not occur prior to six months following vasectomy. The time periods chosen were three weeks, three months, six months and one year following operation. Age matched sham operated rats would be used as controls. The testes of all of these animals would be collected, sectioned and frozen with the application of immunohistochemical techniques to display lymphocyte sub-populations and macrophages.

MATERIALS AND METHODS

Animals and Procedures: Twenty-seven Albino Swiss rats were assigned to one of two groups at three months of age. The first, consisting of fifteen animals, underwent unilateral left sided vasectomy as described earlier (page 34). The second, consisting of twelve animals, had a similar unilateral sham procedure (page 34). The procedural groups were then assigned to time intervals after which sacrifice would occur. These intervals were three weeks, three months, six months and one year each consisting of three animals except the one year vasectomized group which had nine animals. This was to allow us to find some healthy and some degenerated testes as we have been unable to detect a reliable method of predicting which animals would undergo degeneration.

Collection and Freezing of Material: Each animal was sacrificed using a gas chamber into which carbon dioxide was pumped. They were weighed and the scrotum shaved using savalon and then washed in copious warm water. The animals were pinned out on a cork board and the scrotum opened via a midline incision. Each testis and epididymis was exposed and mobilized en block. The spermatic cord was cut and with great care, the testis was separated from the epididymis. The epididymis was then divided into three and placed on dry ice to be used in future work. The testis was weighed and placed on dry ice until frozen. Several of the sham animals also had their spleens removed to provide control material. The spleen was approached via a midline incision, identified, removed and placed on dry ice. The frozen tissue was then wrapped in Nescofilm, labelled and stored at -20 degrees centigrade until cut. This storage was always under 48 hours but varied due to availability of time on the cryostat.

Frozen Sectioning: The proximal 5mm of each frozen testis was removed with a sharp scalpel and stored whilst the remainder was mounted on a chuck in the cryostat (Reichert-Jung 2800 Frigocut E) using OCT compound (Tissue Tek). The testis was then covered in OCT compound and lowered into liquid nitrogen so that only the chuck was in contact with the liquid nitrogen. This prevented cracking of the block due to rapid cooling and also excessive melting of the block due to room temperature OCT compound. Once mounted, the block was cut to full face and sections were then taken sequentially at a thickness of 7 micrometers and mounted on labelled gelatinised slides. The spleen specimens were sectioned in a similar manner to the testes. One section was placed on either end of the slide and allowed to dry in air for ten minutes. The gelatine improved adherence of the section to the slide as did the drying. One section from each testis was labelled with each primary.

Fixation and Storage: After drying, the slides were immersed in acetone for ten minutes and then allowed to dry in air for a further ten minutes. Two slides were then placed back to back and wrapped in cling film. A total of two such packages were then placed in a labelled sealed plastic bag with a small quantity of dehydrated silica gel. They were then placed in a freezer at -40°C until required. Material stored

by this method has been successfully stained by immunocytochemistry after storage for periods in excess of two years.

Antibodies: The primary antibodies were all mouse monoclonal anti-rat in nature and were obtained from Seralab. W3/25 has been shown to label most thymocytes, T-helper lymphocytes and some macrophages (181). OX8 has been shown to label most thymocytes, T-suppressor/cytotoxic lymphocytes and some natural killer cells (181). OX19 has been shown to label all thymocytes and most peripheral mature T lymphocytes (181). These three antibodies were used to identify and subtype T lymphocytes. OX33 is directed to a subfraction of the leukocyte common antigen expressed on B lymphocytes (182) and was used in this study to identify these cells. OX42 has been shown to label the iC3b receptor which exists on a sub-population of macrophages, dendritic cells and granulocytes (183). It therefore has some use, all be limited, as a marker for macrophages in tissues for which purpose it was used in this study (183). OX6 has been shown to bind to class II MHC antigens of all strains of rat tested as well as some loci of the mouse MHC Ia. It has been used to characterise the immune response genes of various strains of rodent (184). OX18 detects a monomorphic determinant of rat RT1A MHC class I antigen (185). OX6 and OX18 were used in this study to determine the distribution of MHC antigens in the testis of the rat after vasectomy.

Immunohistochemical staining: A standard protocol involving the use of the Avidin Biotin Peroxidase Complex (ABC) (Elite Kit, Vector Laboratories) was used throughout the study for all of the antibodies (Table 11). It is a very sensitive technique which would allow identification of small numbers of leukocytes as anticipated in the controls. The concentrations of primary and secondary antibody as well as of the blocking serum were determined in the pilot study and by previous experience (24) (Table 12). Specimens were then counterstained using Mayer's haematoxylin and covered using glass coverslips (Table 13).

Table 11. Protocol for Immunohistochemical staining.

1. Rehydrate specimen from freezer in phosphate buffered saline (PBS) for five minutes in glass trough.
2. Block endogenous peroxidase with 100mls PBS containing 0.3 per cent hydrogen peroxide for twenty minutes in glass trough.
3. Wash in PBS for five minutes three times.
4. Block with 60 microlitres of goat serum (dilutes 1:20 with PBS) for twenty minutes.
5. Drain excess serum.
6. Apply 60 microlitres of primary antibody (Table 2).
7. Incubate overnight at 4 degrees Centigrade in humidified chamber.
8. Rinse in PBS for five minutes three times.
9. Apply 60 microlitres of biotinylated antimouse secondary antibody (Vector) diluted 1:200 in PBS with 10 per cent rat serum.
10. Incubate for sixty minutes at room temperature in a humidified chamber.
11. Make streptavidin/ biotin/ horseradish peroxidase complex (Vector). Allow to incubate for thirty minutes before use.
12. Wash slides in PBS for five minutes three times.
13. Apply 60 microlitres of preformed complex and incubate for thirty minutes at room temperature in a humidified chamber.
14. Add diaminobenzidine developer to 100 mls of PBS and filter in special area (diaminobenzidine has carcinogenic properties).
15. Wash slides in PBS for five minutes three times.
16. Add 0.03 per cent hydrogen peroxide to diaminobenzidine solution and develop slides for fifteen minutes.
17. Wash slides in PBS for five minutes.
18. Wash in distilled water three times.

Table 12. Primary antibody dilutions and specificities.

<u>Antibody</u>	<u>Dilution</u>	<u>Solvent</u>	<u>Specificity</u>
OX19	1:20	PBS with 1% goat serum	T-Lymphocytes
OX 33	1:20	PBS with 1% goat serum	B-Lymphocytes
OX8	1:20	PBS with 1% goat serum	T-Suppressor
W3/25	1:500	PBS with 1% goat and 2% rat serum	T-Helper
OX6	1:20	PBS with 1% goat serum	Class II MHC
OX42	1:20	PBS with 1% goat serum	Macrophages
OX18	1:20	PBS with 1% goat serum	Class I MHC

Table 13. Procedure for counterstaining with Mayer's haematoxylin and covering slides.

1. Immerse slide in Mayer's haematoxylin solution at room temperature for two minutes.
2. Decolourise in running cold water for ten minutes.
3. Immerse in 30 percent ethanol for five minutes.
4. Immerse in 70 percent ethanol for five minutes.
5. Immerse in 90 percent ethanol for five minutes.
6. Immerse in 100 percent ethanol for five minutes.
7. Immerse in pure ethanol for five minutes.
8. Immerse in xylene for five minutes.
9. Immerse in xylene for five minutes.
10. Mount slide using histomount clear and a glass cover slip drying overnight.

Pilot study: The aims of this were to determine the optimum dilutions of the primary antibodies as well as to determine the effects, if any, of long term storage. We also hoped to reduce background staining to a minimum and to identify any

difficulties specific to the staining of testis and to test the suitability of counting methods.

Each antibody was prepared in of dilutions of 1/20, 1/50, 1/100, 1/200, 1/500 and 1/800 and was then used to label sections from a spleen prepared by the above procedure and stored for two years. The dilutions giving the most cell specific staining and least background were noted. This was repeated for spleen stored for two months to give an indication if the storage procedure significantly affected the labelling process. The distribution of staining was then compared with known cell distribution of the spleen as well as previous work on the antibody staining patterns (178, 181, 182). W3/25 caused particular problems with background staining which was reduced by the introduction of two percent rat serum into the solution.

The same dilutions were then tried on sections of control and degenerated vasectomized testes and the dilutions giving the most cell specific and least background were noted. Some of the antibodies appeared to stain relatively few cells although in a highly specific fashion. It was therefore determined to always include positive controls in the form of specimens of spleen in each labelling batch. The identification of cells predominantly in the interstitium with very occasional intratubular cells was of significance for the method of cell counting. OX18 seemed likely to present a particular problem of analysis as it stained extensively in the interstitium (Fig. 47) with only a slight intratubular component (Fig. 48) in healthy testes but had a marked intratubular component in degenerated tubules (Fig. 49).

Experimental Design: In order to spread the work load of this study, it became necessary to store the material once collected. We have demonstrated that long term storage appears not to significantly interfere with the labelling process in this study and in other work (25). The design deviated from a more ideal one in not having all specimens stored for the same time because of practical constraints on the availability of machine time and logistics of staining the large number of specimens involved. Similarly, it was not possible to label all specimens with one primary at a given time.

Testes were stained in batches of three which proved, logistically, to be the greatest number that could be reliably managed at one sitting. The testis were selected by withdrawal of a chit from a box with the operator blinded as to their identity. This was designed to reduce any bias resulting from the necessity of staining in batches. The specimens were stored at -40 degrees celcius for between six and twelve months before use, the precise period being determined by withdrawal of unidentified chits from a box. For each testis, two controls were included consisting of no primary antibody (replaced with normal solvent) (Fig. 50) and no secondary using a primary chosen at random such that in each experiment, six of the seven primaries would be used. Along with the six testes, eight sections of spleen would be included and would be labelled with the seven primaries and one no primary. This functioned as the positive control as the staining characteristics of spleen with many of these antibodies has already been determined in this laboratory and others (183, 186, 187). All of the sections were examined using an Olympus CO11 microscope at a linear magnification of up to approximately 400 times.

Pilot study comparing the numbers of immunolabelled cells between different

testes: Testes were segregated by primary so that all sections stained with a given primary were analysed together. The identity of the primary remained secret as was the identity of the testis except where severe degenerative changes unavoidably implied vasectomy. Complete sections of labelled testis were analysed one at a time at a magnification of 400 times using an Olympus CO11. The slide was placed in a standard manner on a calibrated stage and the overall dimensions of the section were measured. A grid was then prepared on a piece of A4 paper to represent each section by rounding to the nearest mm and marking each vertical and horizontal 1mm division. Each high power field of this grid which was completely filled with tissue was then examined and the number of cells were counted and recorded on the grid (Fig. 51). An eye piece grid (EPM 6) was employed to measure the area of staining and to assist in the counts by allowing for subdivision of the field. The area of the grid was determined using a Graduate S8 stage micrometer which divides 1mm into 100 divisions.

The high powered field measure 0.43mm in diameter and so would not overlap with its surrounding fields provided that reasonable care was taken at arriving at each grid reference. Initial observations in the pilot study had alerted us to the possibility of intratubular as well as interstitial labelling of cells further complicating the process. The recognition of areas of staining as cells would present a further problem because nuclear profiles were not readily identifiable in some cells because of obscurement by diaminobenzidine. Additionally, the number of cells per complete section was expected to be low for some of the primaries. It was therefore decided to count positively stained cell like areas greater than two divisions in maximum diameter on the eye piece grid as cells for the purposes of counts. Cells clearly inside vessels were excluded from the counts. Counts were expressed as the number of labelled cells divided by the number of high powered fields in an attempt to take account of variation in the size of the testes. Cells were described as either being interstitial or intratubular. The background haematoxylin staining did not allow for clear visualisation of the boundary zones and so cells could not be ascribed to this site. Only cells which were clearly surrounded by seminiferous epithelium with no sectional damage due to cutting were included as intratubular. Other cells were classed as interstitial.

It was originally intended to count the number of labelled cells within each section of testis and to compare them for side, vasectomy or sham and time post vasectomy. This proved not to be possible due to the very low numbers of labelled cells on sections with some of the primaries and the inability to reliably identify either the nuclei or the precise cell boundaries of individual cells in regions where focal accumulation with large numbers of labelled cells had occurred. This was further compounded by the change in overall size of the testis in degenerated testes following vasectomy.

RESULTS

Gross appearance: The gross appearance and mass of the testes used in this study can be seen in table 14.

Table 14. Gross appearance prior to immunohistochemistry.

SPECIMEN	TIME	ANIMAL	MASS(g)		APPEARANCE
			Left	Right	
SE7/94	3W	324	1.55	1.54	H
SE8/94	3W	306	1.62	1.49	H
SE9/94	3W	282	1.40	1.34	H
SE10/93	3M	387	1.58	1.60	H
SE11/93	3M	374	1.55	1.51	H
SE12/93	3M	364	1.53	1.47	H
SE7/93	6M	396	1.53	1.53	H
SE8/93	6M	366	1.42	1.42	H
SE9/93	6M	372	1.48	1.46	H
SE1/93	1Y	392	1.55	1.49	H
SE2/93	1Y	394	1.57	1.57	H
SE3/93	1Y	426	1.58	1.59	H
E19/93	3W	312	1.51	1.47	H
E20/93	3W	340	1.49	1.48	H
E21/93	3W	364	1.51	1.54	H
E13/93	3M	368	1.55	1.53	H
E14/93	3M	384	1.47	1.49	H
E16/93	3M	336	1.48	1.45	H
E4/93	6M	396	1.40	1.34	H
E5/93	6M	344	1.39	1.42	H
E6/93	6M	358	1.43	1.39	H
E22/93	1Y	337	1.38	1.33	H
E23/93	1Y	347	1.44	1.43	H
E27/93	1Y	310	1.35	1.31	H
E25/93	1Y	297	0.71	0.62	B
E33/93	1Y	320	1.08	1.59	I
E34/93	1Y	305	1.18	1.57	I

SE = Sham E = Vasectomized

H = Healthy I = Ipsilaterally Degenerated B = Bilaterally Degenerated

On gross examination, all of the testes from sham operated controls appeared healthy regardless of the interval following the procedure. They had a mass ranging between 1.32g and 1.62g. The testes from animals three weeks to nine months following vasectomy all appeared healthy having a mass ranging between 1.34g and 1.58g. The testes from animals twelve months following vasectomy could be divided into two groups, the first consisting of those that were grossly healthy having a mass between 1.31g and 1.59g. The second, degenerated group, had a mass between 0.62g and 1.18g appearing smaller and darker than the rest.

Immunohistochemistry

Immunohistochemistry of control spleen: Sections of spleen used in the pilot study and as controls within each labelling batch showed similar patterns of staining. OX19 labelling was found extensively throughout the periarteriolar lymphatic sheath (PALS) and also scattered thinly through the red pulp (Fig. 52). W3/25 was found in a similar distribution to OX19 but more labelling was found in red pulp areas (Fig. 53). OX 8 was scattered throughout the PALS with relatively few cells in the red pulp (Fig. 54). The labelling pattern of OX19, W3/25 and OX8 observed conformed to that found in other studies (186). OX33 was found to label cells in follicular areas largely sparing the PALS. Some scattered staining was observed in the red pulp (Fig. 55). This is consistent with the pattern of labelling for immunoglobulin which is found particularly although not exclusively on B lymphocytes as observed by others (186). OX18 labelled extensively throughout both the red and white pulp (Fig. 56). The labelling was clearly cellular although some cells were clearly more heavily stained than others (Fig. 57). OX6 labelling was found largely in the mantle of the white pulp and scattered in the red pulp (Fig. 58). This is compatible with the pattern of Ia expression in the spleen suggested by other authors (187). OX42 was found scattered throughout red and white pulp (Fig. 59).

Immunohistochemistry of sham operated control testes: The distribution of labelling for each primary antibody in testis sections at all time periods from both sides of the sham operated animals was noted. OX33 labelled cells were found sparsely in the interstitium of the sham operated testes (Fig. 60). No positively labelled cells were observed inside the seminiferous tubules. OX 19 labelled cells were found confined to the interstitial areas of testes from sham operated animals (Fig. 61). OX 8 Labelled cells were found only in the interstitial areas of testes from sham operated animals (Fig. 62). W3/25 labelled cells were found mostly in the interstitial areas of the testis (Fig. 63) although, one example of an intratubular labelled W3/25 cell was found in the left testis of a sham animal (Fig. 64). OX42 Labelled cells were found mostly in the interstitial areas of the testis (Fig. 65)

although, occasional intratubular labelled OX42 cells were found in the left testis of sham animals. OX6 Labelled cells were found mostly in the interstitial areas of the testis (Fig. 66) although, one example of an intratubular labelled OX6 cell was found in the right testis of a sham animal. OX18 intense labelling was largely confined to the interstitium (Fig. 47) although, some weak staining of spermatids (Fig. 48) was observed along with the occasional labelled intratubular cell (Fig. 67). Overall, no differences were observed between the sides or with time post sham operation. No focal collections of labelled cells were identified for any of the primary antibodies.

Immunohistochemistry of healthy testes following vasectomy: The distribution of labelling for each primary antibody in testis sections from healthy testes of both sides following vasectomy at all time periods was noted. OX33 labelled cells were found sparsely in the interstitium of the healthy testes following vasectomy (Fig. 68) and occasionally within the tubules themselves (Fig. 69). OX 19 labelled cells were found sparsely in both the interstitial and less commonly in intratubular areas of healthy testes following vasectomy (Fig. 70). OX 8 Labelled cells were found in the interstitial and less commonly in intratubular areas of healthy testes following vasectomy (Fig. 71). W3/25 Labelled cells were found in both the interstitial and infrequently in intratubular areas of the testis in healthy testes following vasectomy (Fig. 72). OX42 Labelled cells were found mostly in the interstitial areas of the testis although, occasional intratubular labelled OX42 cells were found in the tubules of healthy testes following vasectomy (Fig. 73). OX6 Labelled cells were found mostly in the interstitial areas of the testis (Fig. 74) with occasional examples within the seminiferous tubules. There were occasional focal accumulations of labelled cells in the interstitium in the grossly healthy testis of one of the two animals with ipsilateral degeneration of the testis (Fig. 75). OX18 intense labelling was largely confined to the interstitium (Fig. 76) although, some weak staining of spermatids was observed along with the occasional labelled intratubular cell. The appearances were similar to those observed in healthy testes from animals following sham procedure. Overall, no differences were observed between the sides or with time post sham operation.

Immunohistochemistry of degenerated testes from rats twelve months following vasectomy:

The distribution of labelling for each primary antibody in testis sections from degenerated testis of animals following vasectomy at all time periods were noted. OX33 labelled cells were found sparsely in the interstitium of degenerated testes following vasectomy (Fig. 77) and occasionally within the tubules themselves. OX 19 labelled cells were found sparsely in both the interstitial and in intratubular areas of degenerated testes following vasectomy (Fig. 78). OX 8 Labelled cells were found in both the interstitial and intratubular areas of degenerated testes following vasectomy (Fig. 79). W3/25 Labelled cells were found in both the interstitial and intratubular areas of degenerated testes following vasectomy (Fig. 80). OX42 Labelled cells were found in the interstitial and intratubular areas of degenerated testes following vasectomy (Fig. 81). OX6 Labelled cells were found mostly in the interstitial areas of the testis (Fig. 82) with occasional examples within the degenerated seminiferous tubules. OX18 labelled cells in severely degenerated tubules included intratubular and interstitial cells (Fig. 83). The intratubular cells appeared to be more frequent in degenerated tubules following vasectomy than in either sham operated controls or healthy testis following vasectomy. The staining of these cells was specific to degenerated tubules as can be seen in the rare cases where degenerated tubules are found close to more healthy ones (Fig. 49).

The testes from animals with degeneration 12 months following vasectomy exhibited areas of focal infiltration with immunoreactive cells. Few OX 33 cells were identified within them (Fig. 84). OX 42, OX8, OX6, OX18 and W3/25 labelled cells could be identified in these collections (Figs. 85, 86 and 87). They were present in the degenerated left testes of animals with both bilateral (Fig. 87) and ipsilateral (Fig. 88) degeneration of the testes twelve months following vasectomy. They were also found in the right testis of the animal exhibiting bilateral degeneration (Fig. 89). Many appeared to be centred on tubules (Fig. 85) while others appeared more interstitial in position (Fig. 88) or to be centred on blood vessels and (Fig. 89).

The pattern of MHC I expression in degenerated tubules following vasectomy as demonstrated with OX18 was markedly different from healthy ones following vasectomy or sham procedure. All intratubular cells were labelled in degenerated

tubules (Figs 49 and 83) as opposed to only late spermatids in healthy tubules (Figs 48, 67 and 76). The interstitial cells were labelled in all testes. The pattern of MHC II expression as demonstrated by OX 6 appeared no different in degenerated tubules following vasectomy from controls or healthy testes following vasectomy. There was possibly an increased number of labelled immunocompetent cells in degenerated tubules following vasectomy compared with healthy testes. To what extent this apparent increase was due to the reduced size of degenerated testes was unclear. There appeared to be many times more cells in the sections from degenerated tubules making simple shrinkage in volume of the testis an unlikely explanation. No differences were observed between the sides in the one animal with bilateral degeneration nor between testes from ipsilateral or bilateral degeneration.

DISCUSSION

This study confirms that there are sporadic immunocompetent cells in the interstitium of healthy rat testes following sham operation. In this study, cells staining with immuno-markers of B lymphocytes (OX 33), T-Helper (W3/25) and T-suppressor lymphocytes (OX 8), macrophages (OX 42) and class II MHC (OX 6) bearing cells have been demonstrated in the interstitial areas of healthy testes following sham operation. The presence of lymphocytes has been previously observed by others using light and electron microscopy in the testis of rats and Rhesus monkeys (145). They found only a few cells in the boundary zone itself and none beyond the myoepitheloid cell layer (145). We have, in addition, found a few labelled cells within the seminiferous epithelium of healthy rats following sham operation. These cells occurred at a very low incidence and only with certain primary antibodies. When observed, they were recorded in only in the absence of any adjacent tissue distortion which was found in some sections particularly near the edge of the specimen. It is therefore unlikely that such cells were an artefact created by the cutting mechanism and brought to their intratubular position by the motion of the knife. A single example of W3/25 and OX 6 labelled intratubular cell was identified. In the case of OX42, three labelled intratubular cells were identified. OX42 had been previously shown to react with only a small number of interstitial

cells in the normal testis (183). Our results suggest that there are a few T-helper, MHC II bearing cells and macrophages in the interstitium of the healthy testis and also within the seminiferous epithelium of the rat. This may reflect the increased ability of immunohistochemistry over conventional histology to identify small numbers of immunocompetent cells. T-lymphocytes and macrophages have been identified in the interstitial space surrounding the rete testes of healthy human testes by immunohistochemistry (180).

The healthy testes following vasectomy show a similar distribution of B cells, T-helper and T-suppressor cells, macrophages and class II MHC bearing cells in the interstitial areas as found in testes from the healthy sham operated rats. The differences being a suggestion of an increase in number which we were unable to quantify and the presence of occasional focal clusters of immunocompetent cells in the grossly healthy right testis of one of the two animals showing ipsilateral degeneration. A further study possibly using computer assisted counting would help to clarify any change in absolute numbers. The number of intratubular cells also appeared to be increased in healthy testes following vasectomy compared with testes of sham operated controls but again, further study is needed to clarify. Examples of intratubular cells were found to include B lymphocytes, T-helper and T-suppressor lymphocytes, macrophages and class II MHC bearing cells.

Degenerated tubules following vasectomy have a similar distribution of B cells, T-helper and T-suppressor cells, macrophages and class II MHC bearing cells in the interstitial areas. However, there appeared to be an increase in number of these cells in degenerated testes when compared with healthy testes following sham operation or vasectomy. This apparent increase may have been related to the reduction in size of the testis. Quantitation proved not possible due to difficulty in distinguishing individual cells and their nuclei which would benefit from further study. The distribution appeared to be the same in all four degenerated testes (two ipsilateral and a bilateral pair). The presence of focal accumulations of immunocompetent cells in sections from degenerated testes which were often centred on tubules themselves raises the possibility that the immune system plays some role in the degeneration. Our observations are similar to those of Experimental Allergic Orchitis (EAO) adult

Wistar rats in which 1.5-2 fold increase in the number of W3/25, OX8 and OX6 labelled cells eighty days following immunisation was demonstrated (179). No labelled cells were observed within the tubules by this group although they have documented a reduced CD4/CD8 antigen ratio in the lymph nodes of rats with severe EAO (188). This raises the possibility of a role for the cell mediated immune system in the degeneration following vasectomy.

The pattern of MHC I expression as assessed by OX 18 labelling within healthy seminiferous tubules of the rat was confined to extensive labelling throughout the interstitium with weak labelling of late spermatids which is consistent with the pattern in the human testis (189, 190, 191). MHC class II was largely confined to the interstitial areas of the testis and absent from the intratubular areas. The only exception to this was a single labelled cell which may represent a macrophage given the overall morphology. In degenerated tubules following vasectomy, there was a marked change in MHC I distribution compared with healthy tubules from controls or following vasectomy (Appendix 7). All of the remaining intratubular cells were labelled. As discussed earlier (page 48), these cells were thought to be Sertoli cells on morphological grounds and so it would appear that degenerated tubules contain Sertoli cells that express MHC I.

CONCLUSIONS

This study represents the latest in a series of works from the Laboratory of Human Anatomy at the University of Glasgow investigating the effects of vasectomy on the Albino Swiss rat (140) (Appendix 1). The model used involved unilateral (left sided) vasectomy which provided an internal control for the effects of operation in that, one side remains untouched. More importantly, it should allow for the separation of local from systemic factors in that, problems with the untouched right side can not be due to simple mechanical interference. A similar left sided sham procedure provided a further control to examine the effects of simple exposure of the vas on the testis. The right side of the sham procedure providing the ultimate control in that neither exposure nor possible systemic effects of vasectomy should be present.

The observation that bilateral degeneration of the testes occurred in some rats, six months or more, following unilateral vasectomy seemed very intriguing to us (139). It seemed possible to explain the ipsilateral degeneration of the testes following vasectomy as a consequence of raised intraluminal pressure (139) but not the bilateral degeneration. There was also no evidence to suggest that granulomas formed in the genital tract following unilateral vasectomy were able to interfere with testicular blood supply (139). One possible explanation for this bilateral degeneration was that it involved an autoimmune reaction to sperm antigens which, would normally be sequestered within the blood testis barrier but because of its breakdown on the vasectomized side, possibly due to pressure effects (139), were now exposed to the immune system. This would not, however, explain how some animals remained with unilateral degeneration unless, the activation of the immune system occurred late in the process. This work was aimed at looking for evidence of immune system activity in the long term following vasectomy.

The second chapter (page 32) examines our model of degeneration of the testes following vasectomy for ultrastructural changes and in particular, for evidence of activation of the immune system. This could take the form of the presence of immunocompetent cells in relation to degenerated tubules or the presence of thickened basal laminae due to the deposition of immunoglobulin, as occurs in the

rabbit with autoimmune orchitis (24). Others have associated the amount of IgG deposition in the basement membrane with the degree of severity of degeneration in the rat (192). We extended our previous work on the model to look at the ultrastructural level for subtle changes in grossly healthy testes following vasectomy and to further examine the changes in degenerated tubules. We were particularly interested in the boundary zone of the seminiferous tubule which includes the basal laminae of Sertoli and myoepithelial cells (143). Thickening of the former had already been reported in Lewis rats (129). Our previous work in the laboratory had focused on the germ cells (139) and so in this chapter we looked at the morphology of the Sertoli cells. Altered morphology of Sertoli cells had been associated with degeneration of the testis resulting from a variety of insults in a number of species (153). Hence changes in either of these components may have given us clues as to the underlying aetiology of the degeneration.

There appeared to be no observed morphological difference between the boundary zones or Sertoli cells from healthy tubules from either testis of sham operated controls and those testes that were grossly normal following vasectomy. This was even true of those right testes from animal with ipsilateral degeneration. In sharp contrast, degenerated testis following vasectomy contained seminiferous tubules with boundary zones and epithelium which differed greatly in appearance from those tubules found in healthy tubules following either sham operation or vasectomy (Appendix 2). There were no recognisable germ cells but a population of Sertoli cells with exaggerated features.

At the light microscopic level, the boundary zone of degenerated seminiferous tubules appeared thicker than their healthy compatriots. On high powered examination, Sertoli cell basal laminae appeared thicker with undulations towards the tubular lumen. On electron microscopy, it appeared that this thickening was more related to the excessive undulations. A similar appearance was found for the myoepithelial cell basal laminae while the cell bodies and nuclei often adopted a triangular profile (Appendices 4 and 5). We found no evidence of immune complex deposition in the boundary zones of any of the sections examined. We did find small numbers of leukocytes in the layers of the boundary zone in degenerated tubules.

These were often beyond the myoepithelial layer (Fig. 26) which was not seen in the healthy tubules following vasectomy or in sham operated controls. Attempts to count these cells (Chapter 2 page 45) suggested that they were more numerous, although the number of tubules assessed was small.

The seminiferous epithelium from degenerated tubules following vasectomy were markedly different from those of healthy testis following vasectomy or sham operated controls. No recognisable germ cells were identified. The epithelium appeared to consist of a population of cells with exaggerated features of Sertoli cells. Their nuclei contained deep intranuclear clefts with many clumps of peripheral heterochromatin. The nuclei were often placed more centrally within the tubule. The cytoplasm showed a sparsity of vacuoles. These features suggest a low turnover and relatively few organelles consistent with low cellular activity. Their numbers appeared increased compared with healthy tubules although, this may have been to reduction in the diameter and possibly length of the tubules. A number of studies have noted changes in Sertoli cell morphology in a variety of circumstances such as cryptorchidism (155, 193), oestrogen treatment (162) and Sertoli cell only syndrome (194). Many of the changes documented are non-specific and not unique for any particular condition and may reflect germ cell loss.

We directly compared degenerated tubules from rats following anti-androgen treatment (flutamide) *in utero* and those following vasectomy (Appendix 3). Both showed very similar changes in both the seminiferous epithelium and in the boundary zones. Additionally, following vasectomy, grossly degenerated testes had similar boundary zones regardless of whether they were from bilaterally or ipsilaterally degenerated animals. The only possible difference being that immunocompetent cells were, perhaps, more frequent in degenerated tubules following vasectomy. A variety of other insults including chemical poisoning (195, 196), experimental allergic orchitis (188) and vitamin deficiencies (175) are capable of producing degeneration of the testes in the rat. Some of these including doxorubicin treatment (197) and zinc toxicity (163) also produce changes in some parts of the boundary zone. Others, although not commenting on boundary zone changes, produce photographic evidence of it (198, 199). Many conditions which lead to disturbed spermatogenesis

in man also produce altered boundary zones (200) including post-pubertal pituitary failure (177) and following vasectomy (88, 90, 95). Given the similarity of the changes we have demonstrated following both bilateral and ipsilateral degeneration post vasectomy to those following maternal in *utero* flutamide administration and those reported in the literature for a variety of insults, it seems likely that these changes are non-specific. They may represent a common pathway following a variety of insults which lead to germ cell loss and shrinkage of the seminiferous tubules.

In the third chapter (page 51), the marked changes observed in Sertoli cells and basal laminae of degenerated tubules following vasectomy compared with healthy ones following vasectomy or after sham procedure lead us to look, in detail, at the structure and function of the blood-testis barrier. Disruption of this barrier has been linked to germ cell loss in chemical poisoning (168) and vitamin A deficiency (169) in rats. It is also thought to play a role along with chemical factors in the maintenance of tolerance to sperm antigens (167). Given the marked change in the seminiferous epithelium we had observed in degenerated tubules following vasectomy along with the occasional report of increased permeability to lanthanum following short term vasectomy (128), we were particularly interested to note if there was any difference in permeability of the blood-testes barrier following bilateral and ipsilateral degeneration.

Typical Sertoli-Sertoli tight junctions, as described in the literature (167), were readily identified in the basal portions of the seminiferous epithelium in healthy testes from sham operated controls, following vasectomy and in the contralateral testis from animals with ipsilateral atrophy nine to fifteen months following. They were also seen in testes with both ipsilateral and bilateral degeneration following vasectomy. These junctions also retained their ability to exclude lanthanum from the lumen even in degenerated tubules following vasectomy. No difference was observed between the junctions from testes with ipsilateral or bilateral degeneration. It would appear that the blood-testis barrier is intact in rats nine to fifteen months following vasectomy or sham procedure, even in degenerated tubules. This is broadly in agreement with the findings of others (166). The notable exception being the finding of increased permeability to lanthanum of degenerated testes from Lewis rats three

months following vasectomy (128). It is possible that the blood-testis barrier has a transient leaky phase around three months followed by a return to impermeability by nine months. Our findings suggest that disruption of the blood-testes barrier is not a feature of either ipsilateral or bilateral degeneration of the testis following vasectomy in the long term.

In the fourth chapter (page 60), we looked for an autoimmune aetiology to degeneration following unilateral vasectomy similar to that occurring in the rabbit (24) and guinea pig (97). We had previously found little direct evidence for this in the first three chapters with the possible exception of the presence of leukocytes in the boundary zone. This may reflect the almost complete nature of the degeneration of the testis at the time post insult at which they are examined. Alternatively, it may reflect the time required to initiate the immune response as in autoimmune orchitis, the active phase typically taking some time to develop (188). Others have found some evidence for the humoral immune response being involved in testicular damage in the linking of antibody titres with degree of testicular degeneration in the rat (133). In our model, ipsilateral degeneration of the testes following vasectomy may have a different aetiology to the bilateral, perhaps involving mechanical pressure phenomena (135) or the production of free radicals (201). We were, however, unable to detect any differences in morphology between degenerated tubules from the ipsilateral and bilateral group in this study.

The distribution of immunocompetent cells in healthy testis following vasectomy appeared to show no difference from those in healthy controls at the same interval following procedure. The only exception was in one section from the contralateral healthy testes from an animal with ipsilateral degeneration (Fig. 75). It is difficult to draw any firm conclusions from this single example and further study is required. There also appeared to be no difference with time following vasectomy in terms of distribution of immunocompetent cells in the interstitium. There is no clear evidence from this study to demonstrate immune cell involvement prior to degeneration.

Degeneration of the testis was not seen earlier than one year following the procedure in this part of the study, nor in sham operated controls. There was no observed

difference between bilateral and unilateral degeneration. The small number of animals with degeneration of the testes following vasectomy in this part of the study was small but is a reflection of the fact that we remain unable to predict which animals will undergo degeneration or whether it will be unilateral or bilateral. The distribution of labelled cells appeared similar to healthy testes following vasectomy or sham operation but there often appeared to be more numerous immunocompetent cells in and around degenerated tubules. We were unable to decide to what degree this was due to a reduction in overall size of the testis. The degenerated testis following vasectomy showed evidence of focal accumulations of immunocompetent cells often in and around atrophic tubules. We were unable to determine whether these accumulations preceded the degeneration or were a consequence of it. Further investigation of testes from vasectomized animals around the time that degeneration appears to occur (around six months post procedure) may help to resolve this. Our observations that degenerated tubules retained their ability to exclude lanthanum suggests that they were unlikely to have simply leaked antigen provoking an immune response. Given the presence of focal accumulations of immunocompetent cells around and within degenerated tubules there is clearly a role for the immune system in the process but it is possible that it follows rather than precedes the degeneration.

There was a marked change in MHC I expression in degenerated tubules compared with healthy tubules in that all intratubular cells were labelled (Appendix 7). These cells were morphologically identified as Sertoli cells implying that these cells expressed MHC I in degenerated tubules. There was no evidence of increased expression of MHC I prior to degeneration. This may be because this represents a sequelae rather than a cause of the degeneration. Sertoli cells are capable of phagocytosis (202) and may therefore be able to initiate an immune response although, experimental work in the mouse has found them not able to initiate certain T-cell responses (203). In our model, animals with high sperm counts and therefore antigen load may overwhelm the clearance mechanisms of the epididymis resulting in a cell mediated immune response as evidenced by the epididymal head granulomas. In high immune responders this may lead to removal of sperm precursors from the ipsilateral testis resulting in unilateral degeneration. Animals with a persisting immune response may develop bilateral degeneration.

Figure 1. Diagram illustrating the division of the testis in to 8 blocks for processing.

Figure 2. An example of part of an initial camera lucida drawing from a healthy left testis following vasectomy. Letters A, B, etc. are used to identify tubules included in the count. Numerical values in the selected tubule represent form factor, area in $1/360\text{mm squared}$ and perimeter in $1/360\text{ mm}$. I = rejected on die roll.

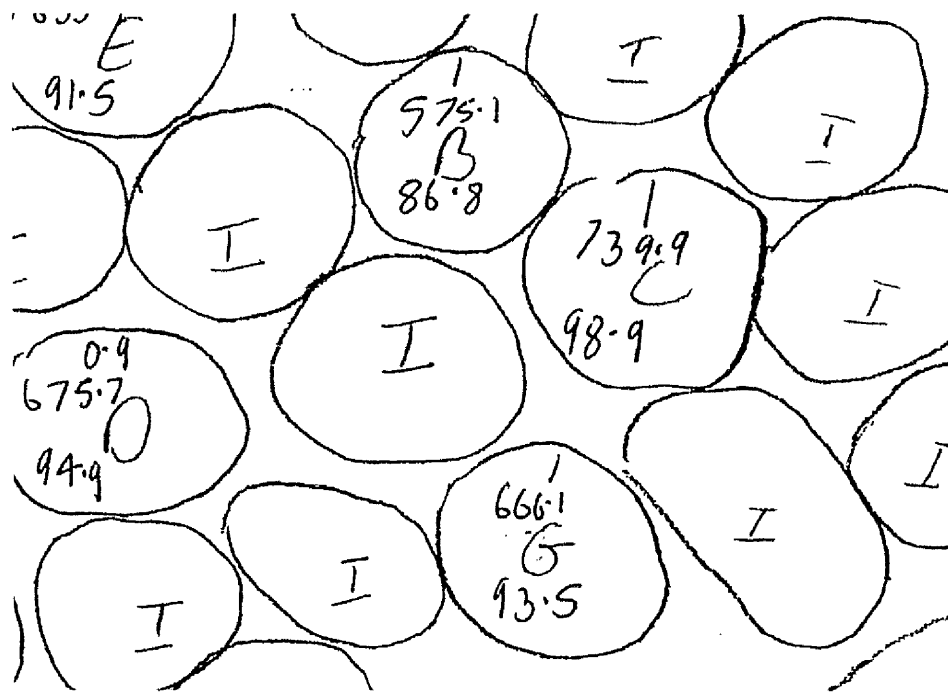
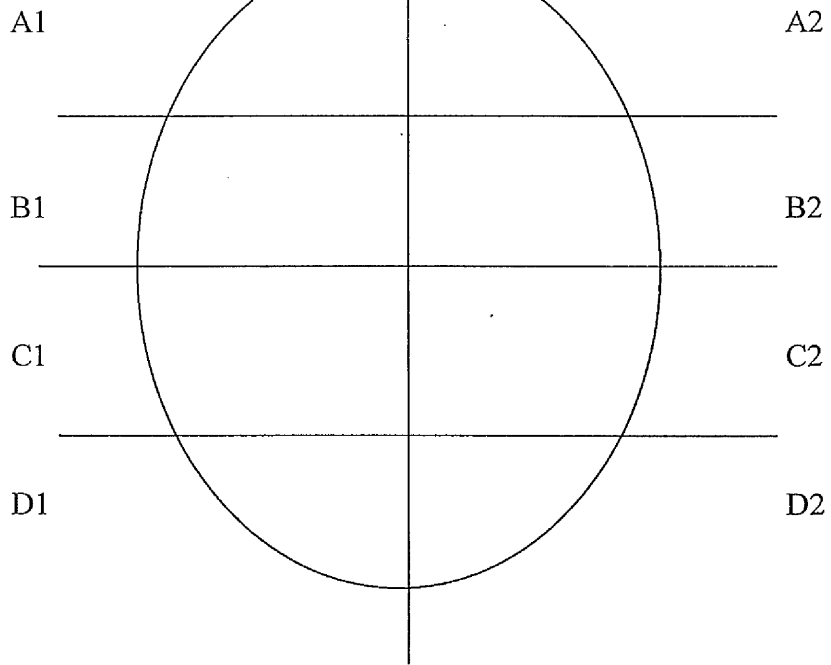


Figure 3. An example of a high powered camera lucida drawing of a section through a single seminiferous tubule from a healthy left testis following vasectomy identified as G on Fig. 2. The position of Sertoli cell nuclei and any leukocyte nuclei identified in the boundary zone are identified.

Figure 4. The typical appearance of a seminiferous tubule from a healthy left testis of a sham operated animal stained with toluidine blue (*400 linear magnification). Seminiferous tubules containing a variety of sperm precursors (S) can be seen to be separated by an interstitium containing Leydig cells, blood vessels (b) and lymphatic space (L).

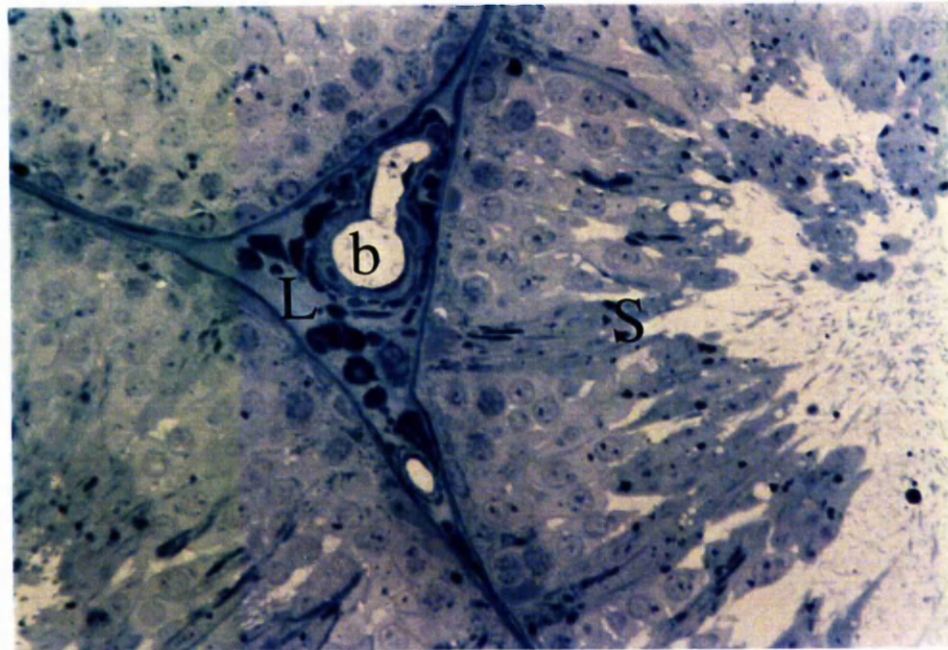
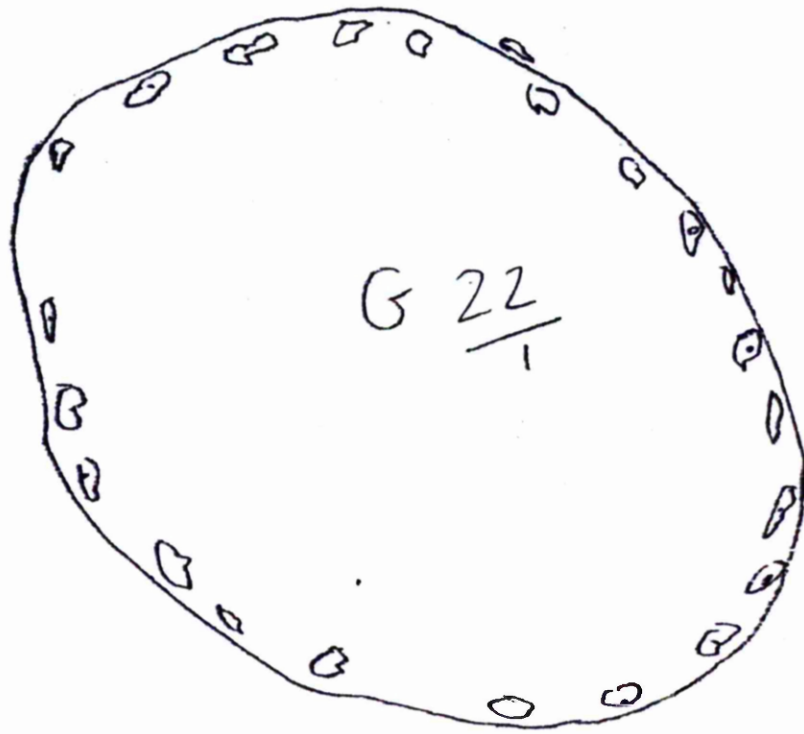


Figure 5. The typical appearance of a seminiferous tubule from a healthy right testis of a sham operated animal stained with toluidine blue (*800 linear magnification). The seminiferous tubule containing a variety of sperm precursors as well as Sertoli cells (S) with their large pale staining nuclei and prominent nucleolus which lie on a boundary zone consisting of two thin blue staining bands. The inner one corresponds to the myoepithelial cell layer (M) and the outer to lymphatic endothelium (L).

Figure 6. An example of the presence of a leukocyte (W) in the boundary zone of a tubule from a healthy right testis of a sham operated animal stained with toluidine blue (*800 linear magnification). Sertoli cell nuclei (S) can also be identified one of which is nearer the lumen. Pachytene primary spermatocytes (P) and type B spermatogonia can also be seen (B).

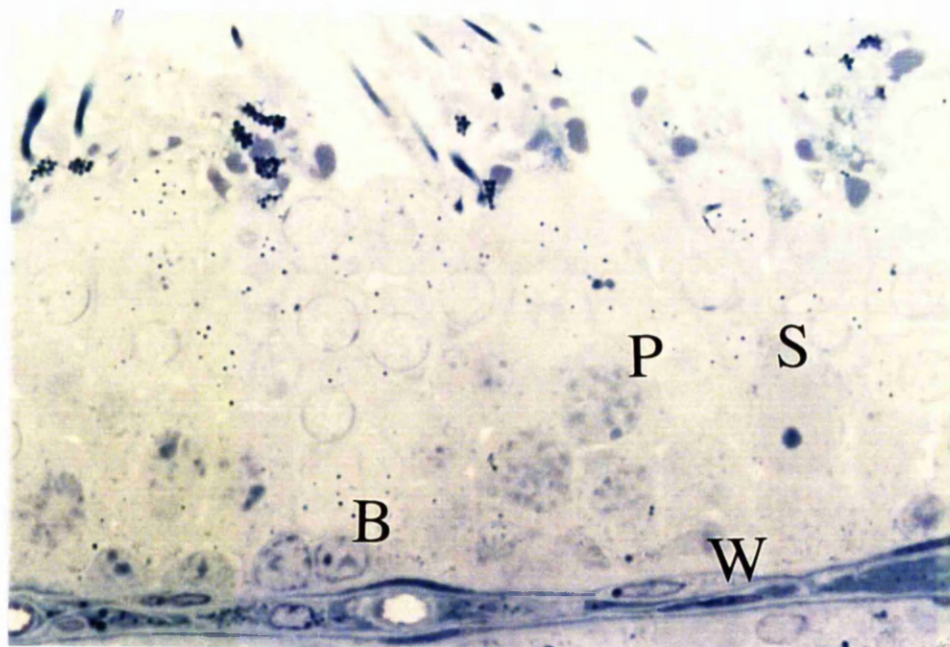
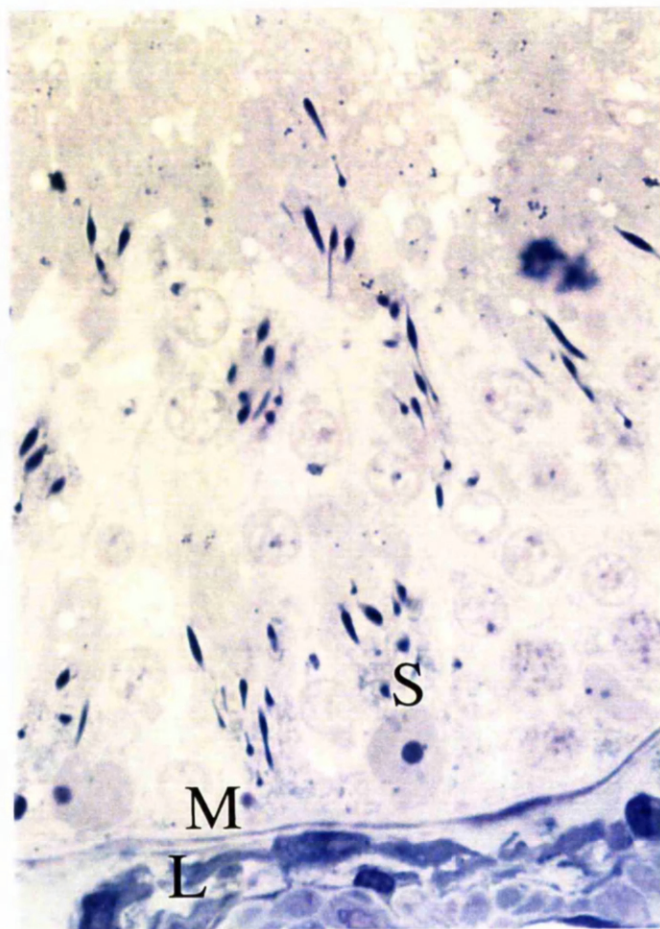


Figure 7. The typical appearance of a tubule from a healthy right testis of a sham operated animal stained with toluidine blue (*800 linear magnification). The Sertoli cell nuclei (S) identified by their large, pale, irregular nuclei, often with prominent nucleoli, are separated from the dark staining myoepithelial cells (M) by their pale staining basement membrane.

Figure 8. The typical appearance of a healthy tubule from a left testis following vasectomy stained with toluidine blue (*400 linear magnification). Sertoli cells (s) and a variety of sperm precursors (P) can be identified along with a typical boundary zone (b).

<

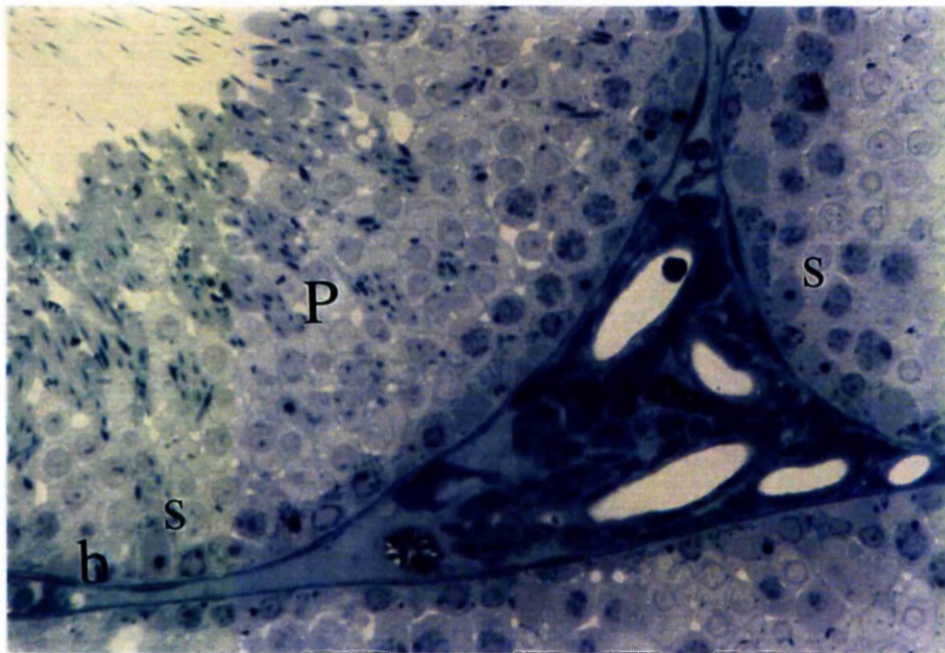
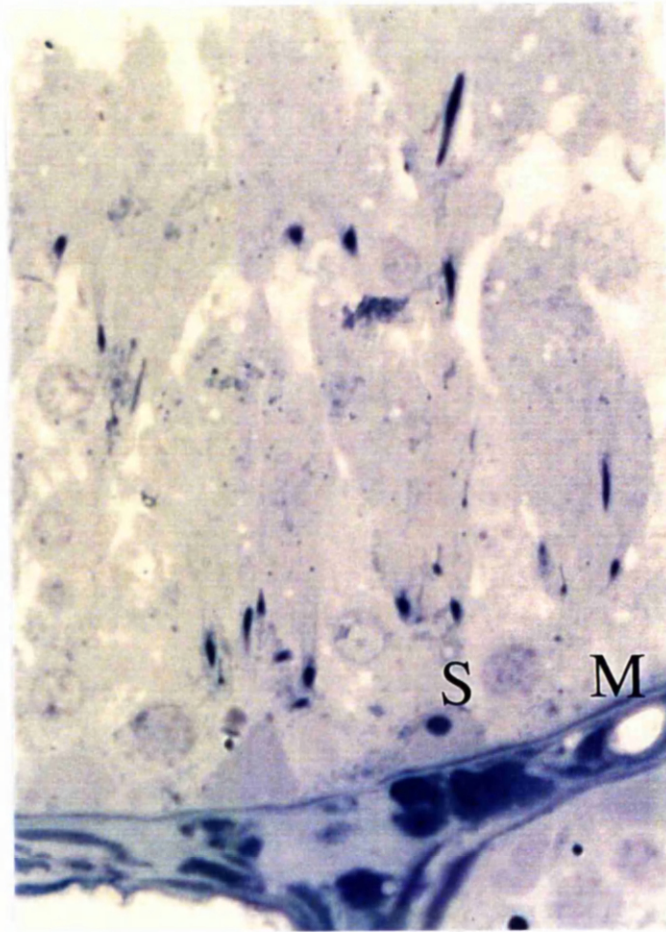


Figure 9. The typical appearance of a seminiferous tubule from a healthy right testis following vasectomy stained with toluidine blue (*400 linear magnification). The Sertoli cells (S) and a variety of sperm precursors can be identified along with a typical boundary zone consisting of two alternate dark and light blue bands. The former correspond to an inner myoepithelial (M) and outer endothelial layer (L). The latter representing basement membranes of Sertoli and myoepithelial cells.

Figure 10. The typical appearance of a healthy right testis from an animal with ipsilateral (left sided) degeneration following vasectomy stained with toluidine blue (*50 linear magnification). Several tubules (t) can be seen with minimal interstitial space occupied by blood vessels and lymphatic space (l).

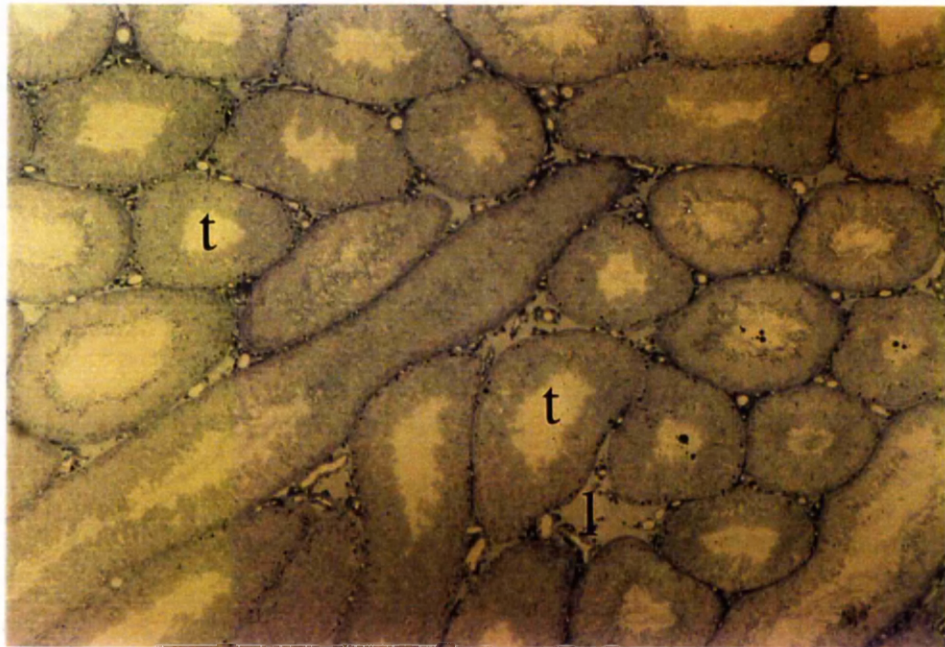
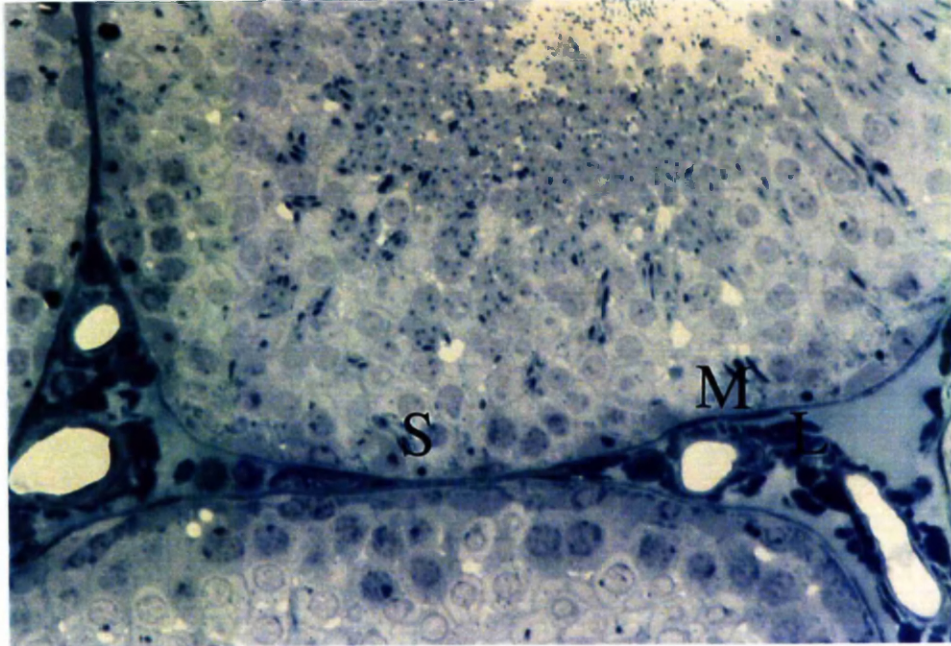


Figure 11. The typical appearance of a tubule in a healthy right testis from an animal with ipsilateral (left sided) degeneration following vasectomy stained with toluidine blue (*400 linear magnification). The Sertoli cells (S) and a variety of sperm precursors can be identified along with a typical boundary zone (B).

Figure 12. The typical appearance of an ipsilaterally degenerated left testis stained with toluidine blue (*50 linear magnification). The seminiferous tubules (t) have reduced in size with no apparent lumen and are separated by grossly enlarged lymphatic spaces (l) containing blood vessels (b).

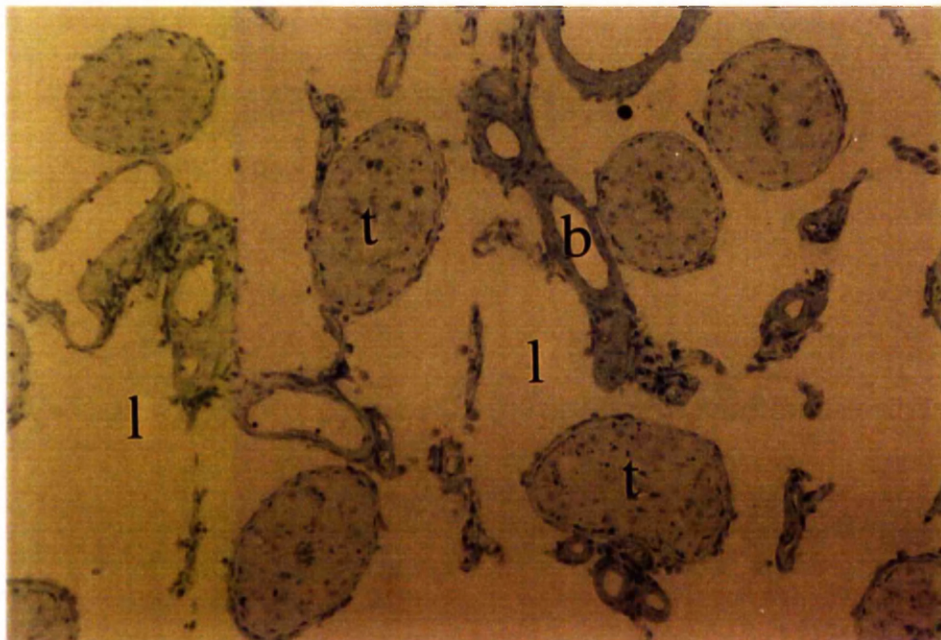
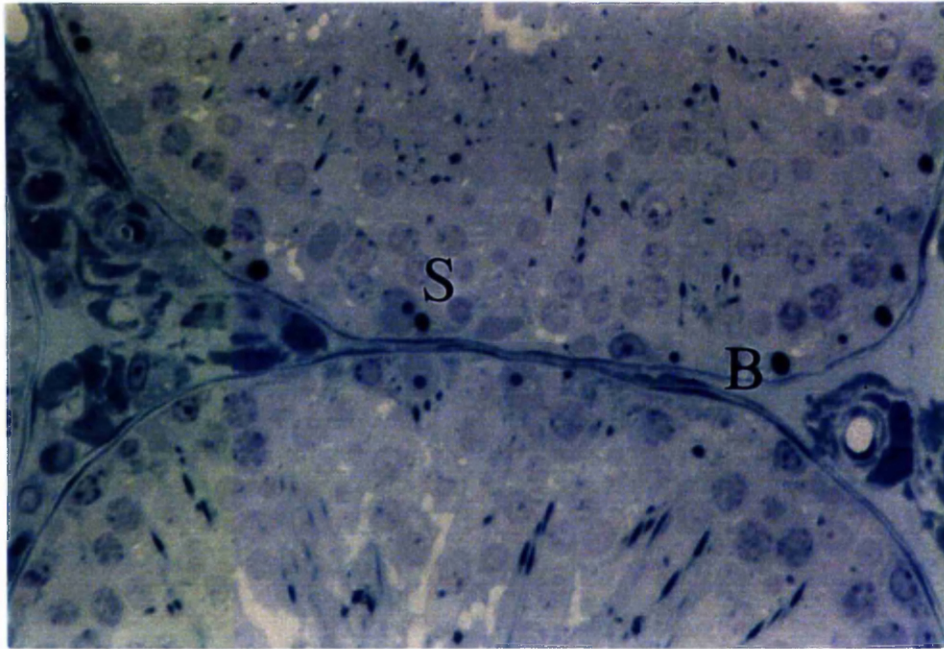


Figure 13. The typical appearance of a seminiferous tubule from a degenerated left testis of an animal with bilateral degeneration following vasectomy stained with toluidine blue (*400 linear magnification). Few sperm precursors remain although, there are several Sertoli cells identifiable by their characteristic nuclear morphology (n) which has become exaggerated. The boundary zone is thickened with some myoepithelioid (m) cells having a triangular profile. Leukocytes can be seen adherent to the outer lymphatic endothelium and in the boundary zone (w).

Figure 14. The typical appearance of a degenerated tubule from a right testis of an animal with bilateral degeneration following vasectomy stained with toluidine blue (*800 linear magnification). Few sperm precursors remain although, there are several Sertoli cells (s) identifiable by their characteristic nuclear morphology which has become exaggerated. The boundary zone is thickened (B) and a lymphocyte (w) can be seen adjacent to two triangular nuclei of myoepithelial cells. The cytoplasm of the lymphatic endothelium also appears almost triangular in profile (E).

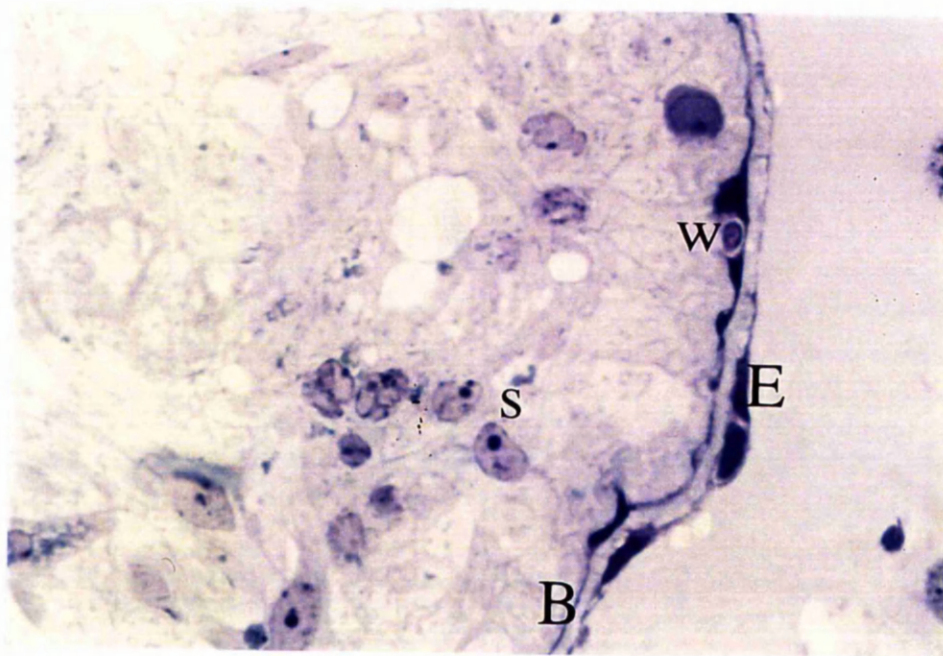
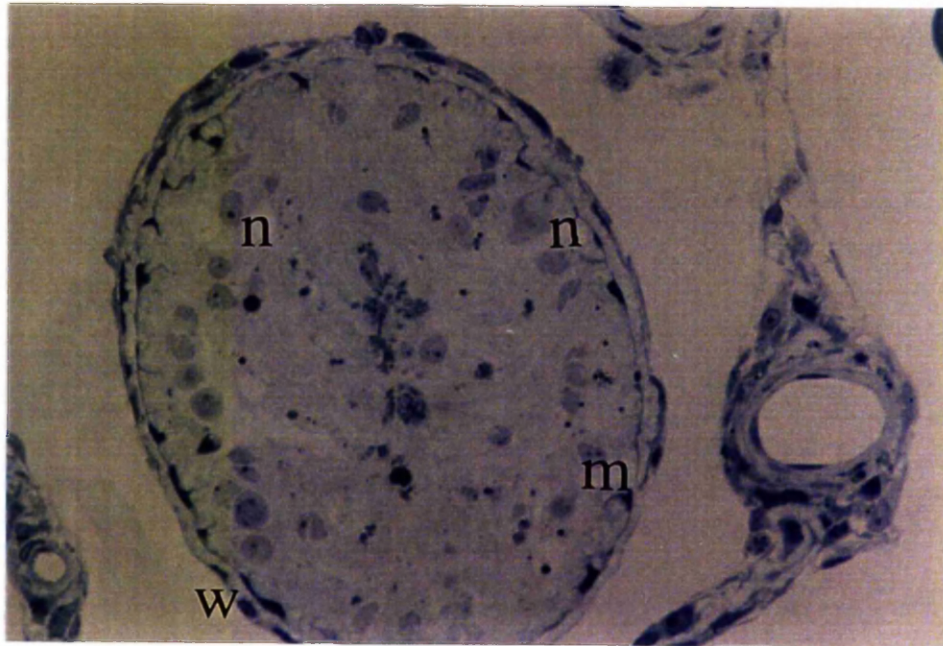


Figure 15. The typical appearance of a degenerated seminiferous tubule from a right testis of an animal with bilateral degeneration following vasectomy stained with toluidine blue (*1000 linear magnification). Sertoli cells exhibit exaggerated clefts (c) and appear close to the lumen. The boundary zone is thickened with some myoepithelioid (m) cells having triangular nuclei. A leukocyte (w) can be seen within the boundary zone adjacent to two myoepithelial cells with triangular nuclei.

Figure 16. An electron micrograph demonstrating the appearance of a grossly degenerated testis from a Swiss Albino rat following *in utero* maternal flutamide administration (*400 linear magnification). Note the enlarged lymphatic (L) spaces and seminiferous tubules (T) containing few sperm precursors.

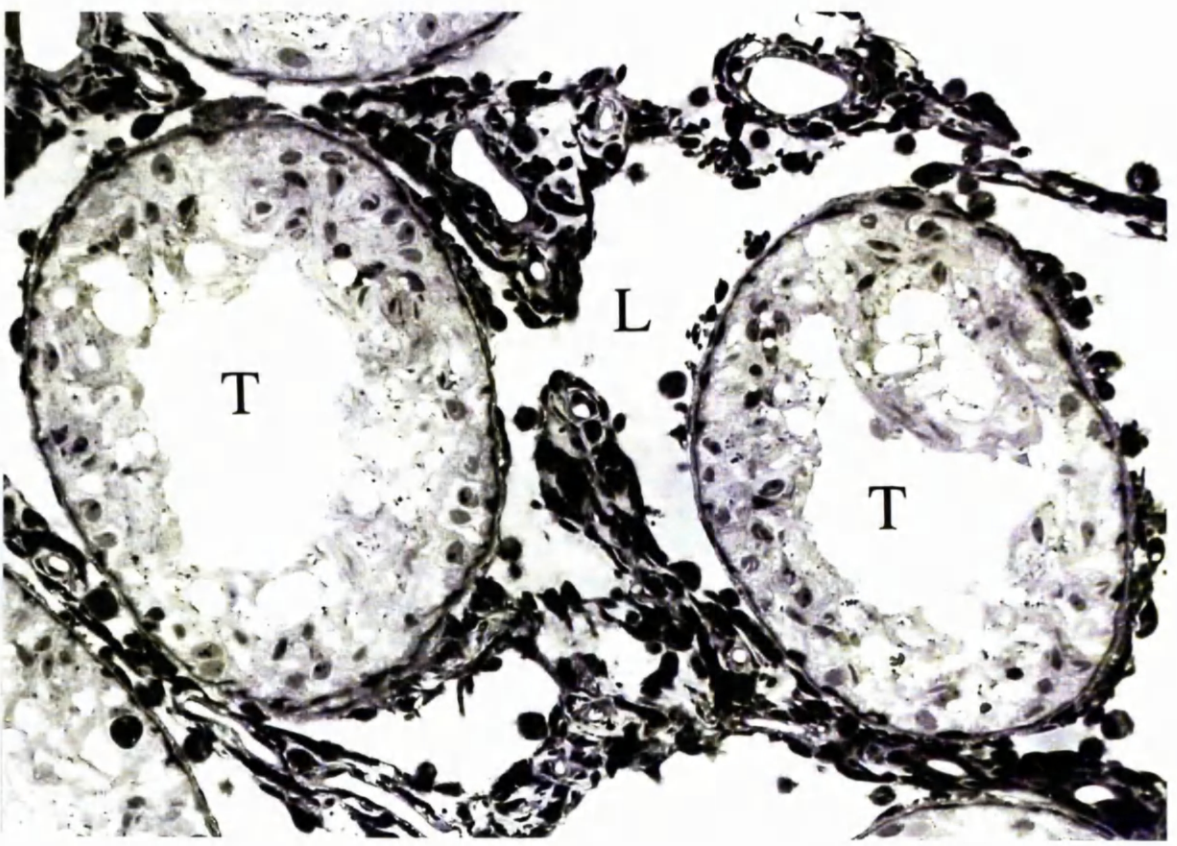
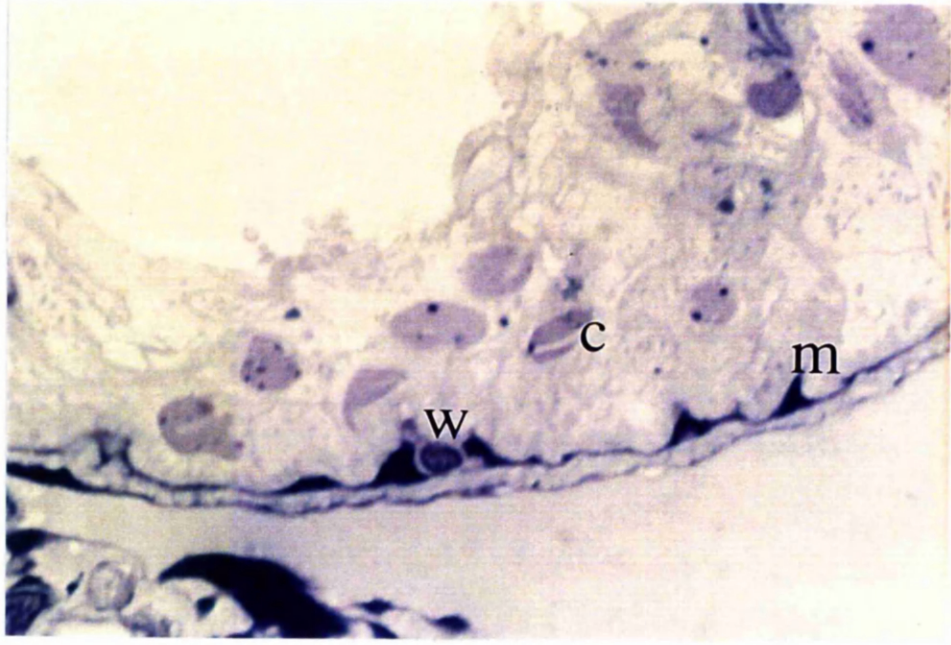


Figure 17. An electron micrograph (*27000 linear magnification) showing a Sertoli cell nucleus from a healthy sham operated left testis. Note the prominent nucleolus (N) and two folds (F) in the nucleolemma. The nucleus lies close to the boundary zone consisting of an inner moderately electron dense layer associated with fibres constituting the Sertoli cell basement membrane. A thin strand of electron dense cytoplasm of the myoepithelial (M) cell is surrounded by a moderately electron dense basement membrane. A thin strand of cytoplasm from the endothelial cell (E) adjacent to which there is a cell.

Figure 18. An electron micrograph (*7500 linear magnification) showing typical boundary zones lying between two adjacent seminiferous tubules from a healthy sham operated right testis. Each boundary zone consisting of an inner moderately electron dense layer associated with fibres constituting the Sertoli cell basement membrane (B). An elongated myoepithelial cell nucleus (N) is surrounded by a moderately electron dense basement membrane. A thin strand of cytoplasm (C) from the endothelial cell lines the lymphatic space.

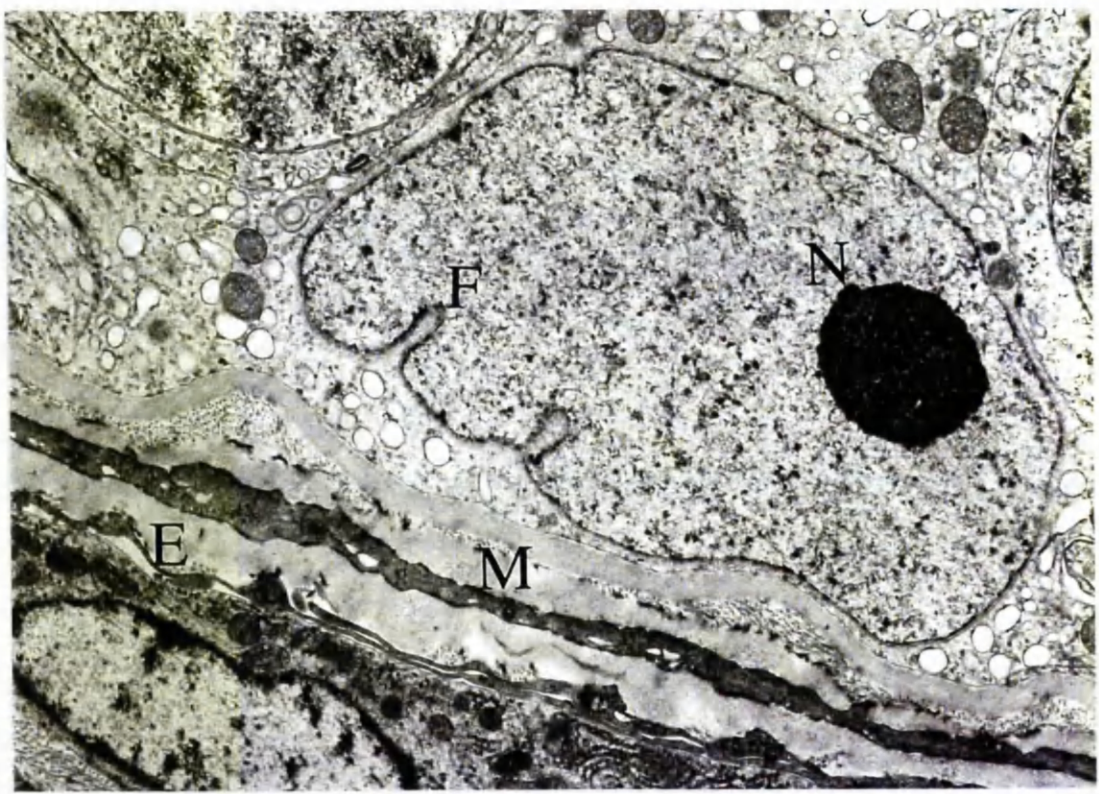


Figure 19. An electron micrograph (*7500 linear magnification) showing a Sertoli cell nucleus and two adjacent boundary zones from seminiferous tubules of a healthy right testis following vasectomy. The nucleus (s) lies close to the boundary zone consisting of an inner moderately electron dense layer associated with fibres constituting the Sertoli cell basement membrane. A thin strand of electron dense cytoplasm of the myoepithelial cell (m) is surrounded by a moderately electron dense basement membrane. A thin strand of cytoplasm from the endothelial cell with its elongated nucleus (l) lines a collapsed lymphatic space.

Figure 20. An electron micrograph (*9400 linear magnification) showing a typical Sertoli cell nucleus from a left testis following vasectomy. Note the prominent nucleolus (n) and intranuclear cleft (c). The nucleus lies close to a typical boundary zone consisting of an inner moderately electron dense layer constituting the Sertoli cell basement membrane. A thin strand of electron dense cytoplasm of the myoepithelial cell (m) is surrounded by a moderately electron dense basement membrane outside which lies the lymphatic endothelium.

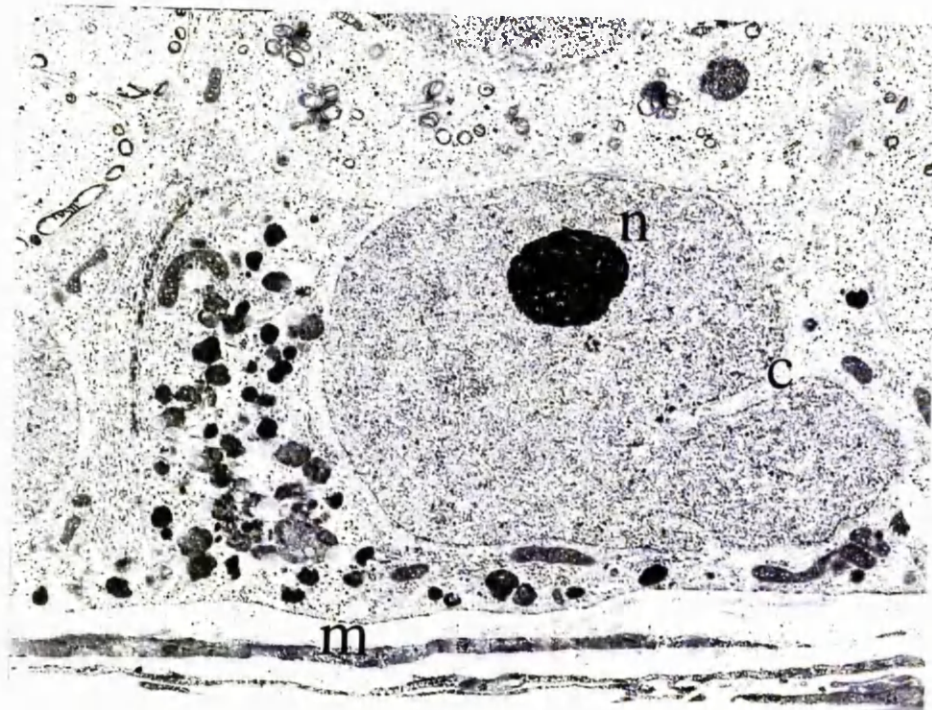


Figure 21. An electron micrograph (*48000 linear magnification) showing typical boundary zones lying between two adjacent seminiferous tubules from a healthy right testis of an animal with ipsilateral degeneration following vasectomy. Each boundary zone consisting of an inner moderately electron dense layer associated with fibres constituting the Sertoli cell basement membrane (s). An elongated strand of myoepithelial cell cytoplasm (m) is surrounded by a moderately electron dense basement membrane. A thin strand of cytoplasm from the endothelial cell (c) lines the lymphatic space (L).

Figure 22. An electron micrograph (*9400 linear magnification) showing the boundary zone of a seminiferous tubule from a left testis of an animal exhibiting bilateral degeneration following vasectomy. The inner moderately electron dense layer is folded and associated with clumps of fibres constituting the Sertoli cell basement membrane (black triangles). The myoepithelial cell and nucleus (open arrowhead) is now triangular in profile surrounded by a folded moderately electron dense basement membrane. Similarly, the endothelial cell and nucleus is triangular with a podocyte (closed arrowhead) of a leukocyte adherent to the outer wall.

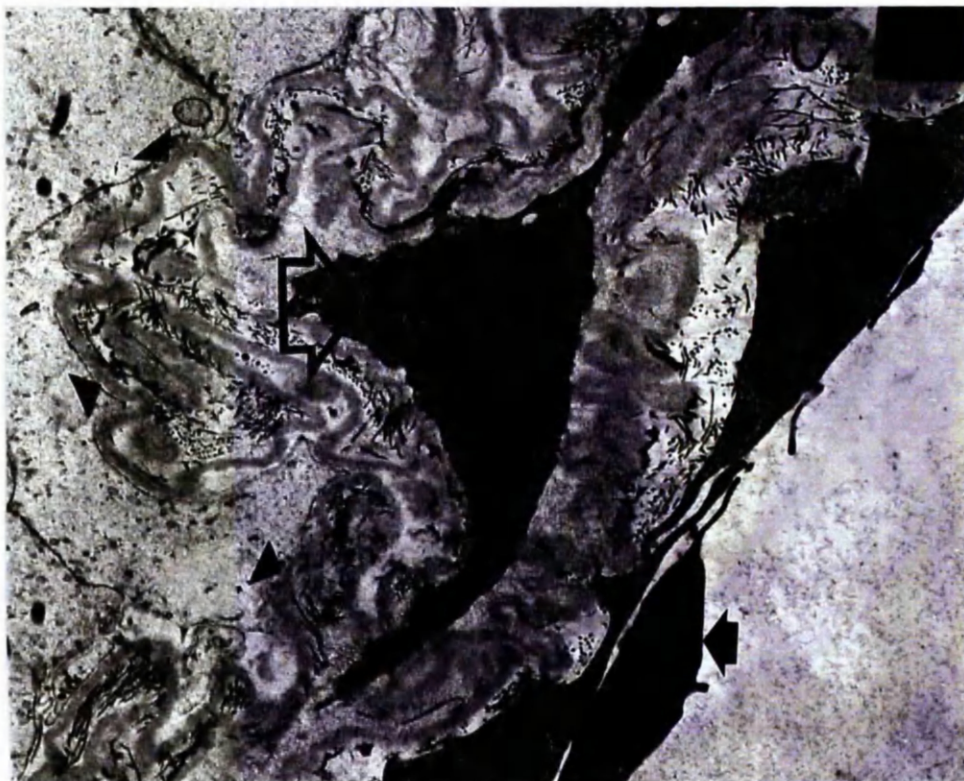
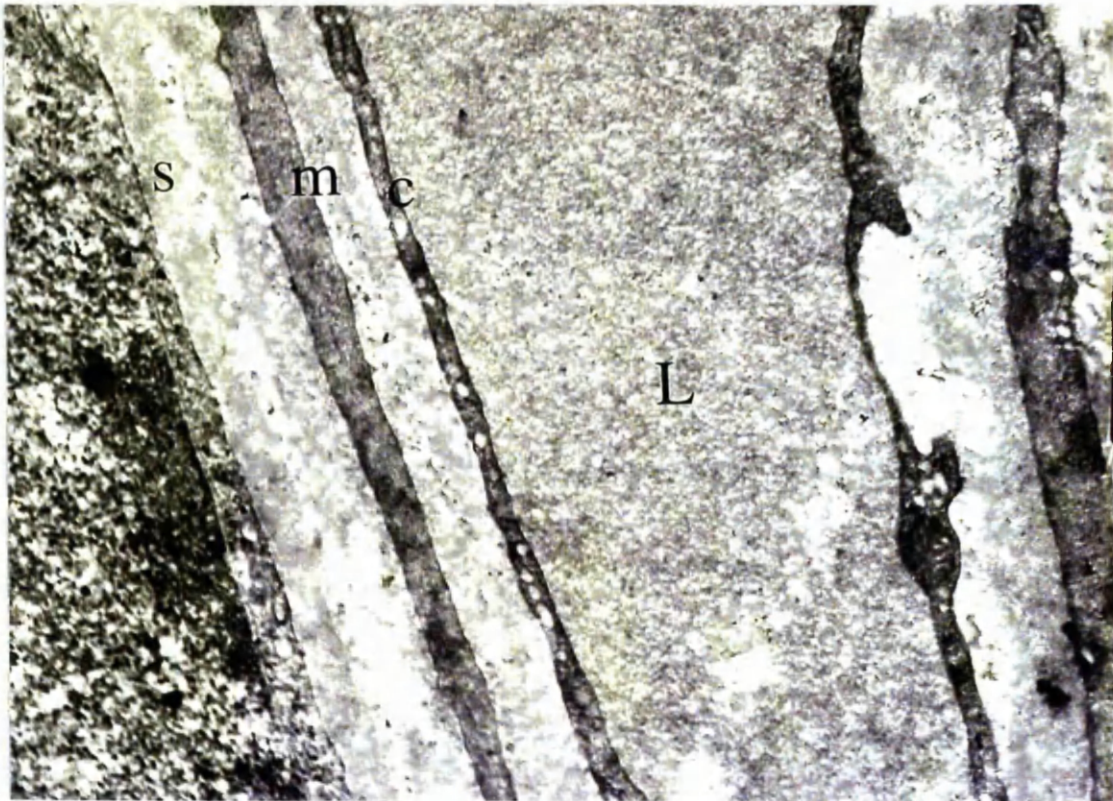


Figure 23. An electron micrograph (*14000 linear magnification) showing the typical boundary zone of a seminiferous tubule from a right testis of an animal with bilateral degeneration following vasectomy. The boundary zone consists of a folded inner moderately electron dense layer associated with clumps of fibres constituting the Sertoli cell basement membrane (black triangle). An elongated strand of myoepithelial cell cytoplasm (m) is surrounded by a moderately electron dense convoluted basement membrane. A thin strand of cytoplasm from the endothelial cell lines the lymphatic space along which podocytes of leukocytes (P) could be identified. Part of a Sertoli cell nucleus is visible with deep intranuclear clefts (C) and peripheral clumps of heterochromatin.

Figure 24. An electron micrograph (*12000 linear magnification) showing typical boundary zones of two adjacent seminiferous tubules from a left testis of an animal with ipsilateral degeneration following vasectomy. Each boundary zone consists of a folded inner moderately electron dense layer associated with clumps of fibres constituting the Sertoli cell basement membrane (black triangle). Several myoepithelial cells and nuclei can be seen to be triangular in section (T) and surrounded by a moderately electron dense convoluted basement membrane with fine cytoplasmic strands (open arrowhead). A thin strand of cytoplasm from the endothelial cells (black arrowhead) line the lymphatic space along which podocytes of leukocytes can be identified.

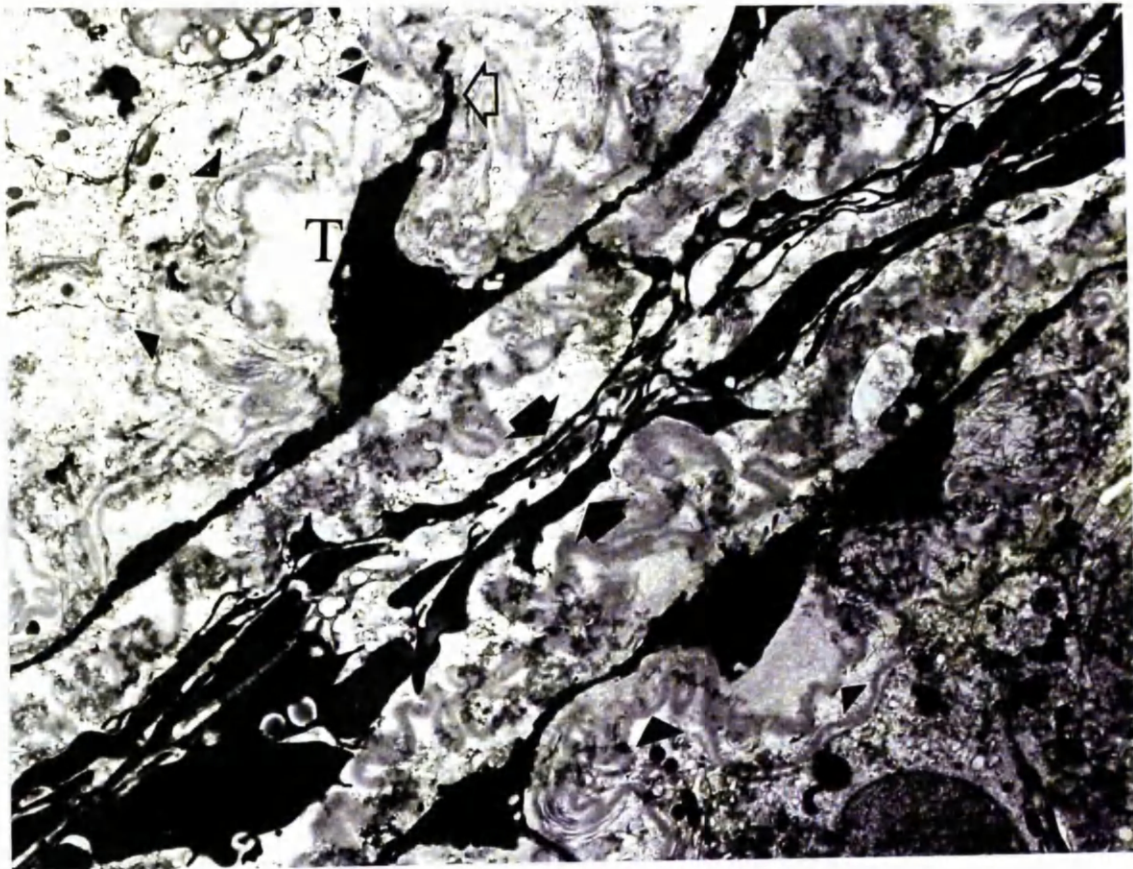
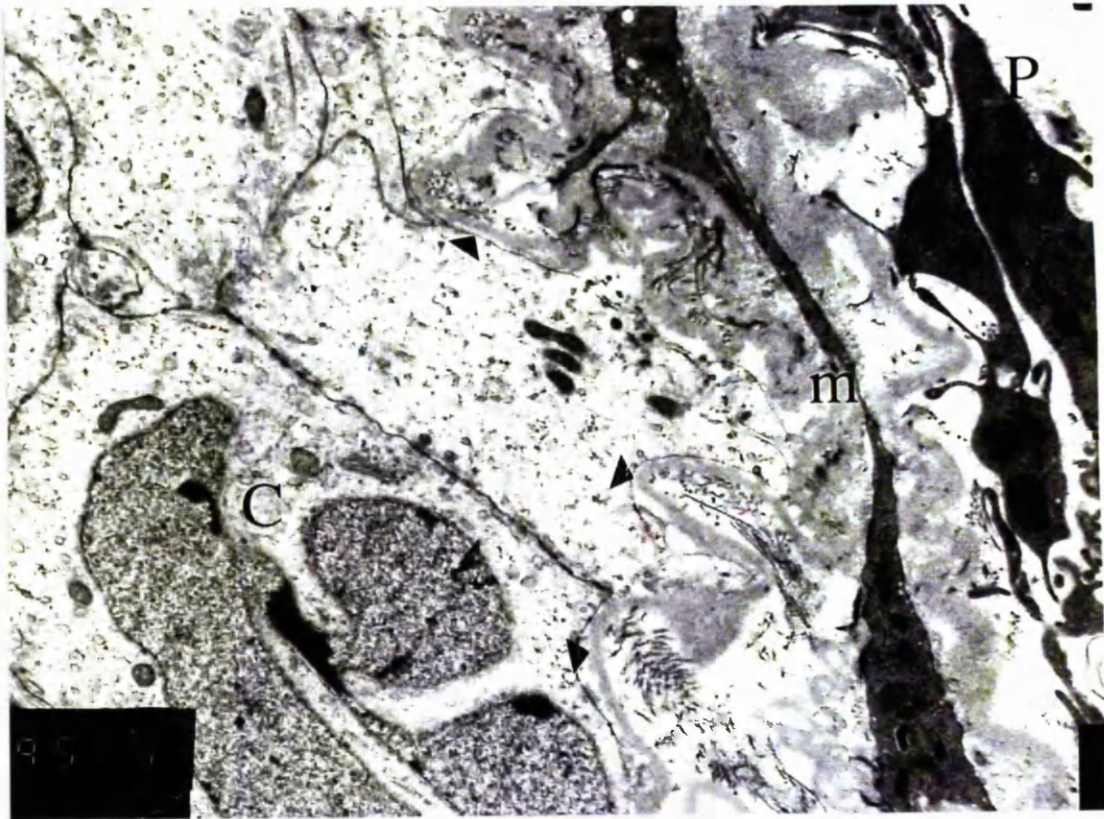


Figure 25. An electron micrograph (*5000 linear magnification) showing the boundary zone of a seminiferous tubule from a left testis from an animal exhibiting bilateral degeneration following vasectomy. The inner moderately electron dense layer is folded appearing to have a double layer constituting the Sertoli cell basement membrane (black triangle). Adjacent to the myoepithelial cell cytoplasm is a small lymphocyte (W) with its large nucleus. A Sertoli cell nucleus is visible with deep intranuclear clefts (C) and peripheral clumps of heterochromatin.

Figure 26. An electron micrograph (*17000 linear magnification) showing a small lymphocyte (W) in the boundary zone of a seminiferous tubule from a right testis of an animal with bilateral degeneration of the testis following vasectomy. The cell lies adjacent to a myoepithelial cell which has a triangular profile (T).



Figure 27. An electron micrograph (*27000 linear magnification) showing a small lymphocyte (W) in the boundary zone of a seminiferous tubule from a left testis of an animal with ipsilateral degeneration of the testis following vasectomy. The cell lies adjacent to a myoepithelial cell which has a triangular profile (T). The Sertoli cell basement membrane (A) can be seen to be extensively folded.

Figure 28. An electron micrograph (*9800 linear magnification) showing the seminiferous epithelium from a left testis of an animal exhibiting bilateral degeneration following vasectomy. The nuclei of several Sertoli cells (S) lie towards the centre of the lumen (E) and exhibit deep intranuclear clefts and peripheral clumps of heterochromatin. No sperm precursors can be identified. The boundary zone shows undulations.

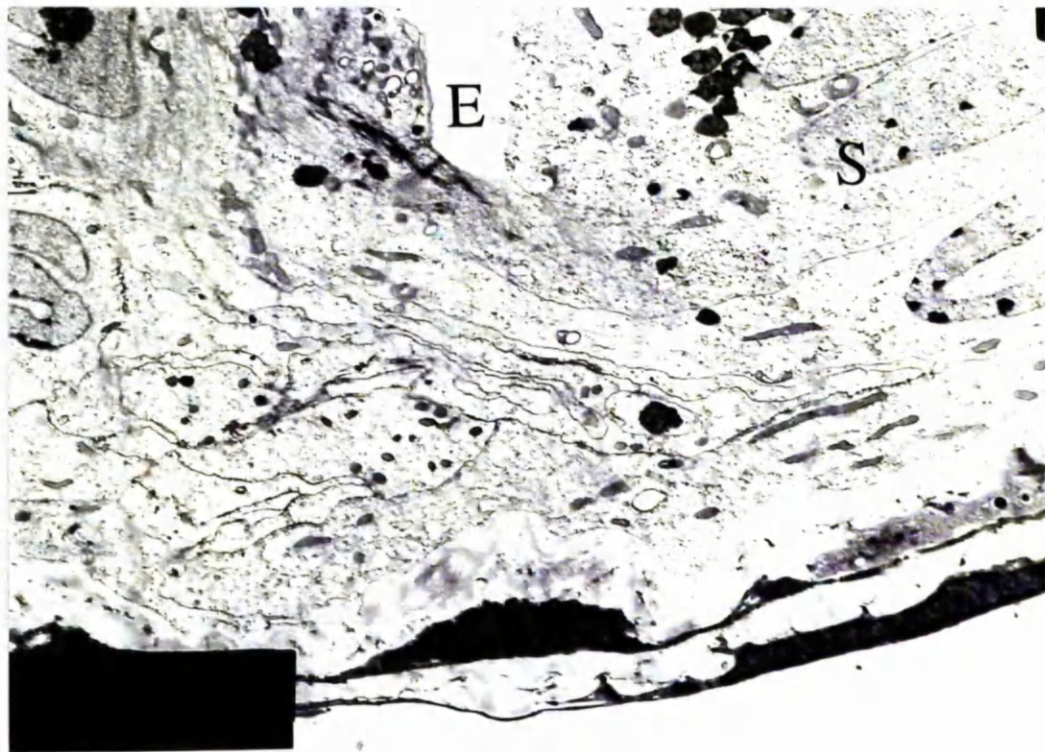
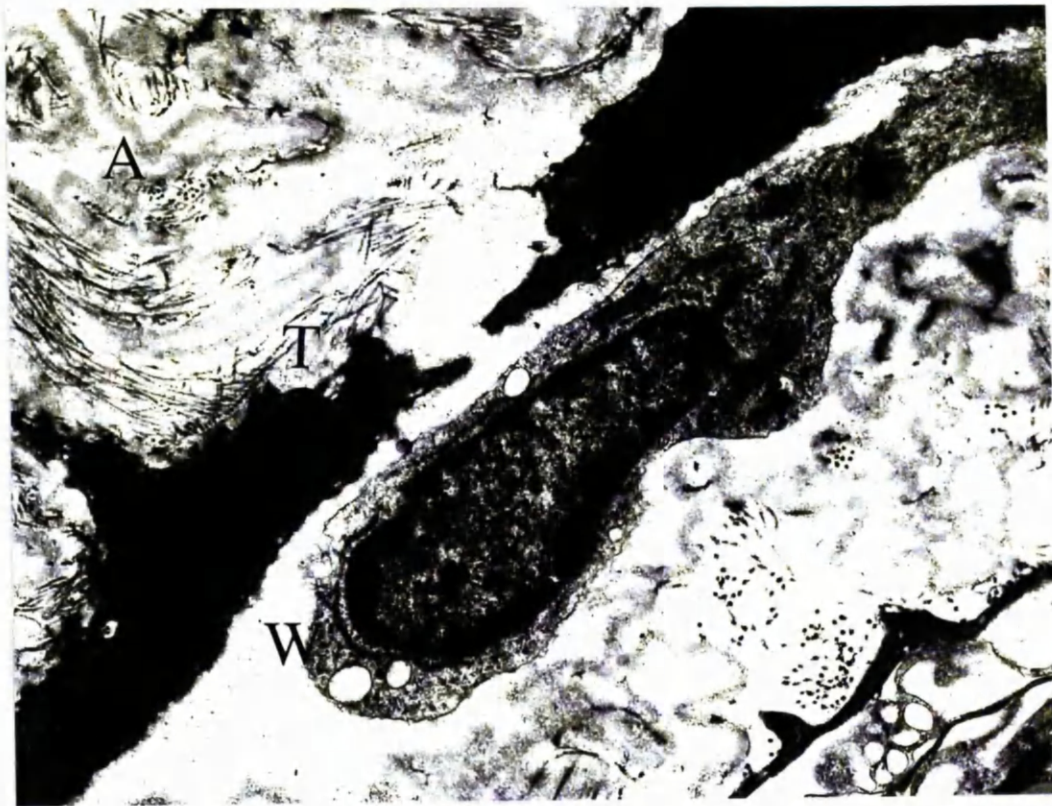


Figure 29. An electron micrograph (*21000 linear magnification) showing the typical appearance of the boundary zone from seminiferous tubules from a degenerated right testis of an animal exposed to flutamide in *utero*. The boundary zone consists of a folded inner moderately electron dense layer associated with clumps of fibres constituting the Sertoli cell basement membrane (black triangles). A myoepithelial cell and nucleus can be seen to be triangular in section (T) surrounded by moderately electron dense convoluted basement membrane. A thin strand of cytoplasm (C) from the endothelial cells line the lymphatic space along which podocytes of leukocytes can be identified. Part of a Sertoli cell nucleus (S) is visible with deep intranuclear clefts and peripheral clumps of heterochromatin.

Figure 30. An electron micrograph (*53000 linear magnification) showing a Sertoli-Sertoli cell junctional complex from a healthy sham operated left testis. The tight junction component consists of areas of apparent membrane fusion (open arrowhead) with adjacent electron dense deposits. Dilated sacs of endoplasmic reticulum (black arrowhead) are seen adjacent to these junctions.

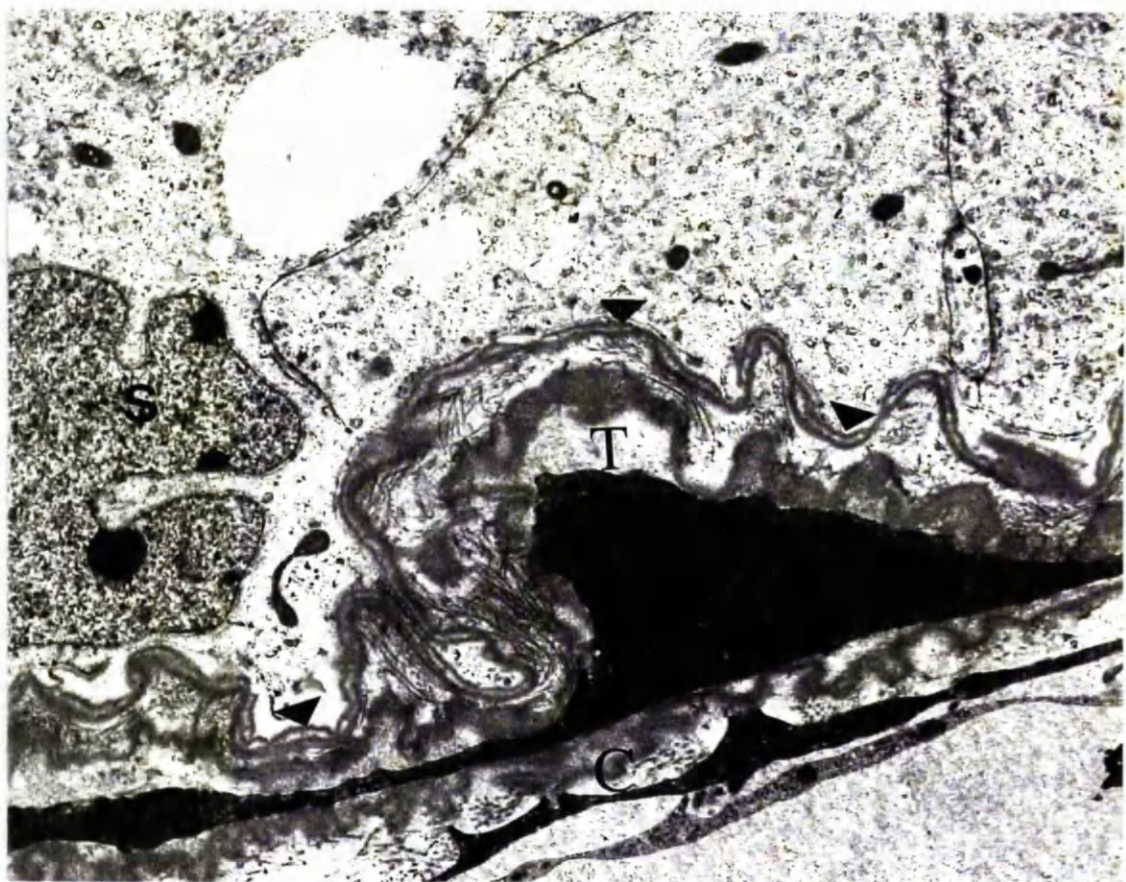


Figure 31. An electron micrograph (*53000 linear magnification) showing a typical healthy Sertoli-Sertoli cell junctional complex from a healthy sham operated right testis. The junction complex consists of areas of apparent membrane fusion (open arrowhead) with adjacent electron dense deposits. Dilated sacs of endoplasmic reticulum (black arrowhead) are seen adjacent to these junctions.

Figure 32. An electron micrograph (*46000 linear magnification) showing a Sertoli-Sertoli cell junctional complex from a healthy left testis following vasectomy. The junctional complex consists of areas of apparent membrane fusion (open arrowhead) with adjacent electron dense deposits. Sacs of endoplasmic reticulum (black arrowhead) are seen adjacent to these junctions.

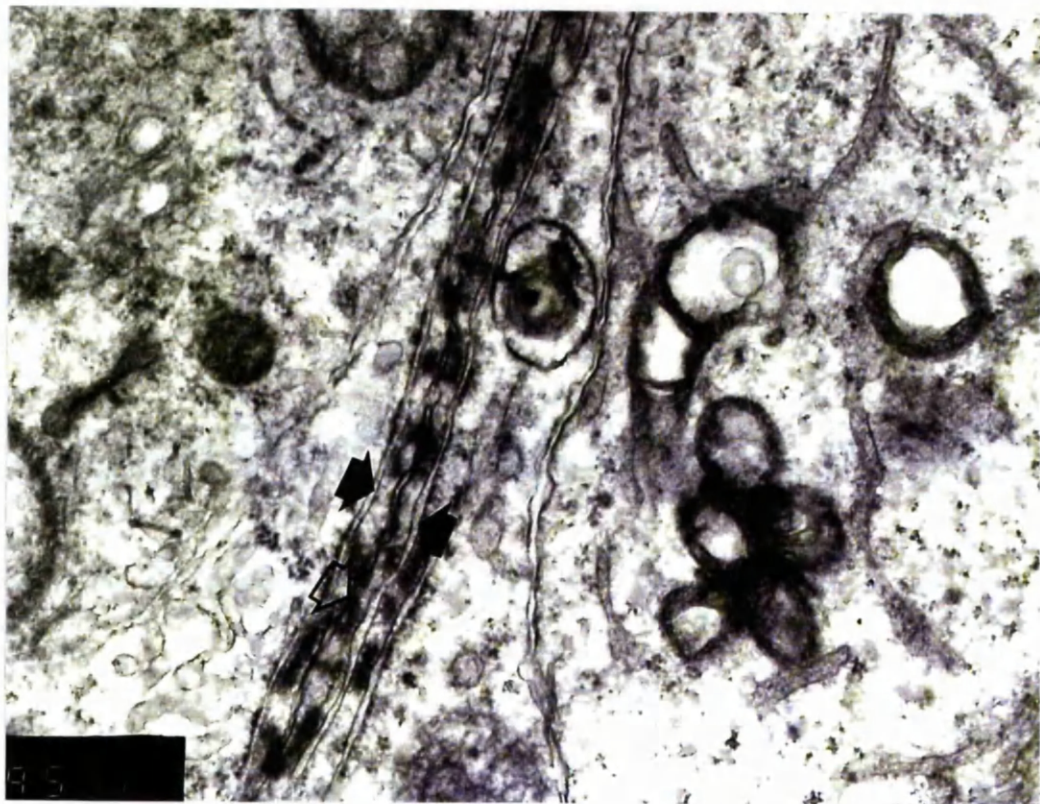


Figure 33. An electron micrograph (*71000 linear magnification) showing a typical Sertoli-Sertoli cell junctional complex from a healthy right testis following vasectomy. The junctional complex consists of areas of apparent membrane fusion (open arrowhead) with adjacent electron dense deposits. Sacs of endoplasmic reticulum (black arrowheads) are seen adjacent to these junctions.

Figure 34. An electron micrograph (*53000 linear magnification) showing a Sertoli-Sertoli cell junctional complex the healthy right testis of a rat exhibiting ipsilateral degeneration following vasectomy. The junctional complex consists of areas of apparent membrane fusion (open arrowhead) with adjacent electron dense deposits. Sacs of endoplasmic reticulum (black arrowhead) are seen adjacent to these junctions

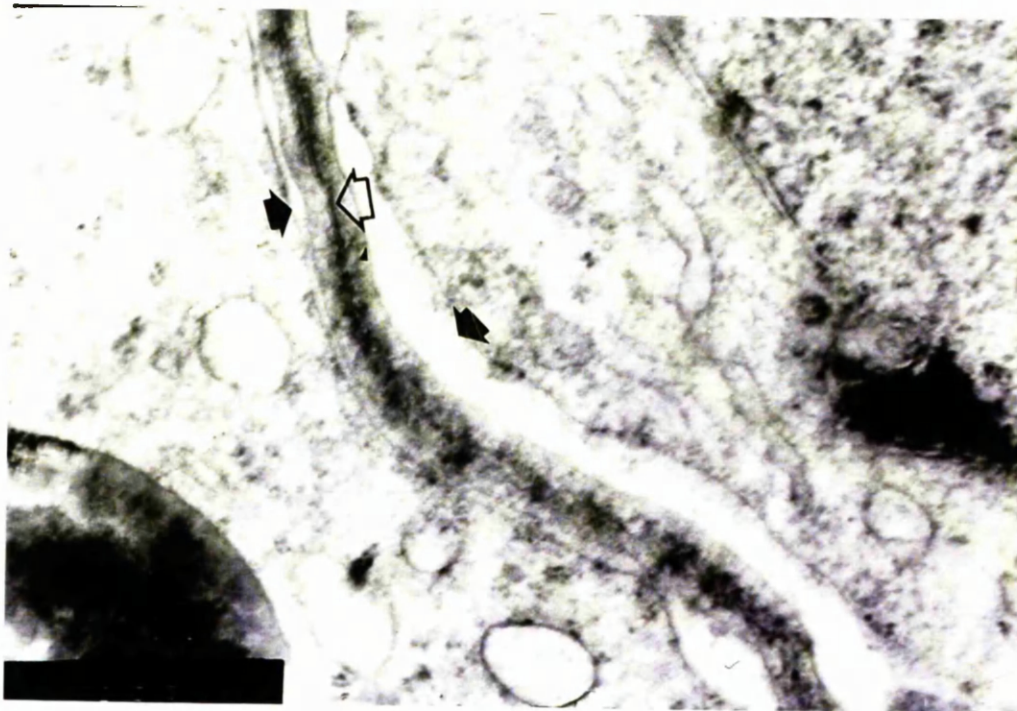
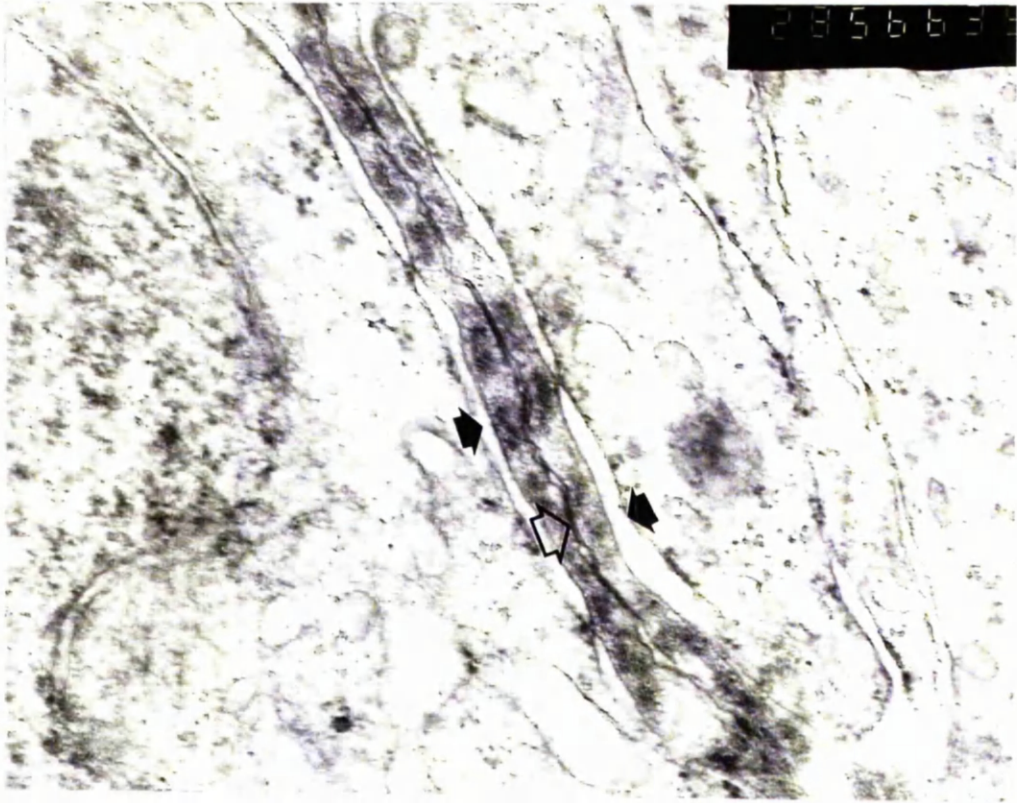


Figure 35. An electron micrograph (*53000 linear magnification) showing a Sertoli-Sertoli cell junctional complex from an degenerated left testis of a rat exhibiting ipsilateral degeneration following vasectomy. The junctional complex consists of areas of apparent membrane fusion (open arrowhead) with adjacent electron dense deposits. Sacs of endoplasmic reticulum (black arrowhead) are seen adjacent to these junctions.

Figure 36. An electron micrograph (*46000 linear magnification) showing a typical Sertoli-Sertoli cell junctional complex from an degenerated left testis of a rat exhibiting bilateral degeneration following vasectomy. The junctional complex consists of areas of apparent membrane fusion (open arrowhead) with adjacent electron dense deposits. Sacs of endoplasmic reticulum (black arrowhead) are seen adjacent to these junctions. The Sertoli cell basement membrane (B) can also be seen with adjacent fibrils.

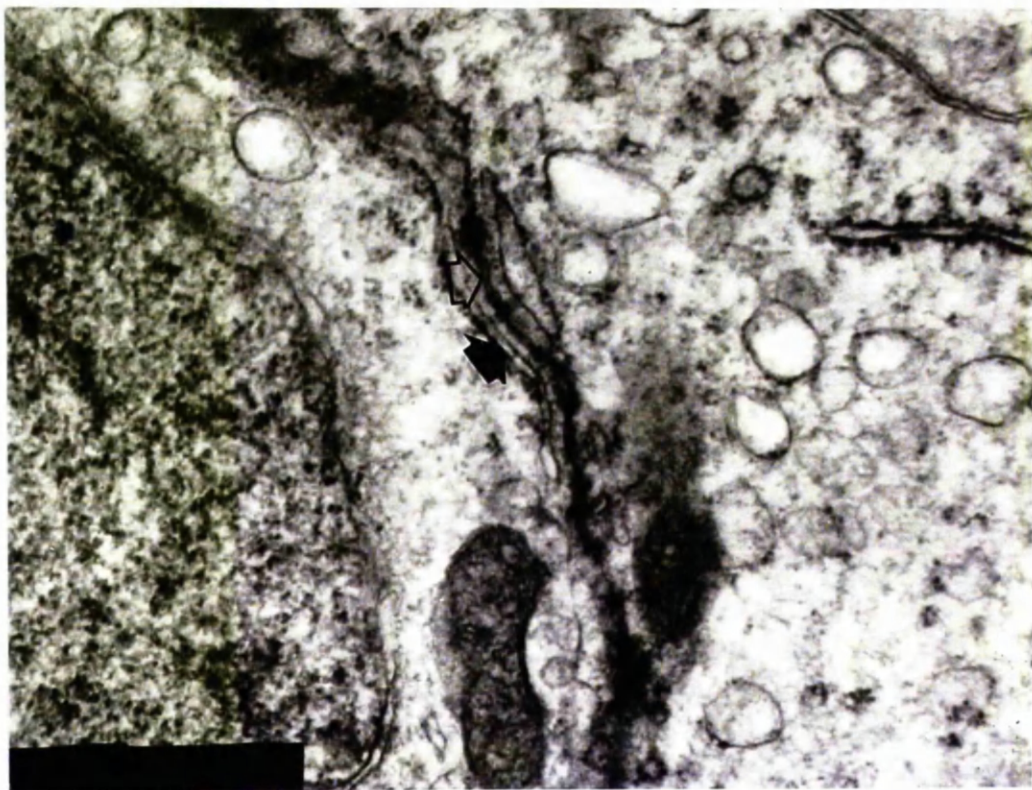


Figure 37. An electron micrograph (*46000 linear magnification) showing a Sertoli-Sertoli cell junctional complex from an degenerated right testis of a rat exhibiting bilateral degeneration following vasectomy. The junctional complex consists of areas of apparent membrane fusion (open arrowhead) with adjacent electron dense deposits. Dilated sacs of endoplasmic reticulum (black arrowheads) are seen adjacent to these junctions. A mitochondrion (D) can be seen within the Sertoli cell cytoplasm.

Figure 38. An electron micrograph (*14000 linear magnification) showing lanthanum confined to the outer compartment of the seminiferous tubule from a healthy sham operated left testis. The lanthanum does not reach the Sertoli-Sertoli junctional complex (R) but stops before (black arrowheads). Lanthanum deposits can be seen widely throughout the boundary zone (open arrowheads).

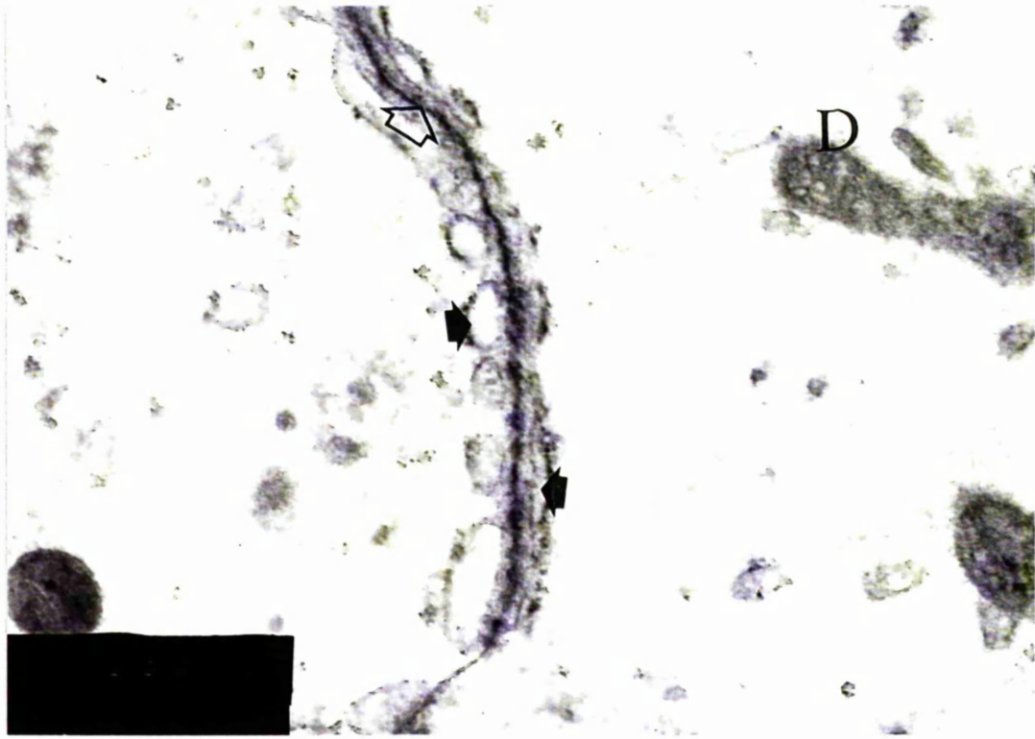


Figure 39. An electron micrograph (*14000 linear magnification) from a healthy sham operated right testis. The lanthanum does not extend into the tubule but can be seen on the vascular endothelium (black arrowheads).

Figure 40. An electron micrograph (*7500 linear magnification) from a healthy left testis following vasectomy. A typical Sertoli cell nucleus (s) can be seen. Lanthanum does not extend beyond the vascular space (black arrowheads).

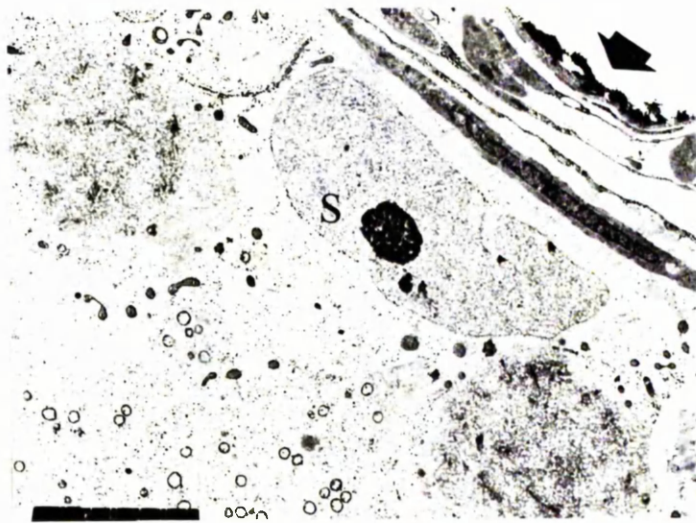
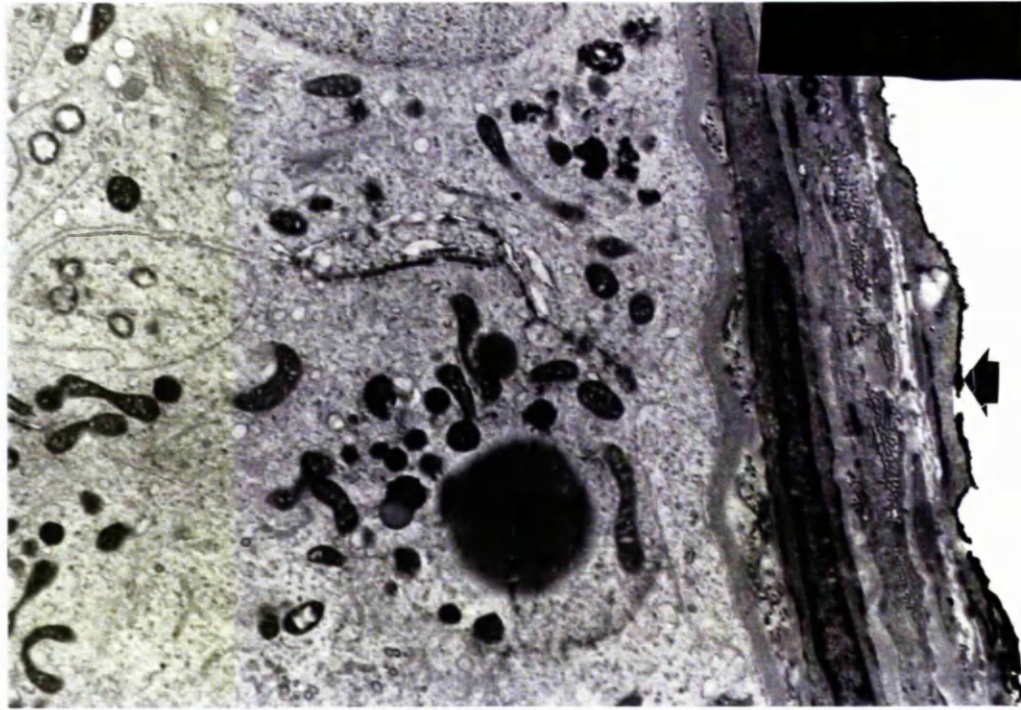


Figure 41. An electron micrograph (*14000 linear magnification) showing lanthanum confined to the outer compartment of the seminiferous tubule from healthy right testis following vasectomy. The lanthanum surrounds a spermatagonium (G) but is stopped at the Sertoli-Sertoli junctional complex (black arrowhead).

Figure 42. A high powered electron micrograph (*46000 linear magnification) of Figure 41. The lanthanum stopped at the Sertoli-Sertoli junctional complex (Black arrowhead) consisting of areas of apparent membrane fusion with adjacent electron dense deposits and dilated sacs of endoplasmic reticulum.

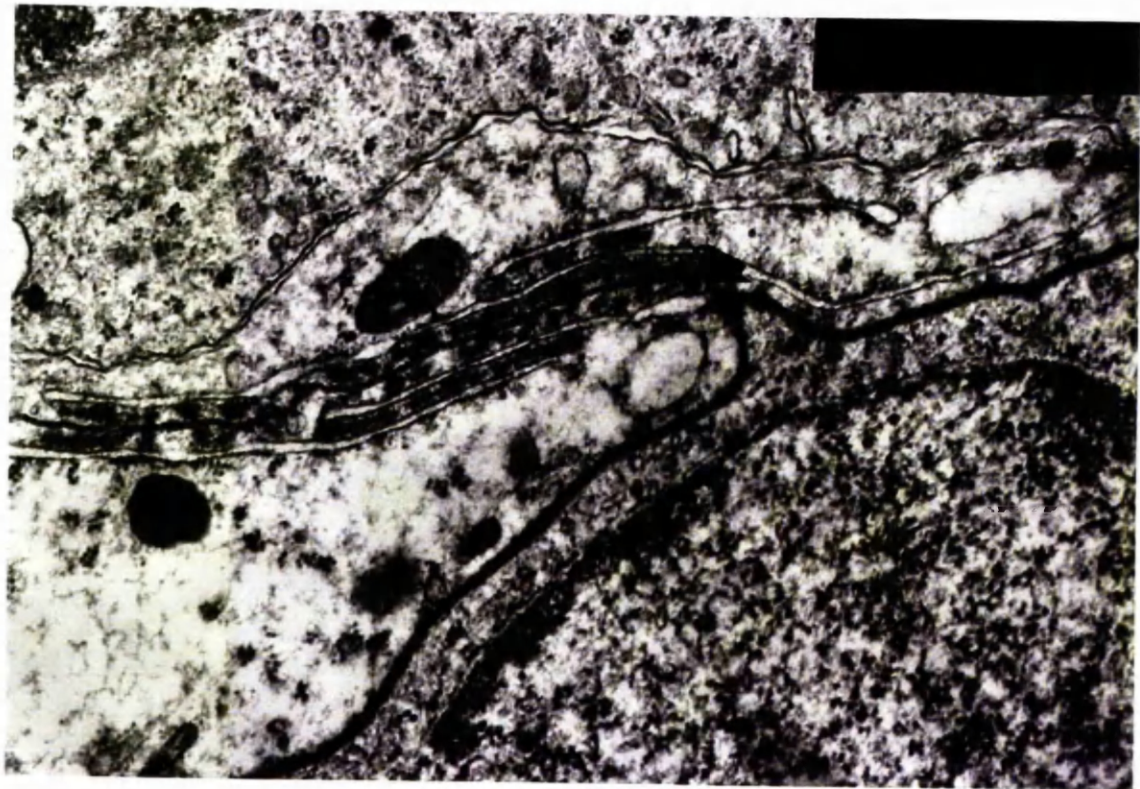


Figure 43. An electron micrograph (* linear magnification) showing the luminal aspect of the seminiferous tubule from a healthy right testis of an animal with ipsilateral degeneration following vasectomy. The lumen (O) can be identified with several sperm precursors present. No lanthanum is identified.

Figure 44. An electron micrograph (*14000 linear magnification) showing lanthanum (black arrowhead) confined to the outer compartment of the seminiferous tubule from an ipsilateral degenerated left testis following vasectomy. A typically convoluted Sertoli cell basal lamina (H) can be seen along with the triangular profile (T) of a myoepithelial cell.

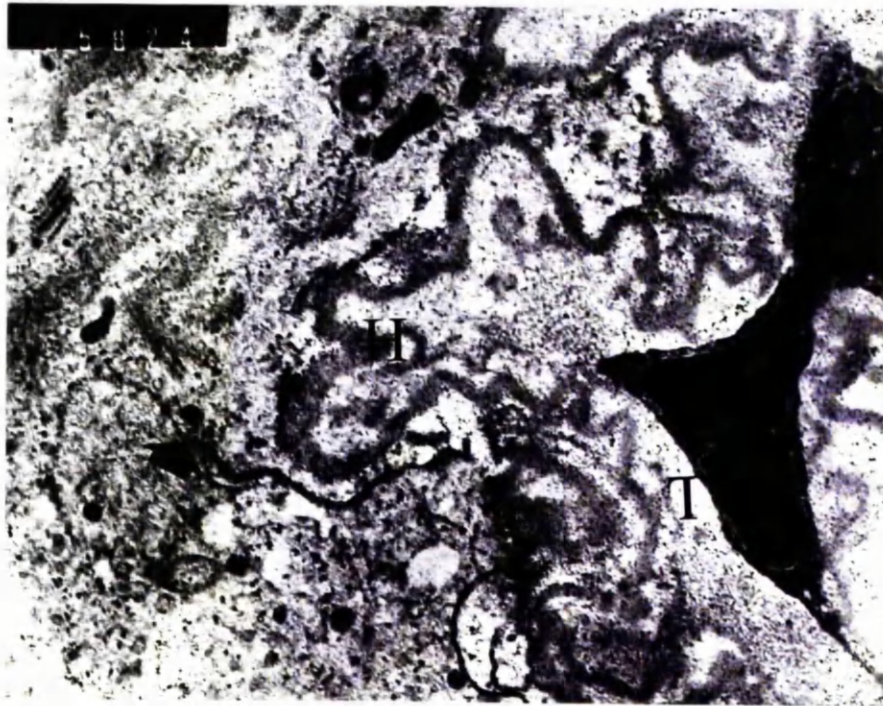
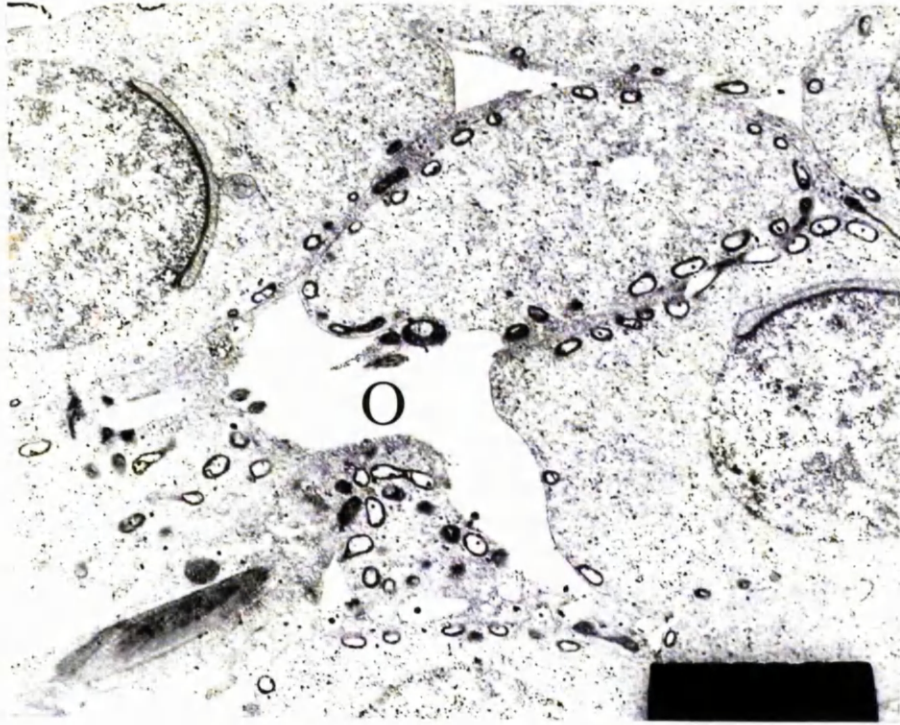


Figure 45. An electron micrograph (*22000 linear magnification) from the left testis of an animal with bilateral degeneration following vasectomy. The lanthanum has stopped (black arrowhead) at the Sertoli-Sertoli junctional complex whose structure is only just resolvable at this magnification. The lanthanum can be seen to surround part of a Sertoli cell (P) in the basal part of the seminiferous tubule.

Figure 46. An electron micrograph (*36000 linear magnification) from the right testis of an animal with bilateral degeneration following vasectomy. The lanthanum has stopped (black arrowhead) at the Sertoli-Sertoli junctional complex with areas of membrane fusion (open arrowheads). The convoluted Sertoli cell basal lamina can also be identified (H).

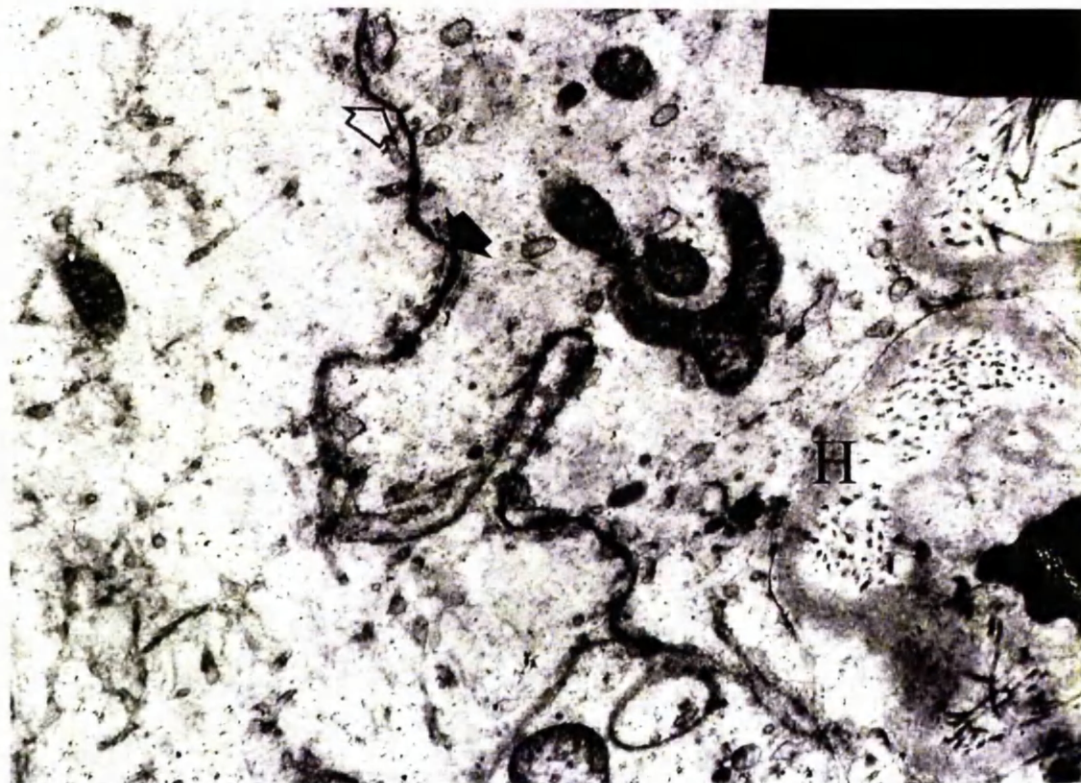
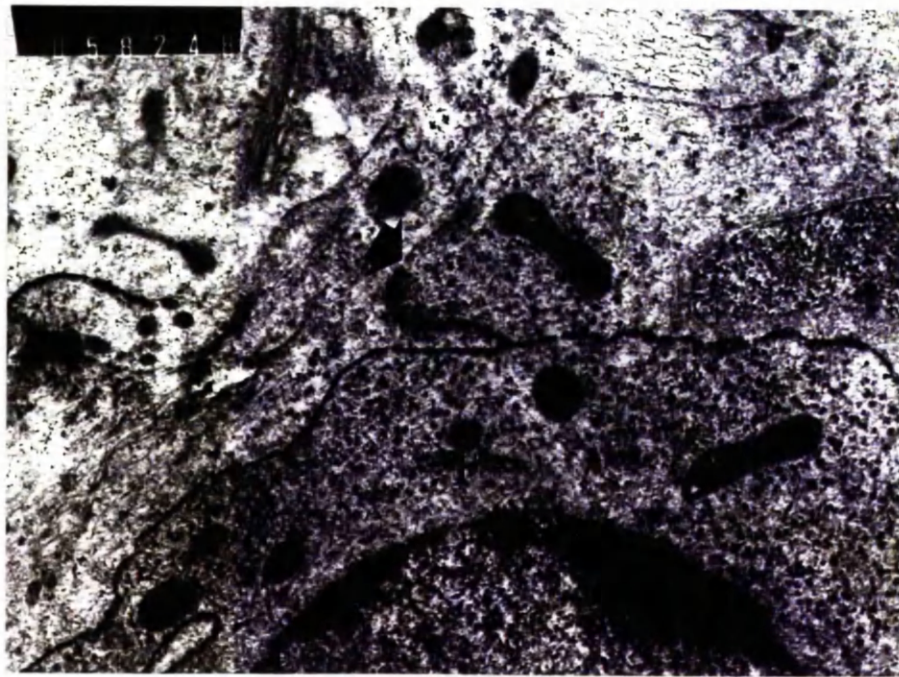


Figure 47. The appearance of OX18 labelling of the seminiferous tubules of a healthy left testis from a sham operated animal 12 months after the procedure (linear magnification *50). The labelling is largely confined within the interstitium between the tubules (open arrowhead) with very slight labelling on mature spermatids nearer the lumen (black arrowhead).

Figure 48. The appearance of OX18 labelling of the seminiferous tubules of a healthy left testis 3 months following vasectomy (linear magnification *200). The labelling is largely confined within the interstitium between the tubules (open arrowhead) with very slight labelling on mature spermatids nearer the lumen (black triangle).

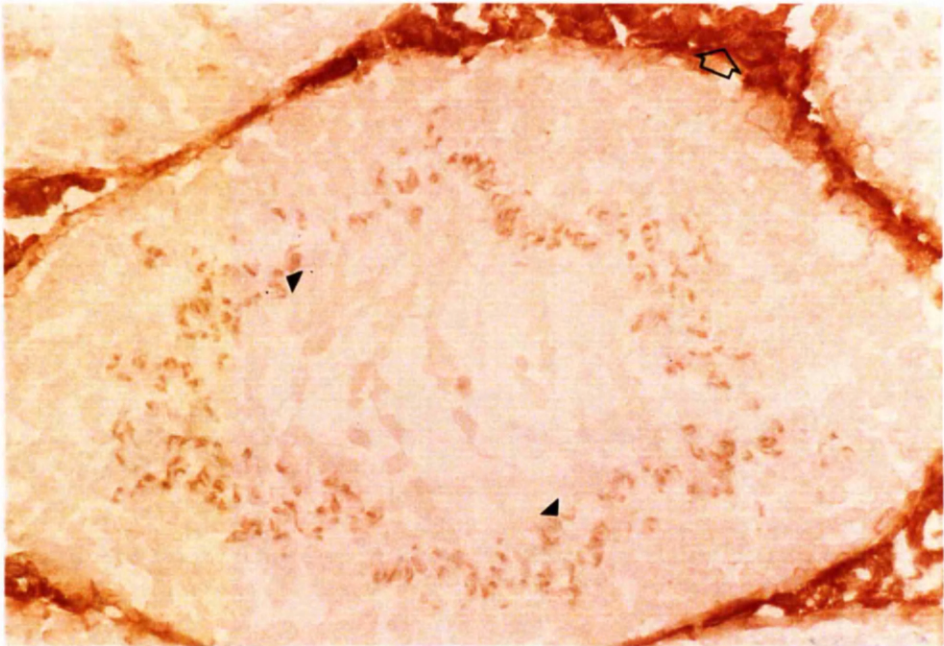
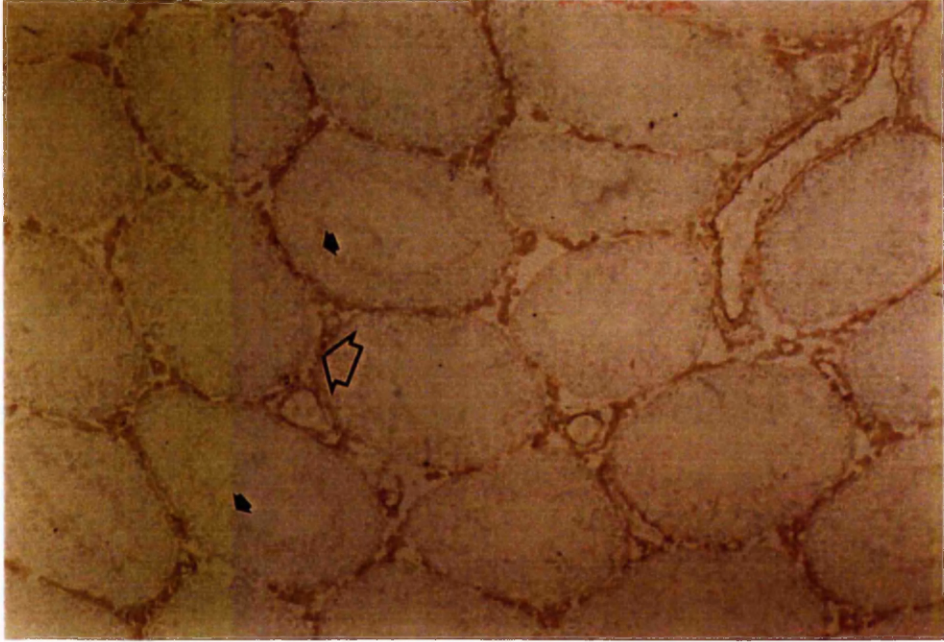


Figure 49. The appearance of OX18 labelling of the seminiferous tubules of a degenerated right testis from an animal with bilateral degeneration 12 months following vasectomy (linear magnification *200). The labelling is largely confined within the interstitium between tubules (open arrowhead) with very slight labelling on mature spermatids nearer the lumen on healthy tubules (black arrow head). In degenerated tubules, however, labelling extends throughout the remaining epithelium (black triangle).

Figure 50. The appearance of testes labelled no primary antibody as a control (linear magnification *100). Only very faint background staining can be seen partly due to the Mayer's haematoxylin.

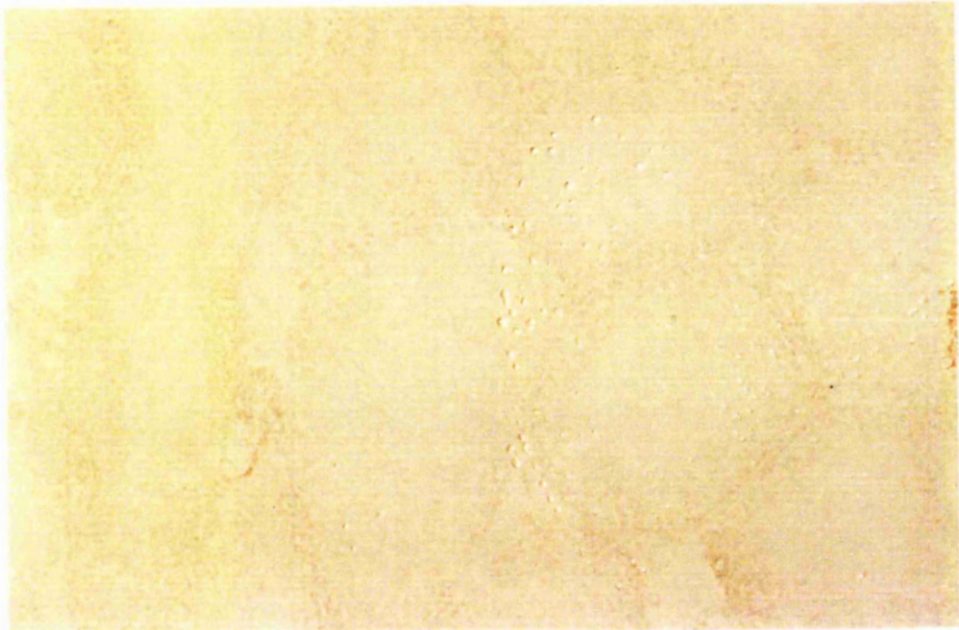
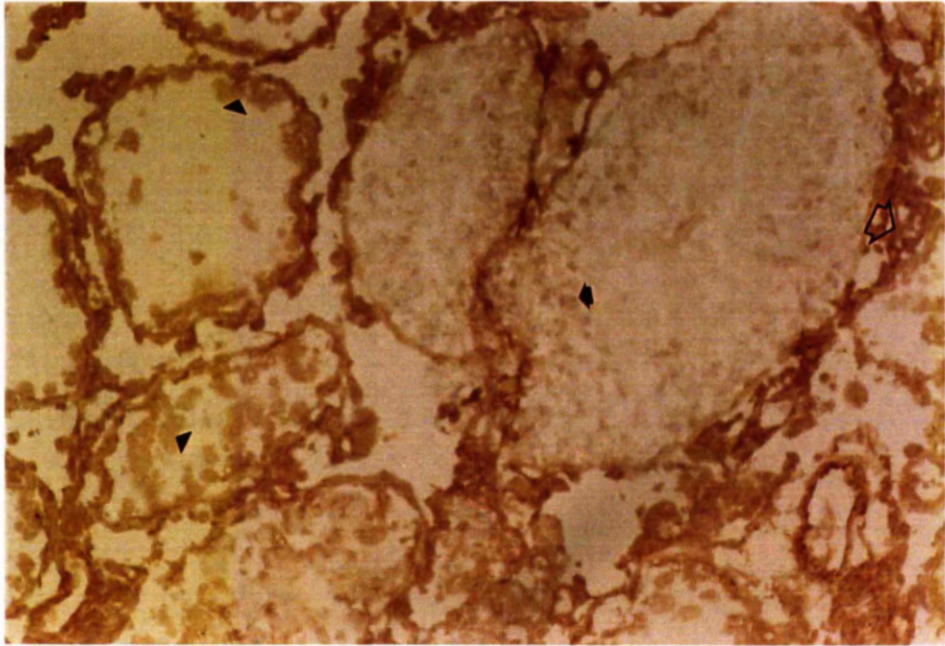


Figure 51. An example of a table recording the number of cells counted on a section. The X and Y co-ordinates refer to the overall dimensions of the section. Each number represents the number of labelled cells identified in the high powered field. Any identified to the right by "/" are within the tubule. The "V" refers to potential photographic opportunities. The identification of the specimen and primary antibody were added after the count to facilitate data collection.

E34143

Rox 42

G000

X 150.3 - 151.7

Y 14.8 - 8.4

	159	158	157	156	155	154	153	152	151
19	1	3	2	3	3V	4	0	-	-
18	2	5	5V	2	6	3	4	2	0
17	2	3	7	1	2	3	2	1	0
16	2	2	3	2	4	2V	2	2	3
15	3	6	4	5V	5	1	2	1	1
14	3	3	1	1	2	2	2	3	0
13	4	2	2	0	5	1	5	5	8
12	4	4V	7	3	2	1	3/1	4	2
11	4	4	2	4	2	6	2	6	3
10	2V	3	2	1	2	4	V	2	2
9	0	1	1	1	3	5	3V	2	2
23	35	35	23	34	30	21	29	14	
11	10	10	11	11	11	11	10	9	

$$\frac{261}{94} + 1$$

Figure 52. The appearance of OX19 labelling of the spleen from a sham operated animal 12 months after the procedure (linear magnification *100). The labelling is largely confined to cells in the periarterial lymphatic sheath (p) with its central artery (a). Scattered labelled cells could also be seen within the red pulp. The appearances are consistent with the distribution of T-lymphocytes in the spleen.

Figure 53. The appearance of W3/25 labelling of the spleen from a sham operated animal 12 months following the procedure (linear magnification *100). The labelling is largely confined to cells in the periarterial lymphatic sheath (p) with its central artery (a). Numerous scattered labelled cells could also be seen within the red pulp (r). The appearances are consistent with the distribution of helper T-lymphocytes in the spleen.

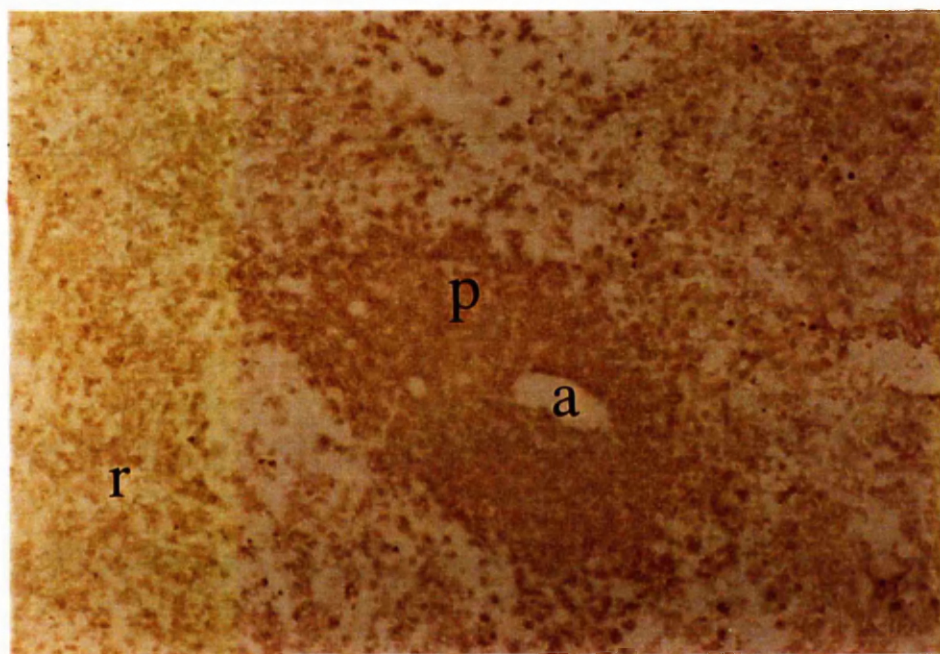
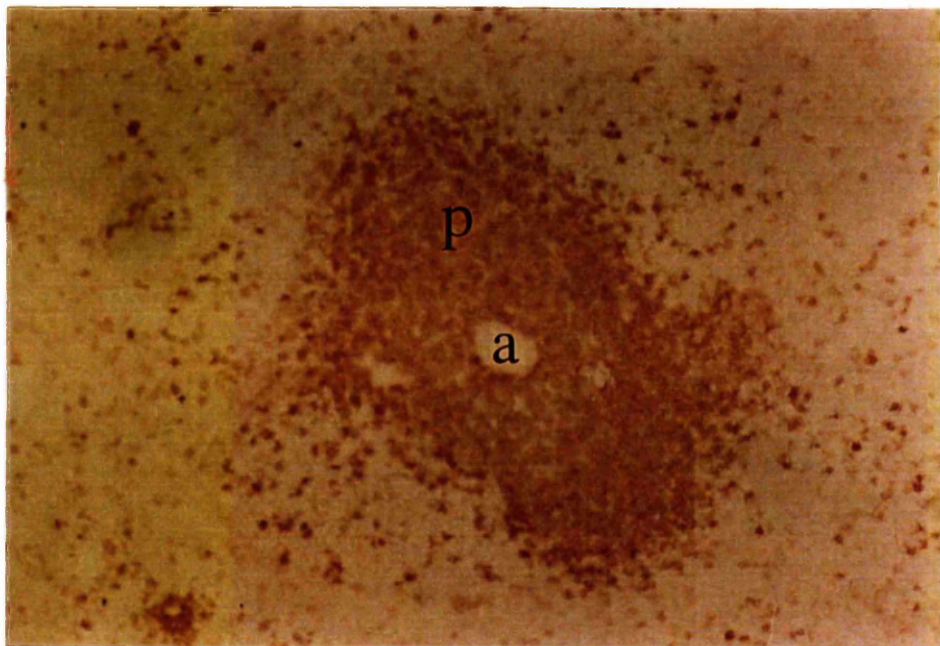


Figure 54. The appearance of OX8 labelling of the spleen from a sham operated animal 12 months after the procedure (linear magnification *100). The labelling is scattered throughout the periarterial lymphatic sheath (p) with its central artery (a). A few labelled cells can be seen in the red pulp. The appearances are consistent with the distribution of cytotoxic T-lymphocytes in the spleen.

Figure 55. The appearance of OX33 labelling of the spleen from a sham operated animal 12 months following the procedure (linear magnification *100). The labelling is largely confined to follicular areas (f) with few cells in the periarterial lymphatic sheath with its central artery (a). A few scattered cells are labelled within the red pulp. The appearances are consistent with the distribution of B-lymphocytes in the spleen.

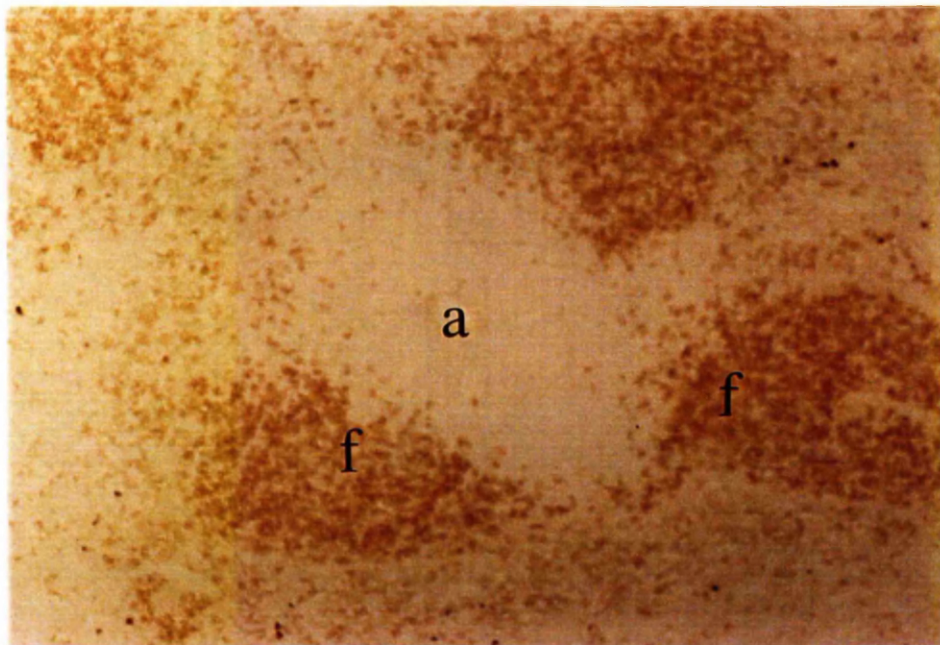
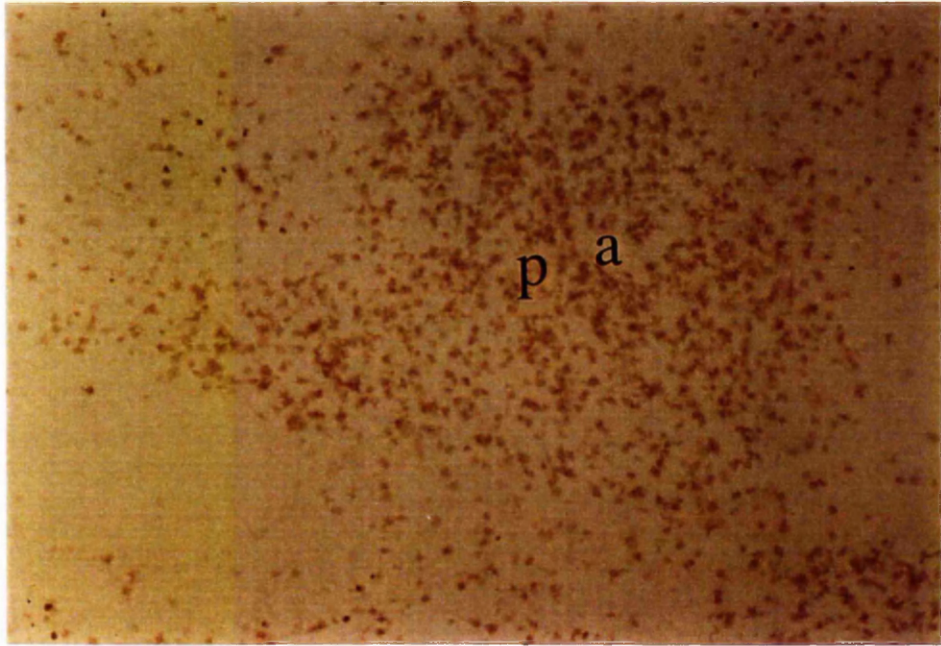


Figure 56. The appearance of OX18 labelling of the spleen from a sham operated animal 12 months after the procedure (linear magnification *100). The labelling is extensive throughout red (r) and white pulp. A central artery (a) with its surrounding periarterial lymphatic sheath (p) can be seen. The distribution is consistent with known Major Histocompatibility Complex class I expression.

Figure 57. The appearance of OX18 labelling of the spleen from a sham operated animal 12 months after the procedure (linear magnification *400). The labelling is extensive but clearly cellular lining the extracellular space/plasma membrane. A central artery (a) is visible.

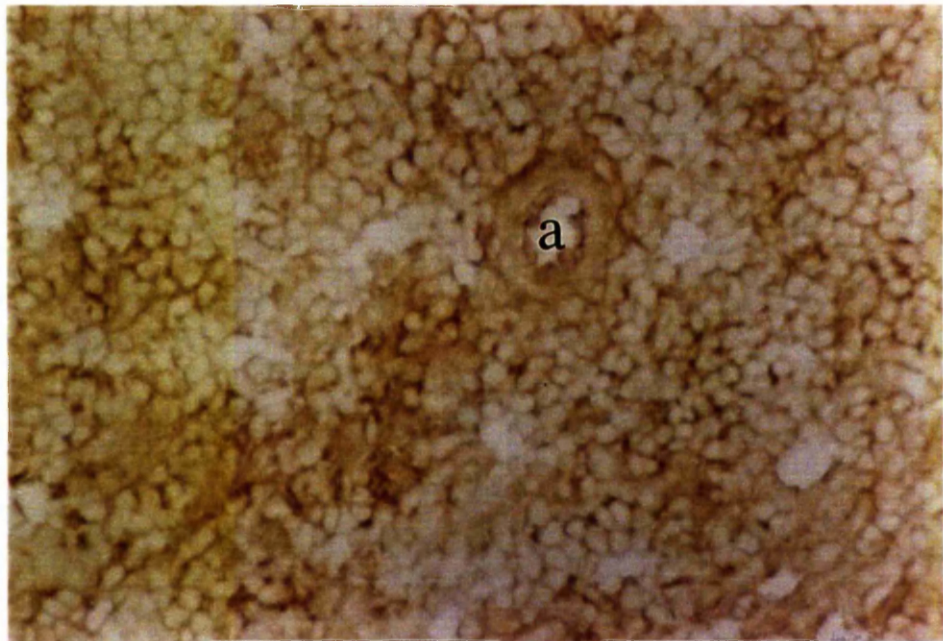
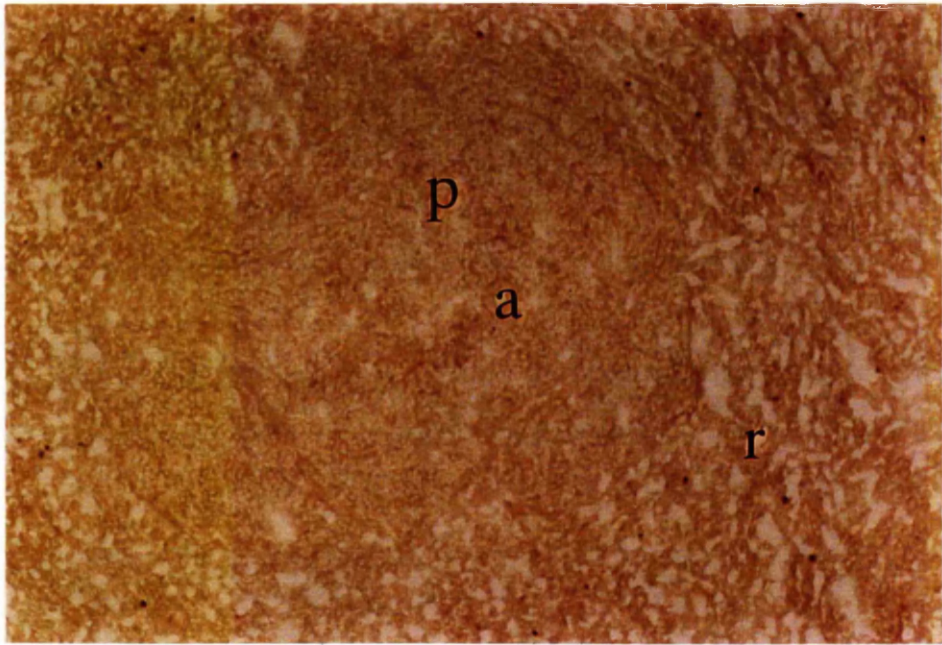


Figure 58. The appearance of OX6 labelling of the spleen from a sham operated animal 12 months after the procedure (linear magnification *100). The labelling is extensive throughout the periarterial lymphatic sheath (p) with its central artery (a) as well as more sparsely in the red pulp (r). The appearances are consistent with the distribution of Major Histocompatibility Complex class II expression in the spleen.

Figure 59. The appearance of OX42 labelling of the spleen from a sham operated animal 12 months following the procedure (linear magnification *100). The labelled cells (black triangle) are scattered throughout the red and white pulps. The appearances are consistent with the distribution of macrophages in the spleen.

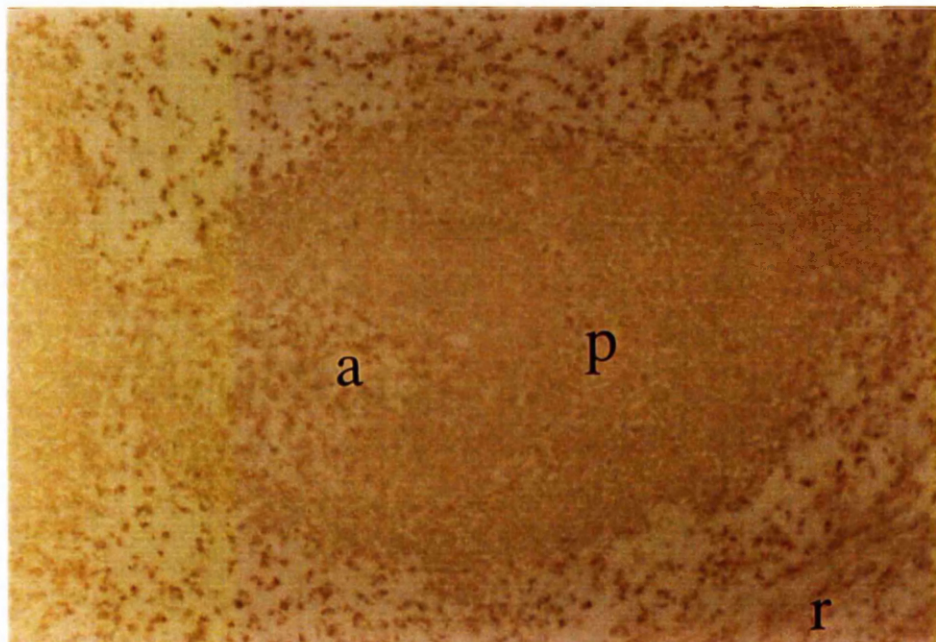


Figure 60. The appearance of OX33 labelling of a healthy left testis from a sham operated animal 6 months following the operation (linear magnification *500). A labelled cell could be identified in the interstitium between two adjacent seminiferous tubules (black triangle).

Figure 61. The appearance of OX19 labelling of a healthy left testis from a sham operated animal 6 months following the procedure (linear magnification *500). Labelled cells could be identified in the interstitium between two adjacent seminiferous tubules (black triangle) and around a blood vessel (open triangle).

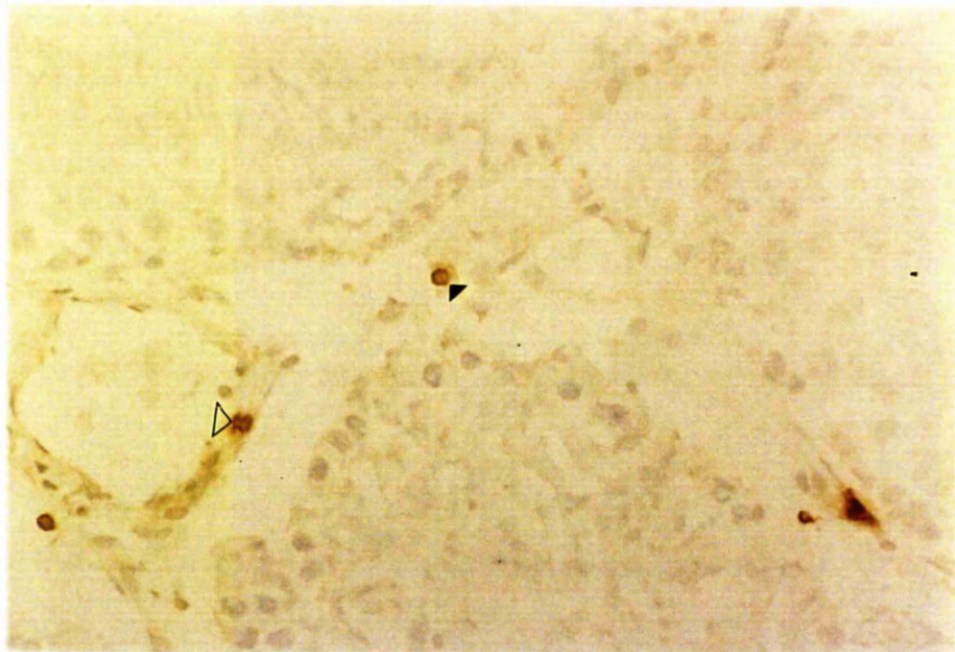


Figure 62. The appearance of OX8 labelling of a healthy left testis from a sham operated animal 12 months following the procedure (linear magnification *300). Labelled cells could be identified in the interstitium (black triangle).

Figure 63. The appearance of W3/25 labelling of a healthy right testis of a sham operated animal 3 weeks following the procedure (linear magnification *300). Labelled cells could be identified in the interstitium between adjacent seminiferous tubules (black triangle).

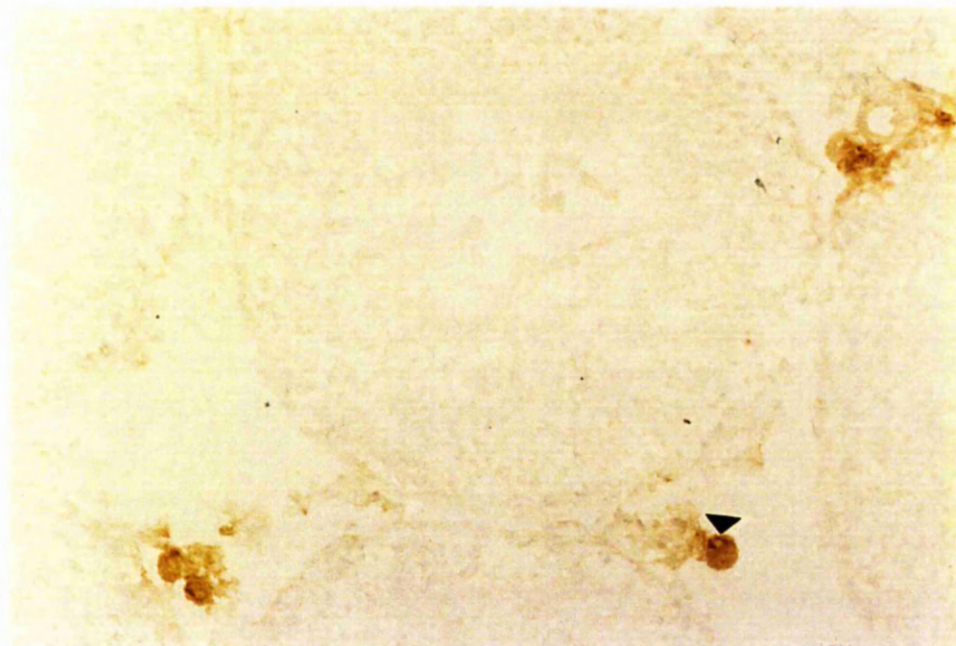


Figure 64. The appearance of W3/25 labelling of a healthy left testis of a sham operated animal 6 months following the procedure (linear magnification *800). A labelled cell could be identified in the seminiferous epithelium (black triangle). Note also the artefact produced by an air bubble in the mounting medium (open triangle).

Figure 65. The appearance of OX42 labelling of a healthy right testis of a sham operated animal 6 months following the procedure (linear magnification *100). Labelled cells could be identified in the interstitium between adjacent seminiferous tubules (black triangles).

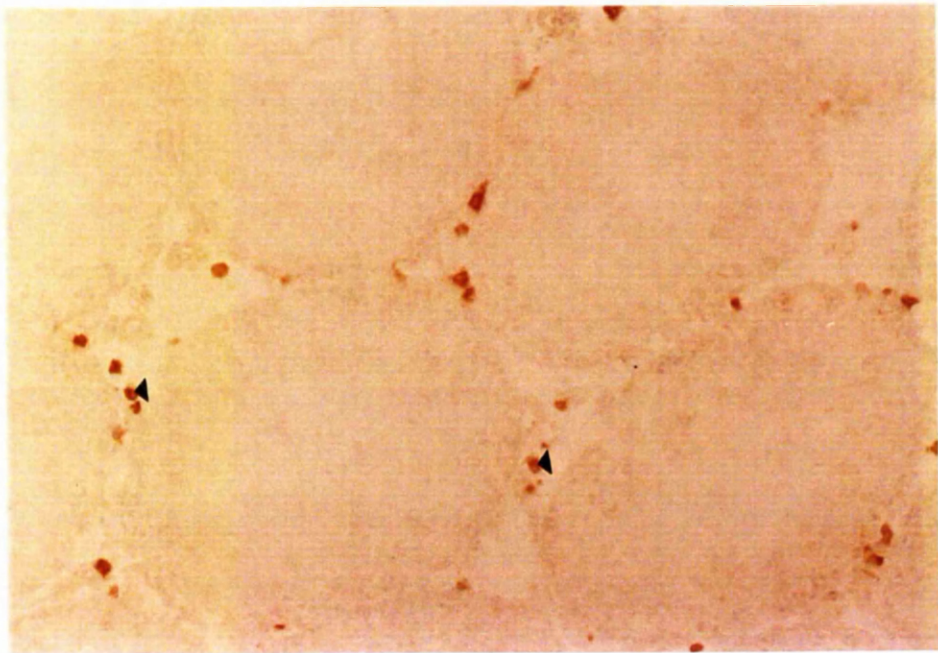
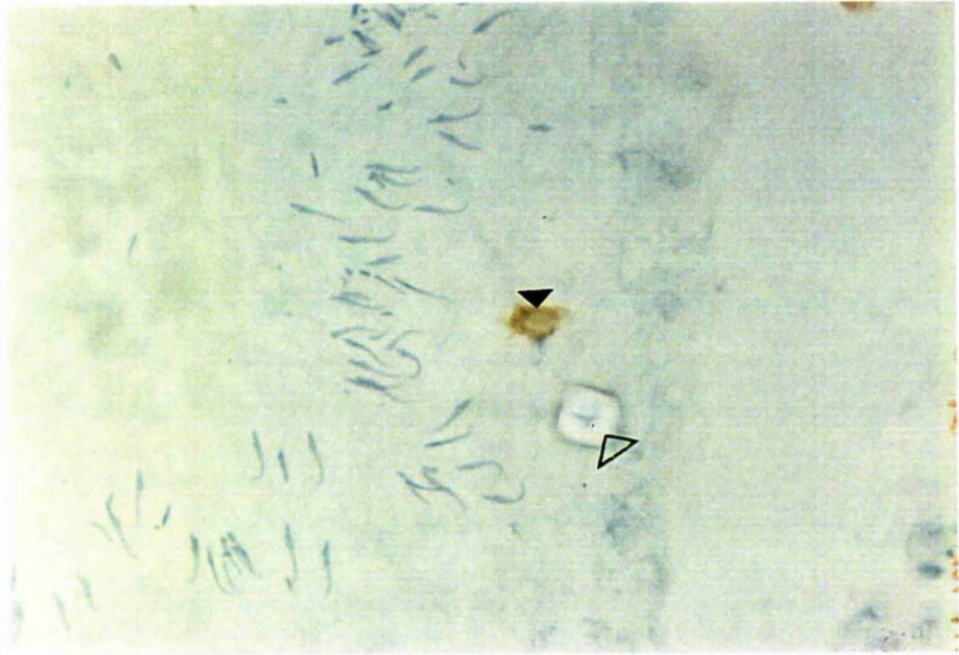


Figure 66. The appearance of OX 6 labelling of a healthy left testis from a sham operated animal 6 months following the procedure (linear magnification *100). Labelled cells could be seen scattered through the interstitium (black triangles).

Figure 67. The appearance of OX18 labelling of a healthy right testis from a sham operated animal 6 months following the procedure (linear magnification *800). Labelled cells could be identified in the interstitium (black triangles) along with a single cell in the tubule (open triangle).

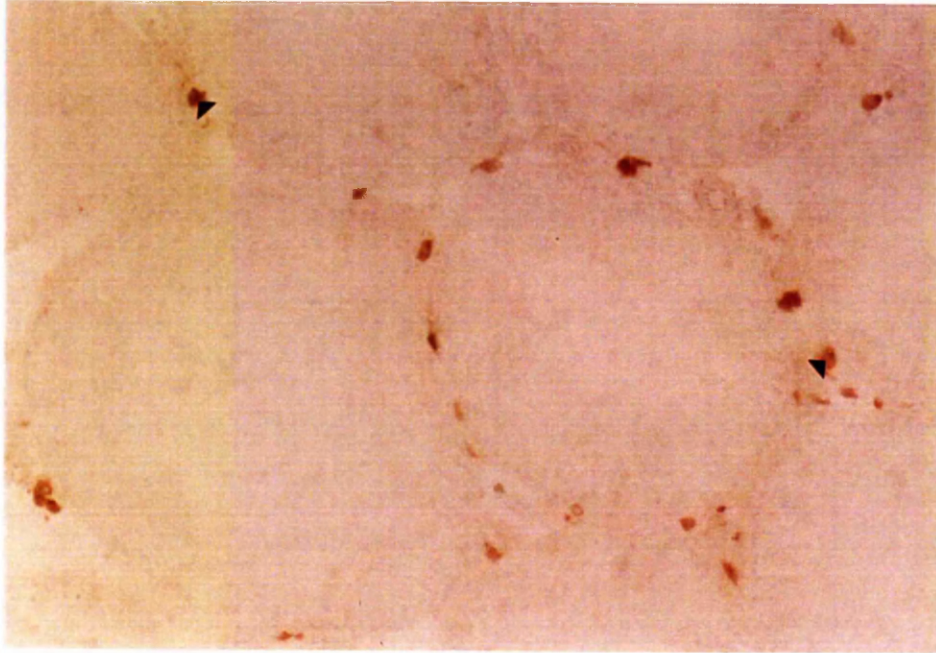


Figure 68. The appearance of OX 33 labelling of a healthy left testis 3 months following vasectomy (linear magnification *50). Occasional Labelled cells could be seen in the interstitium (black triangle).

Figure 69. The appearance of OX 33 labelling of a healthy right testis 12 months following vasectomy (linear magnification *300). A labelled cell can be seen in the seminiferous tubule (black triangle).

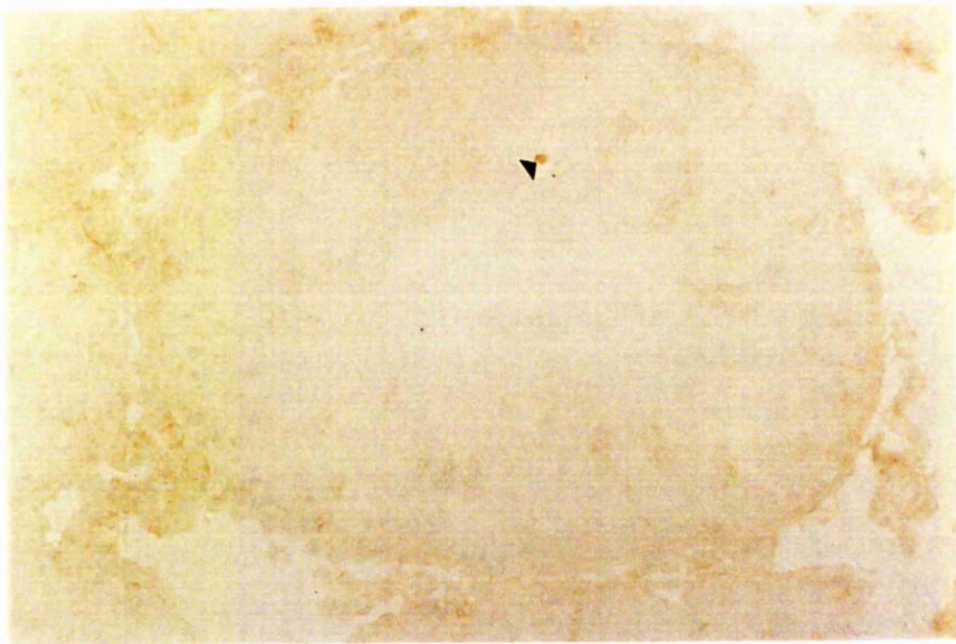
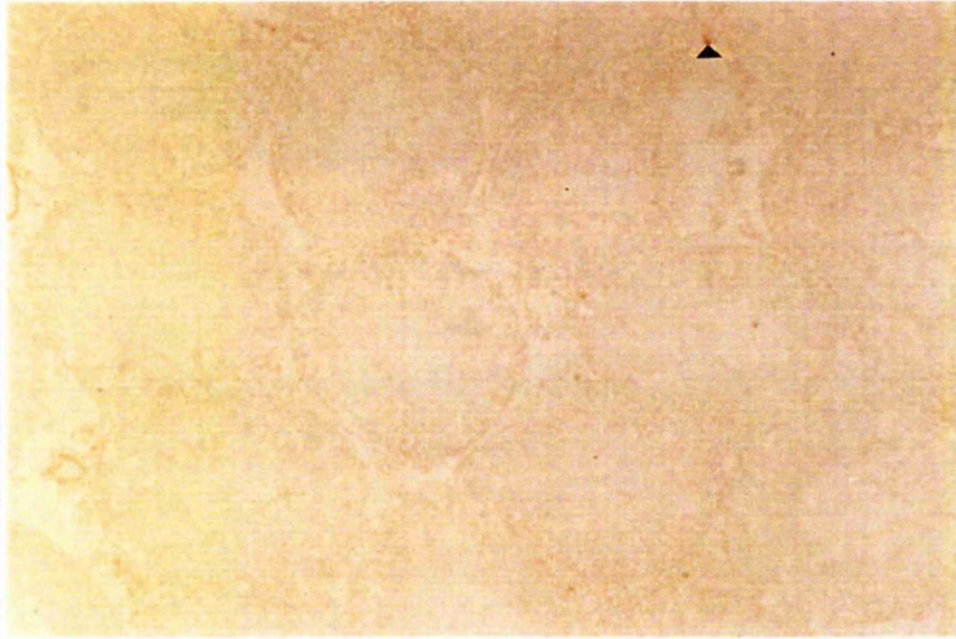


Figure 70. The appearance of OX 19 labelling of a healthy left testis 3 months following vasectomy (linear magnification *50). Labelled cells could be seen scattered sparsely through the interstitium (black triangle).

Figure 71. The appearance of OX 8 labelling of a healthy right testis 12 months following vasectomy (linear magnification *200). Labelled cells could be seen scattered through the interstitium (black triangle).

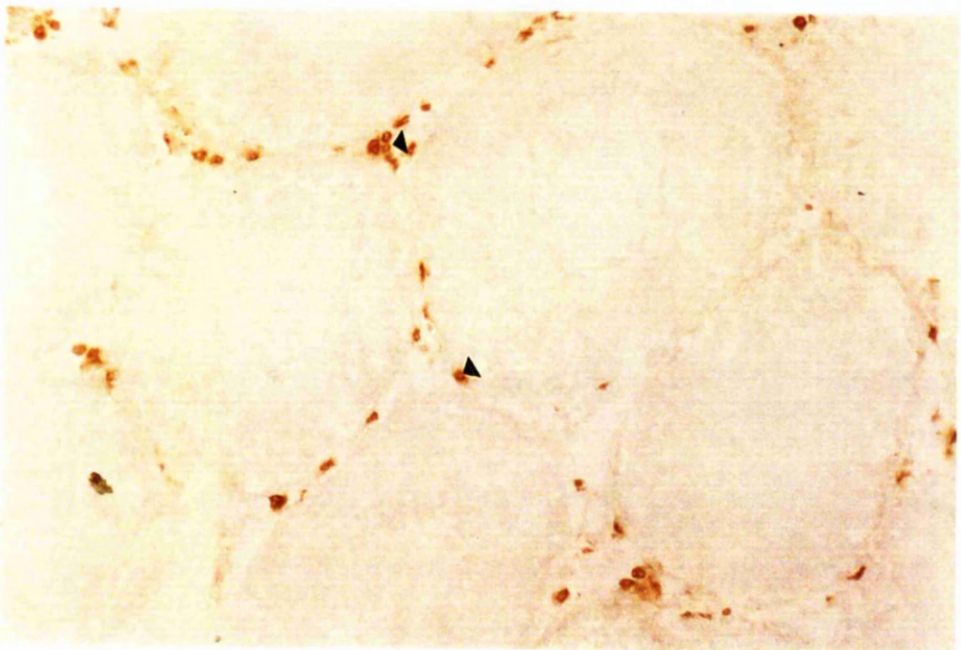
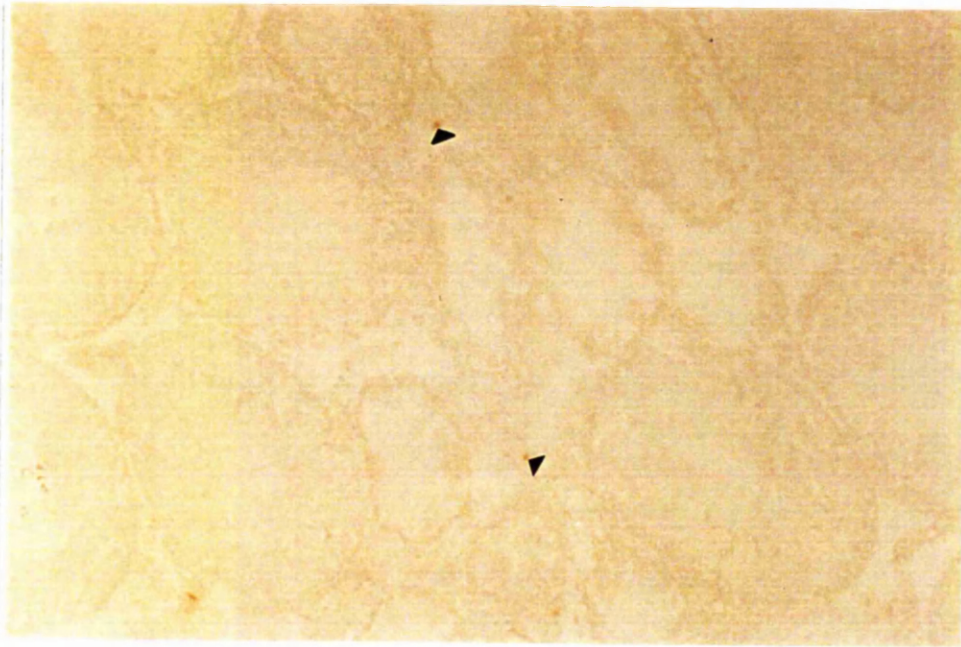


Figure 72. The appearance of W3/25 labelling of a healthy right testis 12 months following vasectomy (linear magnification *100). Labelled cells could be seen scattered sparsely through the interstitium (black triangle).

Figure 73. The appearance of OX 42 labelling of a healthy left testis 3 months following vasectomy (linear magnification *200). Labelled cells could be seen scattered sparsely through the interstitium (black triangle).

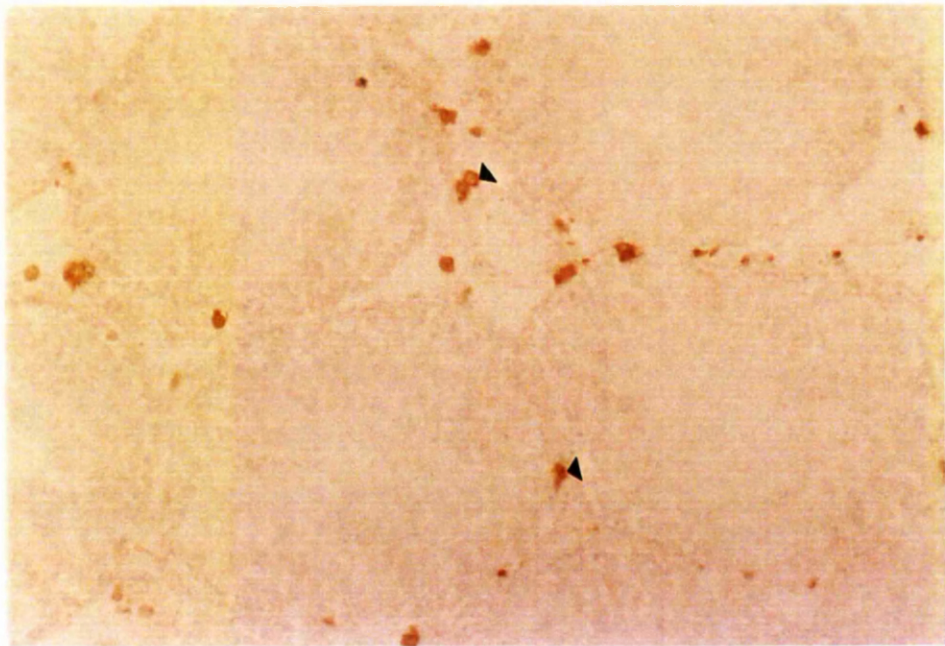
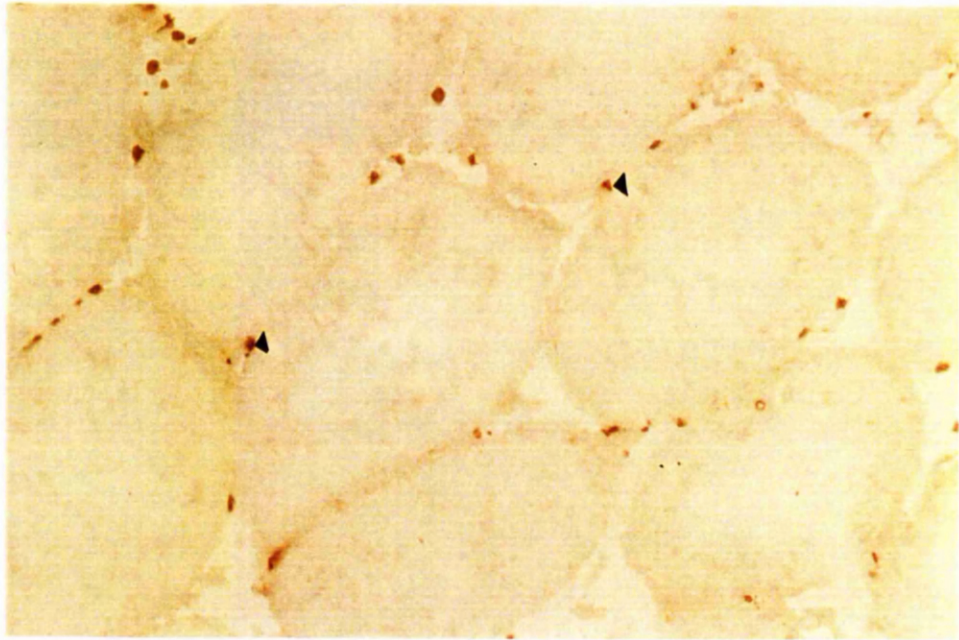


Figure 74. The appearance of OX 6 labelling of a healthy left testis 3 months following vasectomy (linear magnification *100). Labelled cells could be seen scattered sparsely through the interstitium (black triangles).

Figure 75. The appearance of OX 6 labelling of a healthy right testis from an animal with ipsilateral degeneration 12 months following vasectomy (linear magnification *200). Labelled cells could be seen scattered sparsely through the interstitium (black triangle). A focal accumulation of labelled cells (black arrowhead) could be seen in relation to a blood vessel (b).

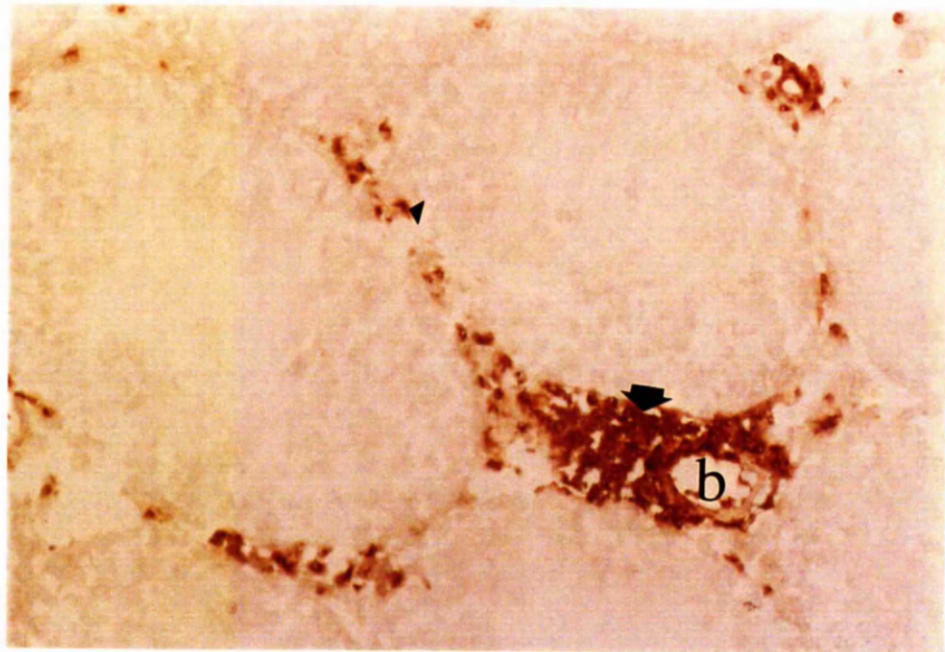
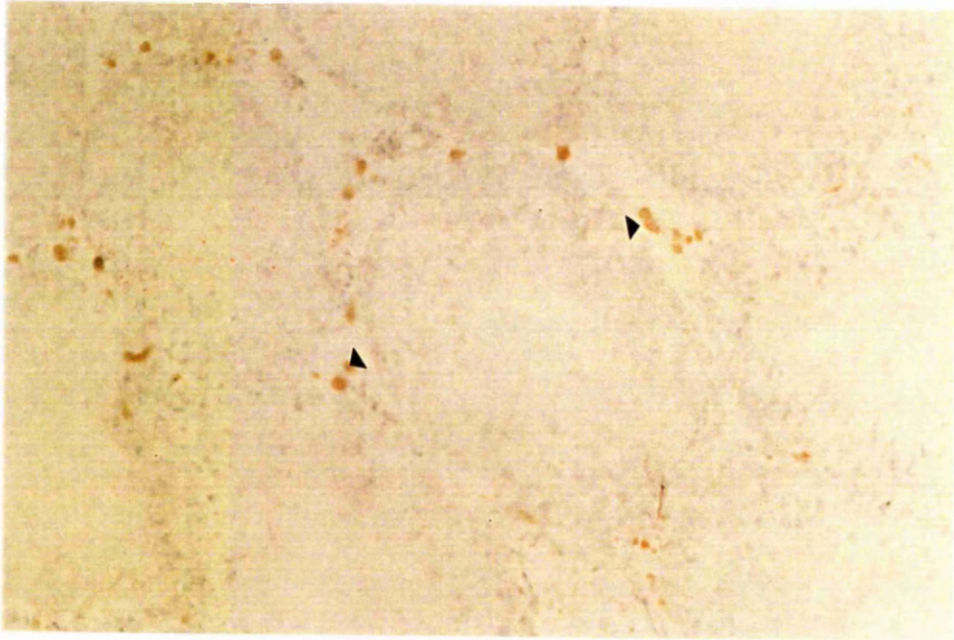


Figure 76. The appearance of OX 18 labelling of a healthy right testis 12 months following vasectomy (linear magnification *200). Labelled cells could be seen in the interstitium (open arrowhead) with some weak staining of late spermatids (black triangle).

Figure 77. The appearance of OX 33 labelling of a degenerated left testis from an animal with bilateral degeneration 12 months following vasectomy (linear magnification *100). A labelled cell could be seen in the interstitium (black triangle). Note the grossly abnormal seminiferous tubules (t) and dilated lymphatic spaces (l).

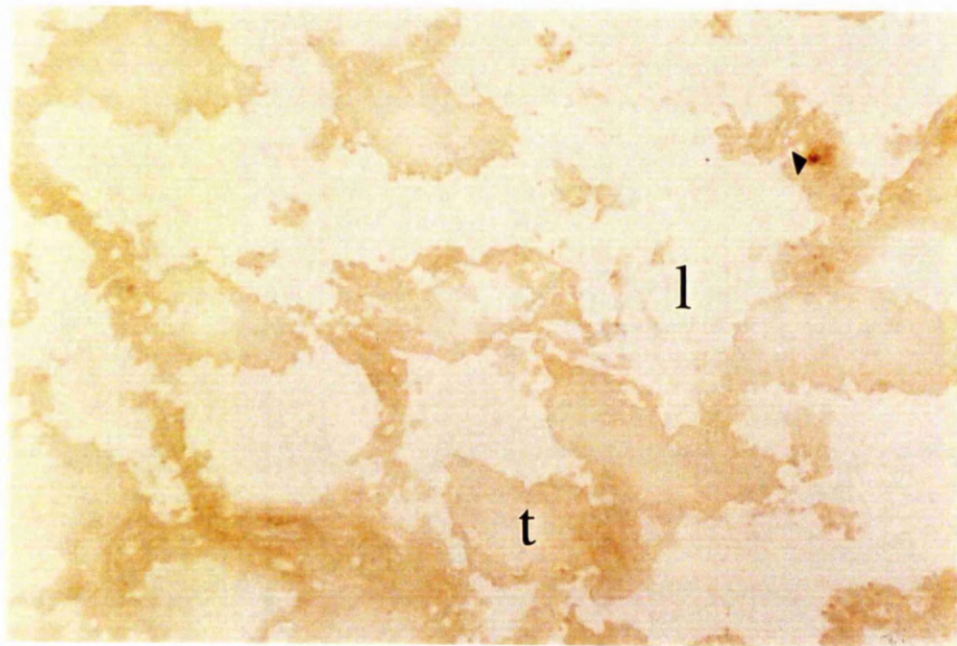
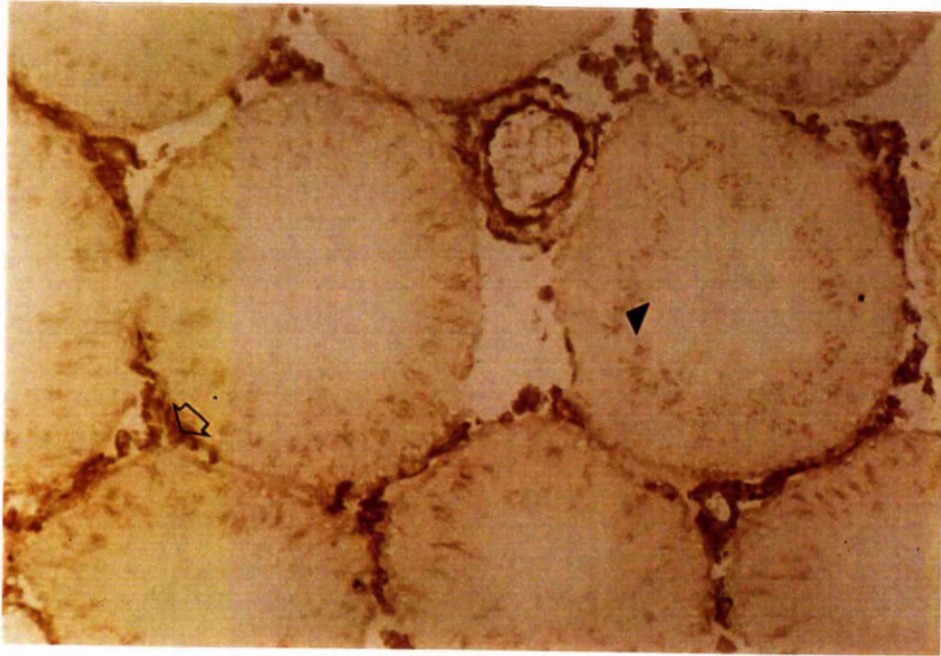


Figure 78. The appearance of OX 19 labelling of a degenerated left testis from an animal with ipsilateral degeneration 12 months following vasectomy (linear magnification *300). Labelled cells could be seen in the interstitium (black triangle) with a labelled cell in the degenerated tubule (black arrowhead).

Figure 79. The appearance of OX 8 labelling of a degenerated left testis from an animal with bilateral degeneration 12 months following vasectomy (linear magnification *100). Labelled cells could be seen in the interstitium (black triangles).

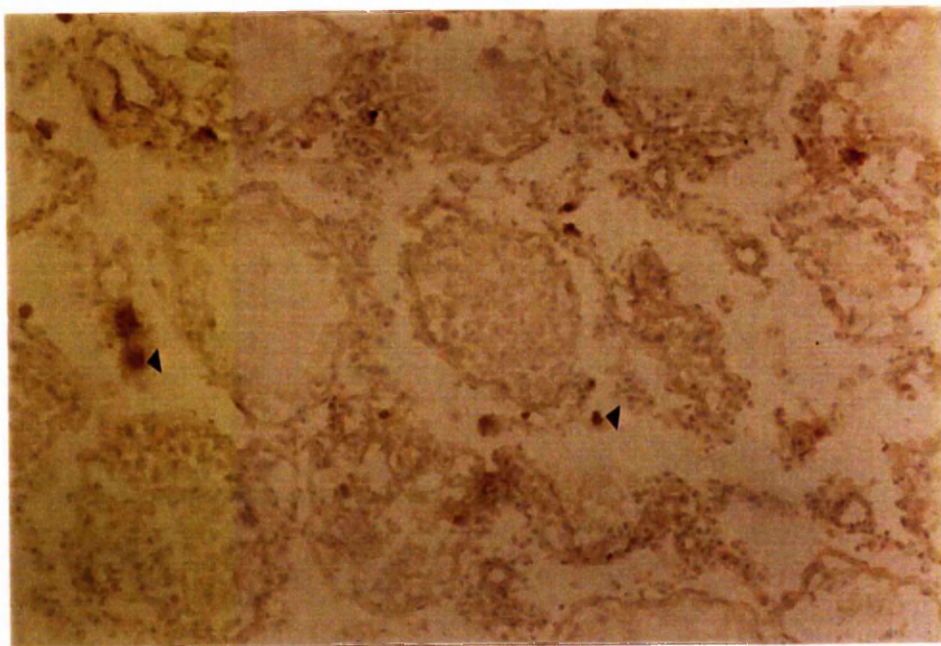


Figure 80. The appearance of W3/25 labelling of a degenerated left testis from an animal with ipsilateral degeneration 12 months following vasectomy (linear magnification *400). Labelled cells could be seen in the interstitium with a labelled cells in the degenerated tubule.

Figure 81. The appearance of OX 42 labelling of a seminiferous tubule from a degenerated right testis from an animal with bilateral degeneration 12 months following vasectomy (linear magnification *400). Labelled cells could be seen in the interstitium (black triangle) but also in the tubule (open arrowhead).

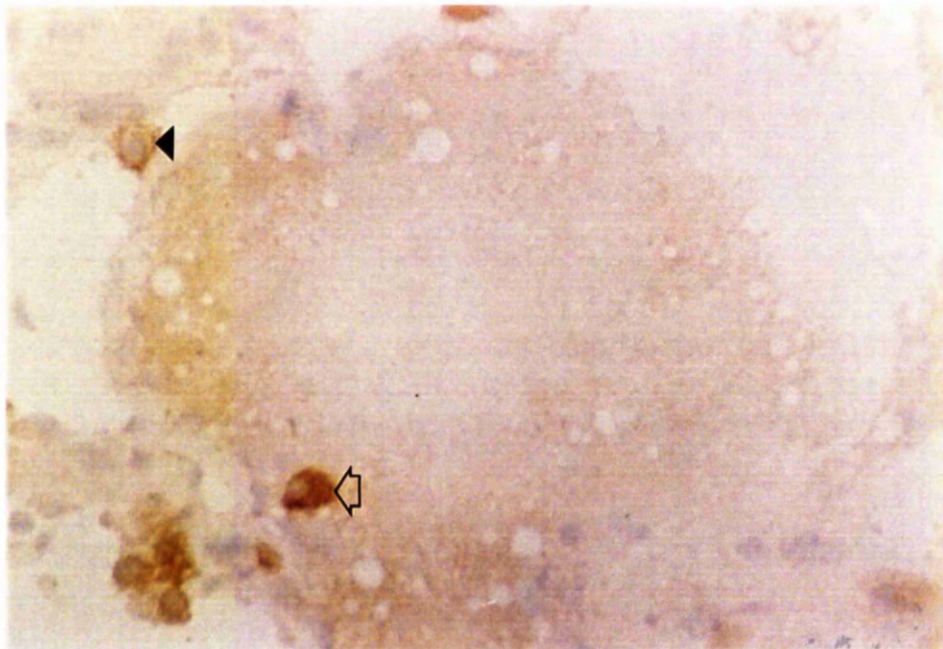
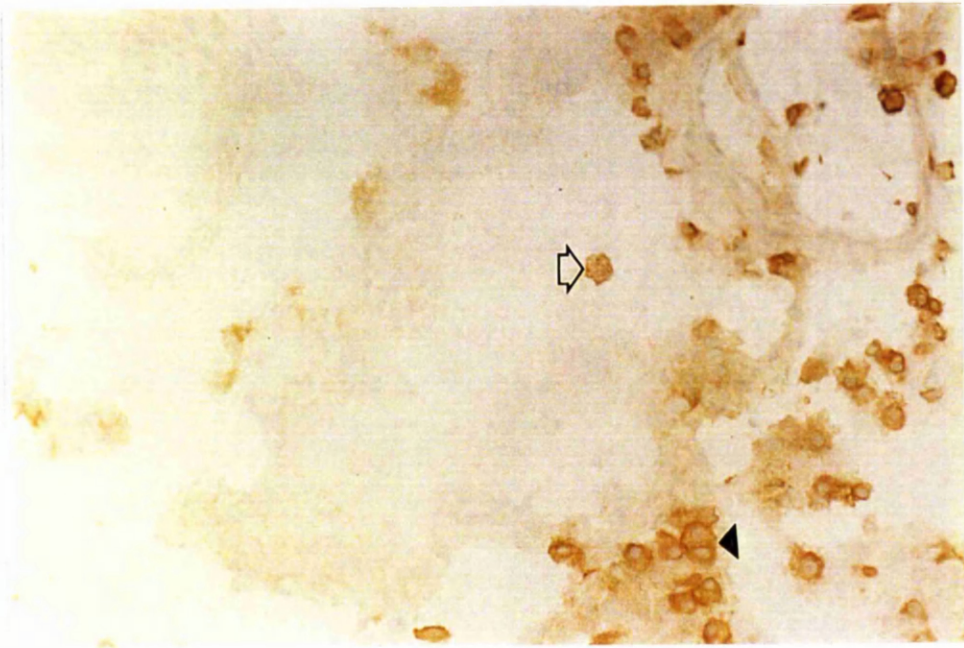


Figure 82. The appearance of OX 6 labelling of a degenerated right testis from an animal with bilateral degeneration 12 months following vasectomy (linear magnification *100). Labelled cells could be seen in the interstitium (black triangles).

Figure 83. The appearance of OX 18 labelling of a seminiferous tubule from a degenerated left testis from an animal with bilateral degeneration 12 months following vasectomy (linear magnification *400). Cells both in the interstitium (black triangle) and within the tubule (open arrowhead) are labelled.

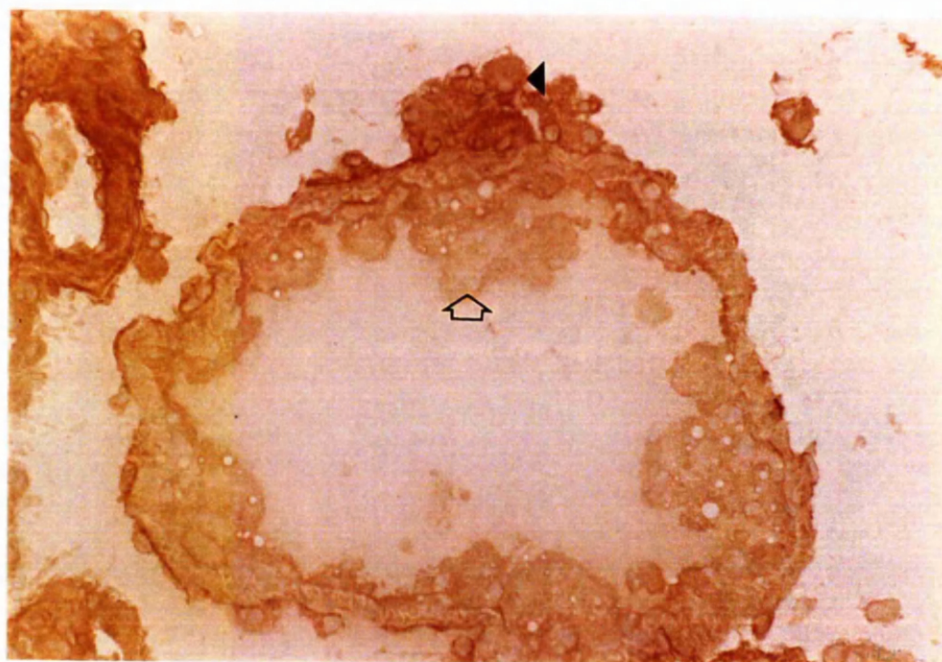


Figure 84. The appearance of OX 33 labelling of a degenerated left testis from an animal with bilateral degeneration 12 months following vasectomy (linear magnification *300). A collection of cells could be seen around a degenerated tubule (t). No labelled cells could be seen.

Figure 85. The appearance of OX 42 labelling of a seminiferous tubule from a degenerated left testis from an animal with bilateral degeneration 12 months following vasectomy (linear magnification *300). A collection of labelled cells (C) could be seen around an degenerated tubule. A few labelled cells could be seen within it (open arrowhead).

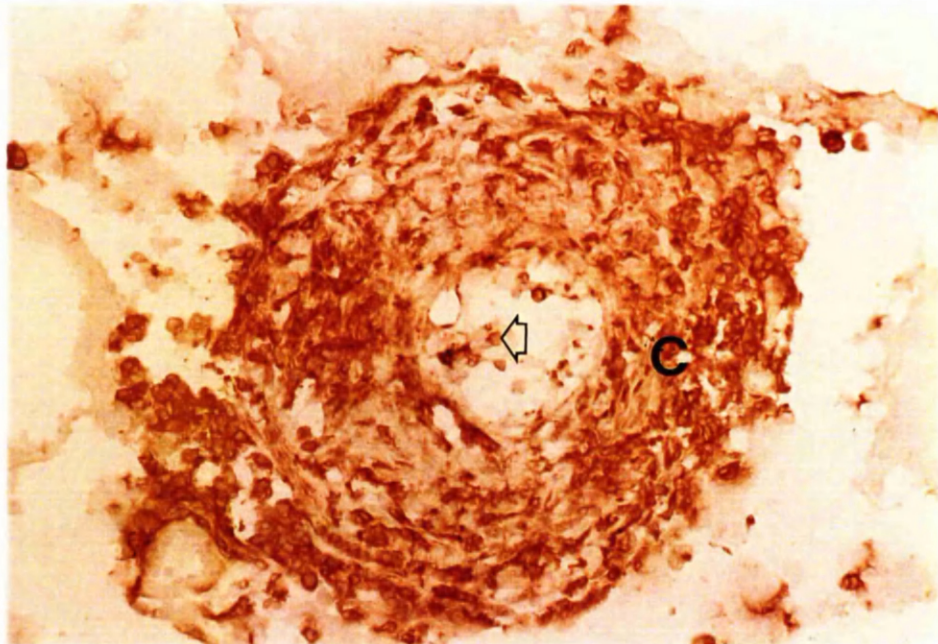
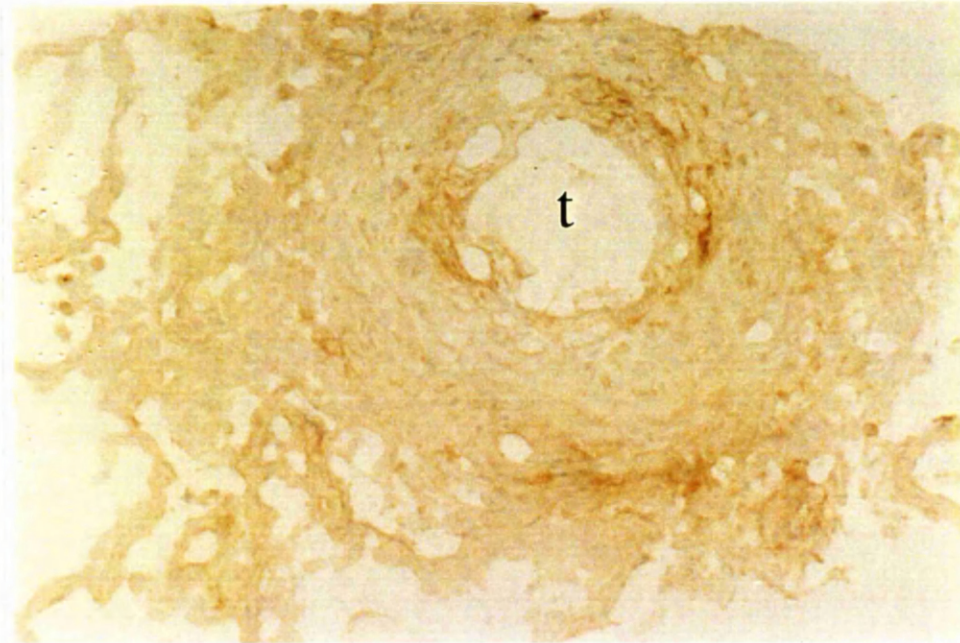


Figure 86. The appearance of OX 6 labelling of a degenerated left testis from an animal with bilateral degeneration 12 months following vasectomy (linear magnification *200). A collection of labelled cells (C) could be seen around an degenerated tubule. A few labelled cells can be seen within it (open arrowhead).

Figure 87. The appearance of W3/25 labelling of a seminiferous tubule from a degenerated left testis from an animal with bilateral degeneration 12 months following vasectomy (linear magnification *300). A collection of labelled cells (C) could be seen around an degenerated tubule. A few labelled cells can be seen within it (open arrowhead).

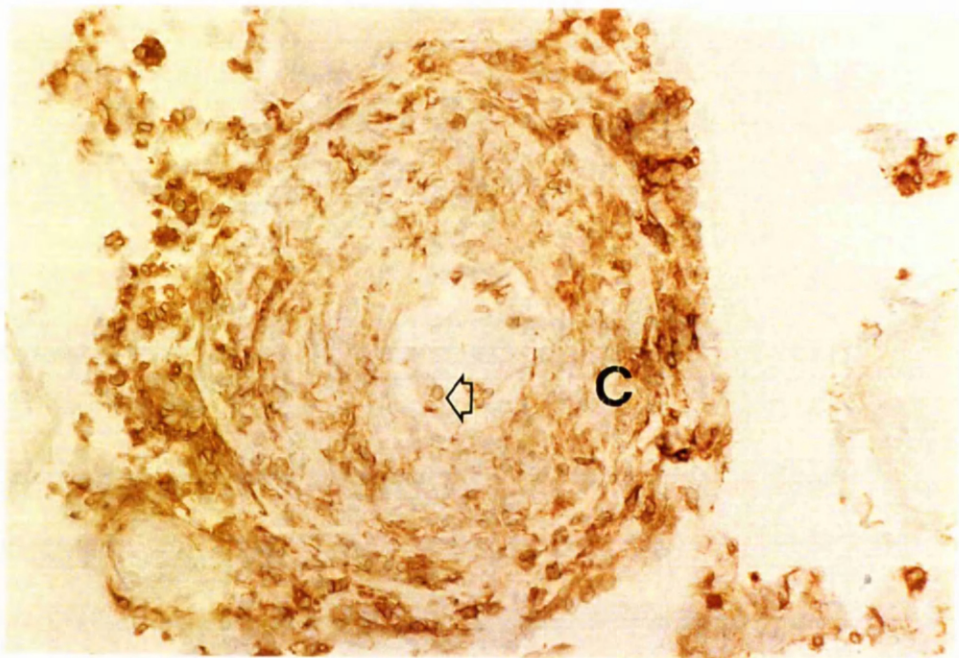
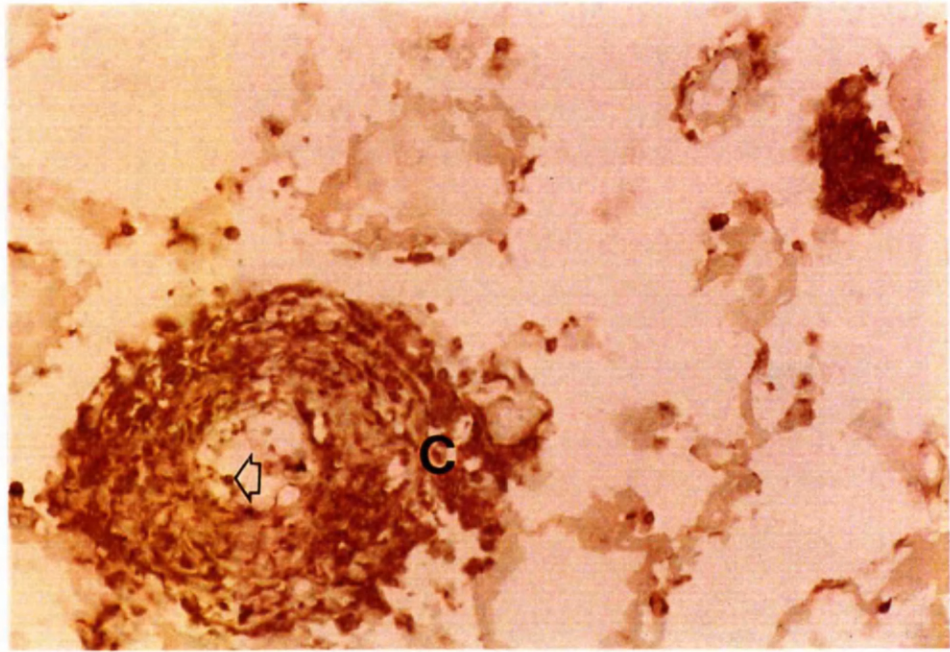
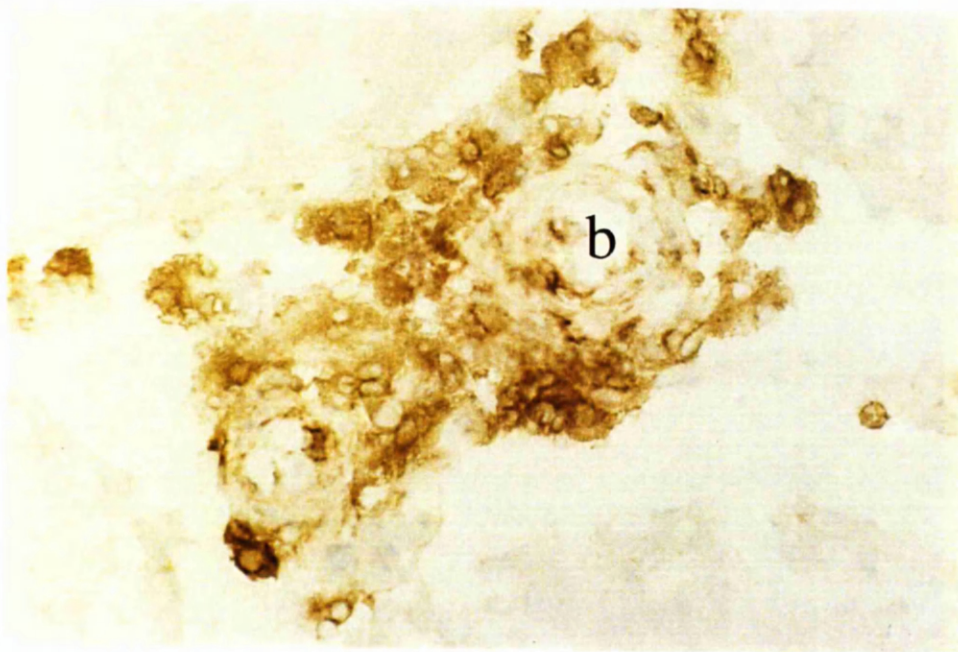
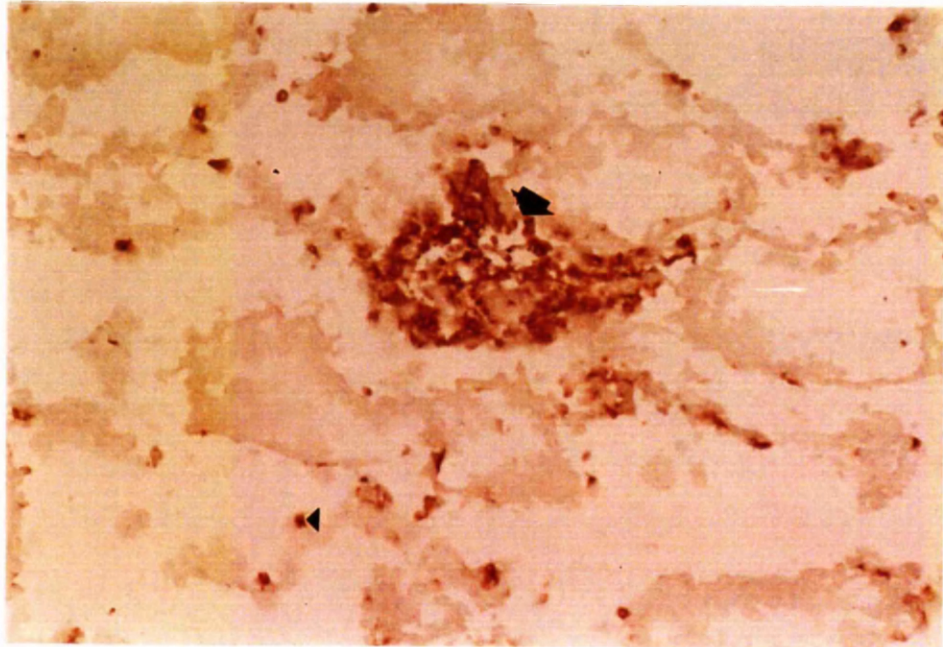


Fig 88. The appearance of OX 42 labelling of a degenerated left testis from an animal with ipsilateral degeneration 12 months following vasectomy (linear magnification *100). A collection of labelled cells (black arrowhead) could be seen with some scattered cells in the interstitium (black triangles).

Figure 89. The appearance of W3/25 labelling in a degenerated right testis from an animal with bilateral degeneration 12 months following vasectomy (linear magnification *400). A collection of labelled cells could be seen around a blood vessel (b).



Appendix 1

The effect of vasectomy on the seminiferous tubule boundary zone in the Albino Swiss rat. Clinical Anatomy in press.

C. C. DOBSON, O. REID, N. K. BENNETT AND S. W. McDONALD

Laboratory of Human Anatomy, University of Glasgow, Glasgow, Scotland.

ABSTRACT

The boundary zone of a seminiferous tubule consists of the basement membrane of the seminiferous epithelium, its myoid cells and their basal laminae. This study examines the boundary zones of seminiferous tubules in healthy and degenerated testes following longterm left-sided vasectomy in the rat and compares them to those of sham-operated controls and adult rats exposed *in utero* to the anti-androgen, flutamide. Degenerated tubular profiles showed similar changes, irrespective of whether the degeneration was ipsilateral or bilateral. In transverse tubular profiles, the basal laminae of the seminiferous epithelium and the myoid cells became more undulating, that of seminiferous epithelium showing complex folding. The collagen layer of the boundary zone, which lies between the basal laminae of the seminiferous epithelium and the myoid cells, thickened and its fibres became irregularly orientated. Rather than being flattened as in controls, the region of the myoid cell near the nucleus and the nucleus itself developed triangular profiles in the transversely sectioned tubules. Similar features were also seen in the degenerated tubules of rats exposed to flutamide. The changes in the boundary zone are not specific for vasectomy and probably reflect reduction in the cross-sectional area of tubular profiles and possibly in their length. We also noted occasional leukocytes infiltrating the boundary zone; they may have increased in number in those tubules that showed degeneration following vasectomy.

INTRODUCTION

The effect of vasectomy on the human testis is incompletely understood and the significance of reports of structural changes is unclear (reviewed by McDonald, 1990). Our group has been studying the Albino Swiss rat with the aim of gaining a thorough understanding of the sequelae of vasectomy in this species and insight into possible effects in patients. We have previously reported that ipsilateral testicular degeneration following unilateral vasectomy in the rat is frequently associated with sperm granuloma formation in the epididymal head (McDonald *et al.*, 1996), an observation also reported in other species (Bedford, 1976). We also documented that bilateral testicular atrophy is common in the long-term after unilateral vasectomy. This seems unrelated to the site of sperm granuloma formation and its mechanism is unknown. The present study investigates the effect of vasectomy on the boundary zone of the seminiferous epithelium in the Albino Swiss rat. The boundary zone consists of the basement membrane of the seminiferous epithelium with the surrounding myoid cells and their associated basal laminae (Hadley and Dym, 1987; Christl, 1990). In the vasectomized rabbit, this region is reported to exhibit deposition of immune complexes (Alexander and Tung, 1979; Bigazzi, 1979).

MATERIALS AND METHODS

Vasectomy and sham operation

Eight young adult Albino Swiss rats from the inbred colony maintained in the Laboratory of Human Anatomy which had undergone left unilateral vasectomy were available for study. Surgery was carried out with pentobarbitone sodium anaesthesia supplemented with halothane via a facemask and with sterile precautions. The ductus deferens was occluded by two silk ligatures, about 4 mm apart, within 2 cm of the origin of the ductus deferens from the epididymis. The portion of ductus between the two ligatures was then excised. A further three rats had undergone a left-sided control sham operation, identical to the vasectomy procedure except that the two ligatures were only loosely tied around the ductus deferens which was not transected. A greater number of rats underwent vasectomy than sham operation because testicular atrophy occurs in only about 50 percent of long-term vasectomized rats (McDonald *et al.*, 1996). The vasectomized and sham-operated rats were sacrificed between 9 and 15 months after operation and tissue harvested for resin histology and electron microscopy.

Preparation of material

Rats were sacrificed by intraperitoneal injection of pentobarbitone sodium. Immediately after death, the tissues were fixed by intracardiac perfusion with 200 ml Ringer's solution containing 1% lignocaine for 5 minutes at a pressure of 130 cm water followed by 200 ml fixative (1% paraformaldehyde + 3% glutaraldehyde in cacodylate buffer at pH 7.8) for 20 minutes. The testes were excised and immersed in the fixative for a further 24 hours. They were then rinsed in 3 changes of cacodylate buffer, weighed and divided into portions. The tissue was postfixated in 1% osmium tetroxide in 0.1M buffer and processed for resin histology using

standard techniques. Sections 1 μm thick were cut on glass knives, mounted on slides and stained with Azur II.

Image analysis

Image analysis was carried out on the bilaterally healthy and degenerated testes following unilateral vasectomy and on the control testes. The testes of the rats showing unilateral atrophy were not included in this part of the study; there were only two animals in this category, insufficient for statistical analysis.

One section of a block from the equator of each testis was selected for image analysis and had its label masked. A drawing of one corner of the section, decided on the toss of a coin, was made at a magnification of X 360 using a camera lucida drawing tube. Measurements of the tubular profiles drawn were then made using a Kontron MOP-AMO2 image analysis system. The 10 tubular profiles with form factors greater than 0.80 nearest the selected corner of the specimen were identified. The form factor is a measure of the roundness of a profile: a perfect circle would have a value of 1.00. Other shapes would have values ranging from 0 to 1.00. The cross-sectional area of each of these ten tubular profiles was obtained for each testis section. The numbers of Sertoli cell nuclei and of any leukocytes in each tubular profile were counted and their positions recorded on the drawing.

Transmission electron microscopy

Sections for electron microscopy, 80 nm thick, were obtained on a Reichert-Jung Ultracut E microtome using a glass knife. Sections were mounted on uncoated copper mesh grids and double-stained with uranyl acetate and lead citrate. They were examined on a Philips EM301 transmission electron microscope.

Flutamide administration

Ultrastructural studies were also made of the degenerated testes of a further three male rats whose mothers had been treated prenatally with flutamide, an anti-androgenic agent which can produce degeneration of the testis (Husmann *et al.*, 1994; Kassim *et al.*, 1997). The mothers had received daily subcutaneous injections of 10 mg flutamide in 0.1 ml propylene glycol from Day 10 following timed mating until birth. The three male offspring were sacrificed at 12 months of age. Resin-embedded blocks were kindly donated by Professor A. P. Payne. Testicular weights were not available but on gross examination all three rats had shown unilateral testicular atrophy. The left testis was affected in one rat and the right in two.

RESULTS

Gross appearance and weights

At sacrifice all three control rats showed testes of healthy size and shape. After fixation, they weighed between 1.21 g and 1.69 g. Three of the rats subjected to unilateral vasectomy showed healthy testes at dissection. These ranged in weight from 1.11 g to 1.61 g. Of the other five animals, three showed bilateral testicular atrophy and two showed ipsilateral degeneration. The affected testes were markedly shrunken and, before fixation, were of flaccid consistency. Their weights ranged from 0.48 g to 1.01 g, considerably lighter than the controls.

Light microscopy

Controls:

Both testes of all three sham-operated control rats showed healthy seminiferous tubules and interstitium.

The boundary zone of the testicular tubules which separates the seminiferous epithelium from the interstitium could be recognised in the resin sections. A single

layer of flattened myoid cells surrounded each tubular profile. These cells showed elongated darkly stained nuclear profiles. A narrow pale zone could be discerned between the myoid cells and the seminiferous epithelial cells. A similar but more readily identified pale zone separated the myoid cells from the interstitium.

Infrequently, leukocytes were related to this outer layer of basement membrane.

Healthy testes following vasectomy:

The two healthy testes from each of three unilaterally vasectomized rats (Fig. 1), and the contralateral testes of the two rats with ipsilateral atrophy, resembled the control material in every way.

Atrophic testes following vasectomy:

All the atrophic testes had markedly different histology from the controls (Figs 2 - 4). There were many degenerated tubules whose cross-sectional profiles were smaller than those of the control tubules. Few spermatogenic cells were present. Most remaining cells had the general features of Sertoli cells but there were differences from those of controls. Their nuclei were more dispersed within the diminished epithelium and seemed more variable in orientation. They exhibited large intranuclear clefts. Many retained their prominent nucleoli but some had scattered clumps of heterochromatin. Regions of the cytoplasm contained large vacuoles.

In the interstitium Leydig cells were associated with blood vessels as in control material but lymphatics were enlarged.

In the boundary zone, the myoid cells remained as a single layer around the perimeter of the tubular cross-sections but their nuclei frequently appeared triangular in profile. On the luminal aspect of the myoid cell, the pale layer representing the basement membranes of the Sertoli and myoid cells appeared thicker than in controls. It was also thrown into folds which projected into the Sertoli cell layer.

Occasionally, leukocytes were seen adjacent to the myoid cells in this zone. The pale zone between the myoid cells and the interstitium, representing the outer layer of the myoid cell basement membrane, was also thicker than in control specimens.

Image analysis

Table 1 shows the values obtained by image analysis.

One-way analysis of variance and multiple range tests indicated a significant reduction in the cross-sectional areas of the tubular profiles in the grossly atrophic testes ($p < 0.01$; $F = 50.47$; $df = 12$).

One-way analysis of variance and multiple range tests indicated that the Sertoli cell nuclei were significantly more numerous in atrophic tubular profiles ($p < 0.01$; $F = 12.14$; $df = 5$) suggesting that atrophic seminiferous tubules were reduced both in length and in cross-sectional area.

For each testis, the number of leukocytes counted in the boundary zone was totalled. Analysis of variance and multiple range tests indicated that while the degenerated testes showed significantly higher numbers than controls, the number of leukocytes in the boundary zones of healthy tubules was not different from that in either the controls or the atrophic testes ($p < 0.01$; $F = 10.32$; $df = 5$).

For each testis, the total number of leukocytes was divided by the total number of Sertoli cells and a ratio obtained. The calculation allows for the possibility that the number of leukocytes in atrophic tubular profiles might increase because of a reduction in tubular length. One-way analysis of variance, however, indicated a significant difference between the groups ($p < 0.01$; $F = 9.55$; $df = 5$). Multiple range tests again suggested that numbers were higher in the atrophic testes but that values for healthy testes were not significantly different from the controls or from the atrophic testes.

Electron microscopy of the boundary zone

Controls and healthy testes following vasectomy

In the basal regions of the seminiferous epithelium of healthy testes following vasectomy or sham operation, Sertoli cell nuclei were readily recognised by their euchromatic character. When sectioned appropriately, prominent nucleoli and intranuclear clefts were observed. Their cytoplasm contained numerous vesicles and scattered mitochondria.

Electron microscopy resolved the components of the boundary zone (Fig. 5). External to the Sertoli cells was a relatively electron-lucent amorphous layer, the basal lamina of the seminiferous epithelium. This was of uniform thickness but was occasionally thrown into slight undulations towards the lumen. External to this basal lamina was a layer of fine collagen fibrils. Most were cut in transverse section in transversely sectioned tubules, indicating that their predominant orientation was parallel to the long axis of the tubule. The fibrillar layer was thicker where there was an inward undulation of the basal lamina of the seminiferous epithelium.

Between the fibrillar layer and the myoid cells, and adjacent to them, was a second amorphous layer, the inner basal lamina of the myoid cells. This was thinner and less distinct than the basal lamina of the seminiferous epithelium but was of similar electron density. The myoid cell cytoplasm showed many fine filaments, a few vacuoles and occasional mitochondria. The markedly elongated nuclei were moderately electron-dense and were darker at their periphery. Between the myoid cells and the interstitium was a third basal lamina. It was similar to, but of more variable thickness than, that of the seminiferous epithelium and had the same amorphous quality and electron density. Sparse fibrils were often seen external to it

but these may have belonged to the interstitium. Frequently, lymphatic endothelium lay adjacent to this layer.

Degenerated testes following vasectomy:

The degenerated testes, both unilateral (Fig. 6) and bilateral (Figs 7, 8), had similar appearances but were very different from control or healthy testes following vasectomy. The Sertoli cells from degenerated tubules had nuclei with deep intranuclear clefts and peripheral clumps of heterochromatin. The cytoplasm contained few organelles. As in the healthy tubules, however, no remnants of sperm precursors were recognised.

The basal lamina of the seminiferous epithelium was highly undulating towards the Sertoli cells. In some areas this was so marked that an impression of multiple layers was given. The myoid cells still consisted of a single layer but in many tubular cross-sections the regions containing the nucleus appeared triangular rather than elongated in profile. The nuclear profiles were also triangular. The apex of these triangular regions faced towards the seminiferous epithelium and often seemed to give a fine cytoplasmic extension towards it. The inner layer of the myoid cell basal lamina was also folded and, in places, had clearly separated from the cell. The collagen fibrils between the seminiferous epithelial and inner myoid cell basal laminae were more numerous and random in arrangement than in healthy tubular profiles. The outer layer of the myoid cell basal lamina was also highly undulating. In some tubules it appeared much thicker than in controls but this may have been due to extensive folding.

The lymphatics of the interstitium were greatly enlarged but were still lined by a layer of endothelium. Pseudopodia of leukocytes were frequently observed on the interstitial aspect of the endothelium. Occasional lymphocytes were seen in the

boundary zone, usually between the myoid cells and their outer basal lamina (Fig. 9).

They were also occasionally found on the tubular aspect of the myoid cells (Fig. 7).

Flutamide treatment:

The three degenerated testes from the three rats which had been exposed to flutamide *in utero* showed boundary zones which were similar in every way in light and electron microscopical appearances to those of degenerated testes following vasectomy (Fig. 10). Although leukocytes were seen in lymphatics close to the seminiferous tubules, none was seen in the boundary zone.

DISCUSSION

This article is the most recent in a series investigating the effect of vasectomy in the Albino Swiss rat. McDonald and Scothorne (1988) examined the tubules of healthy testes in the longterm following vasectomy and found no alterations in their dimensions or in the structure and cycle of the seminiferous epithelium. McDonald *et al.* (1996) also reported ipsilateral testicular degeneration to be common more than 6 months after unilateral vasectomy and associated with sperm granuloma formation in the epididymal head. Granulomas in this region may compress and obstruct adjacent delicate loops of the epididymal duct resulting in raised intraluminal pressure to which the seminiferous epithelium soon succumbs. Several instances of bilateral degeneration were also reported but its etiology remains unclear. It is curious that unilateral vasectomy can result in bilateral testicular degeneration, while flutamide treatment, which might be expected to affect both testes equally, frequently results in asymmetrical changes. The present study shows that when seminiferous tubules degenerate in the vasectomized Albino Swiss rat, marked structural changes occur in their boundary zones.

Cross-sectional tubular profiles of degenerated seminiferous tubules were significantly reduced in area compared to the intact tubules of healthy testes following vasectomy and control sham operation. The degenerated tubules contained higher numbers of Sertoli cell nuclei per cross-sectional profile, suggesting that Sertoli cells persist after germ cells are lost and that the degenerated tubules had shrunk both in length and in cross-sectional area. Occasional leukocytes were identified in the boundary zone of tubules and may have shown a slight increase in absolute numbers following vasectomy, particularly in degenerated tubules. The numbers of testes studied and tubules assessed, however, were relatively small.

The ultrastructural study showed marked changes in the boundary zones of the degenerated seminiferous tubules. While others have noted changes in this region in the vasectomized rat using light microscopy (Flickinger *et al.*, 1987), no ultrastructural study has been specifically devoted to it. Such work in vasectomized rabbits documented deposition of immune complexes (Alexander and Tung, 1979; Bigazzi, 1979). No such features were, however, observed in the present study.

Our investigation confirmed the work of others that, in the healthy rat testis, several layers are to be seen in the periphery of the seminiferous tubules: the basal lamina of the seminiferous epithelium, fine collagen fibers of the basement membrane, the inner basal lamina of the myoid cells, the myoid cells themselves and their outer basal lamina (Hadley and Dym, 1987; Christl, 1990). When testes degenerated following vasectomy, changes occurred in all layers of the boundary zone. The myoid cells persisted as a single layer of cells but the nucleus and the region of the cell in which it lay assumed a triangular profile. All three basal laminae, that of the seminiferous epithelium and the two layers belonging to the myoid cells, became more undulating. This was particularly marked in the basal lamina of the

seminiferous epithelium which became extensively folded. The myoid cell basal laminae were also folded and became separated from the cells in places. There was thickening of the layer of fine collagen fibers that forms part of the basement membrane between the Sertoli and myoid cells. The fibers seemed more numerous and irregular in their orientation. Occasional leukocytes, mostly lymphocytes, were observed among the layers of the boundary zone and seemed more numerous in degenerated tubules. This suggests possible immunological activity. Dym and Romrell (1975) did not find leukocytes internal to the myoid layer in healthy seminiferous tubules.

Interestingly, we were unable to detect any structural differences between the tubules of unilaterally and bilaterally degenerated testes and both groups had similar boundary zones. We also found no evidence for alterations of the boundary zone preceding degeneration. Altered boundary zones were only found in degenerated tubules. This suggests that the boundary zone changes were a result, rather than a cause, of degeneration of the seminiferous tubules. The striking similarity of the boundary zone changes reported here to those observed following X-ray irradiation in the rat (Lacy and Rotblat, 1960) led us to examine the possibility that the changes would be similar for all causes of degeneration.

A variety of other insults including chemical poisoning (Gaunt *et al.*, 1974; Lee and Gillies, 1984; Saxena *et al.*, 1989; Kaido *et al.*, 1992), experimental allergic orchitis (Doncel *et al.*, 1989) and vitamin deficiencies (Ismail and Morales, 1992) can produce degeneration of the testis in the rat. At least some of these, including doxorubicin treatment (Fuse *et al.*, 1992) and experimental allergic orchitis (Doncel *et al.*, 1989), produce changes in the boundary zone. Others, although not commenting on boundary zone changes, produce photographic evidence of them

(Collins and Lacy, 1969). Disturbed spermatogenesis in man may be associated with altered boundary zones (Siew *et al.*, 1977). Specific causes include post-pubertal pituitary failure (Furuya *et al.*, 1980) and possibly vasectomy (Jarow *et al.*, 1985; Mehrotra *et al.*, 1985).

Comparison of the material from our vasectomized rats with that from flutamide-treated animals confirmed that the changes we saw were not specific for vasectomy. Both showed similar boundary zones except that leukocytes seemed absent in the flutamide-treated material. Perhaps the lack of leukocytes in the latter reflects impairment of sperm production throughout adult life in this group rather than the late impairment which occurs following vasectomy. The similarity of the boundary zone changes in degenerated tubules from both causes, along with evidence from the literature, leads us to suggest that a variety of insults to the seminiferous tubules of the rat results in a common response in the boundary zone, probably related to a decrease in tubular cross-section.

REFERENCES

Alexander, N.J., Tung, K.S.K. 1979 Vasectomy in the rabbit: immunological and morphological effects. In *Vasectomy: Immunologic and Pathophysiologic Effects in Animals and Man*. I.H. Lepow and R. Crozier (eds). New York: Academic Press pp. 355-377.

Bedford, J.M. 1976 Adaptations of the male reproductive tract and the fate of spermatozoa following vasectomy in the rabbit, rhesus monkey, hamster and rat. *Biol. Reprod.* 14: 118-142.

Bigazzi P.E. 1979 Immunopathological findings in vasectomized rabbits. In *Vasectomy: Immunologic and Pathophysiologic Effects in Animals and Man*. I.H. Lepow and R. Crozier (eds). New York: Academic Press pp. 339-353.

Christl, H.W. 1990 The lamina propria of vertebrate seminiferous tubules: a comparative light and electron microscopic investigation. *Andrologia* 22: 85-94.

Collins, P., Lacy, D. 1969 Studies on the structure and function of the mammalian testis. II Cytological and histochemical observations on the testis of the rat after a single exposure to heat applied for different lengths of time. *Proc. Roy. Soc. B* 172: 17-38.

Doncel, G.F., Di Paola, J.A., Lustig, L. 1989 Sequential study of the histopathology and cellular and humoral immune response during the development of an autoimmune orchitis in Wistar rats. *Am. J. Repro. Immunol.* 20: 44-51.

Dym, M., Romrell, L.J. 1975 Intraepithelial lymphocytes in the male reproductive tract of rats and rhesus monkeys. *J. Reprod. Fert.* 42: 1-7.

Flickinger, C.J., Herr, J.C., Howards, S.S., Caloras, D., Yarbrow, E.S., Spell, D.R., Gallien, T.N. 1987 The influence of vasovasostomy on testicular alterations after vasectomy in Lewis rats. *Anat. Rec.* 217: 137-145.

Furuya, S., Kumamoto, Y., Ikegaki, S. 1980 Blood-testis barrier in men with idiopathic hypogonadotropic eunuchoidism and postpubertal pituitary failure. *Arch. Androl.* 5: 361-367.

Fuse, H., Iwasaki, M., Katayama, T. 1992 Endocrine/ histological parameters of spermatogenic damage in doxorubicin-treated rats. *Adv. Cont. Deliv. Syst.* 8: 33-40.

Gaunt, I.F., Sharratt, M., Grasso, P., Lansdown, A.B.G., Gangolli, S.D. 1974 Short term toxicity of cyclohexylamine hydrochloride in the rat. *Food Cosmet. Toxicol.* 12: 609-624.

Hadley, M.A., Dym, M. 1987 Immunocytochemistry of extracellular matrix in the lamina propria of the rat testis: electron microscopic localization. *Biol. Reprod.* 37: 1283-1289.

- Husmann, D.A., Boone, T.B., McPhaul, M.J. 1994 Flutamide-induced testicular undescend in the rat is associated with alterations in genitofemoral nerve morphology. *J. Urol.* *151*: 509-513.
- Ismail, N., Morales, C.R. 1992 Effects of vitamin A deficiency on the inter-Sertoli cell tight junctions and on the germ cell population. *Micro. Res. Tech.* *20*: 43-49.
- Jarow, J.P., Budin, R.E., Dym, M., Zirken, B.R., Noren, S., Marshall, F.F. 1985 Quantitative pathologic changes in the human testis after vasectomy. A controlled study. *N. Engl. J. Med.* *313*: 1252-1256.
- Kaido, M., Mori, K., Koide, O. 1992 Testicular damage caused by inhalation of ethylene oxide in rats: light and electron microscopic studies *Toxic. Path.* *20*: 32-43.
- Kassim, N.M., McDonald, S.W., Reid, O., Bennett, N.K., Gilmore, D.P., Payne, A.P. 1997 The effects of pre- and postnatal exposure to the nonsteroidal antiandrogen flutamide on testis descent and morphology in the Albino Swiss rat. *J. Anat.*, *190*: 577-588.
- Lacy, D., Rotblat, J. 1960 Study of normal and irradiated boundary tissue of the seminiferous tubules of the rat. *Exp. Cell Res.* *21*: 49-70.
- Lee, K.P., Gillies, P.J. 1984 Ultrastructural alterations in hexafluoroacetone-induced testicular atrophy in the rat. *Exp. Mol. Pathol.* *40*: 29-37.
- McDonald, S.W., Scothorne, R.J. 1988 A quantitative study of the effects of vasectomy on spermatogenesis in rats. *J. Anat.* *159*: 219-225.
- McDonald, S.W. 1990 Vasectomy and the human testis (editorial). *Br. Med. J.* *301*: 618-619.
- McDonald, S.W., Lockhart, A., Gormal, D., Bennett, N.K. 1996 Changes in the testes following vasectomy in the rat. *Clin. Anat.* *9*: 296-301.
- Mehrotra R, Nath, P., Singh, K.M., Tandon, P., Kumar, H., Pandey, R.K., Mehrotra, R.M.L. 1985 Changes in seminiferous tubules after vasectomy. *Ind. J. Pathol. Microbiol.* *28*: 371-378.
- Saxena, R., Bedwal, R.S., Mathur, R.S. 1989 Zinc toxicity and male reproduction in rats: a histological and biochemical study. *Trac. Elem. Med.* *6*: 119-133.
- Siew, S., Troen, P., Nankin, H. R. 1977 Ultrastructure of testicular biopsies from infertile men. In *The Testis in Normal and Infertile Men*. P. Troen and H. R. Nankin (eds.) New York: Raven Press.

Table 1

	Mean area of tubular image (mm²)	Mean number of Sertoli cells per profile	Total no. leukocytes	No. leukocytes per Sertoli cell nucleus
Control left testes	724.7	19.9	1	0.005
	751.5	20.3	0	0
	697.2	19.8	1	0.005
Control right testes	858.8	20.3	1	0.005
	959.3	20.8	2	0.010
	770.1	20.4	2	0.010
Healthy left testes after vasectomy	636.2	20.4	2	0.010
	821.3	19.2	4	0.021
	657.7	19.3	4	0.021
Healthy right testes after vasectomy	737.2	20.4	6	0.029
	616.4	18.8	4	0.021
	682.4	19.4	7	0.036
Atrophic left testes after vasectomy	193.2	21.8	10	0.046
	243.2	22.6	11	0.049
	292.2	21.4	8	0.037
Atrophic right testes after vasectomy	241.7	24.1	9	0.037
	179.2	22.6	12	0.053
	189.0	22.0	4	0.017

LEGENDS

Figs. 1 - 9 are from rats subjected to left-sided vasectomy.

Fig. 1 Healthy left testis. Four profiles of seminiferous tubules show normal spermatogenesis. Myoid cell nuclei are elongated and flattened (arrows). A clear zone internal to the myoid layer (arrowheads) represents the basement membrane of the seminiferous epithelium. Lymphatics (L) and an artery (A) are seen. Interstitial (Leydig) cells (I) are clustered around capillaries. Resin; toluidine blue; X 312.

Fig. 2 Atrophic seminiferous tubule of left testis from rat showing ipsilateral testicular degeneration. The lumen is collapsed and the epithelium contains only Sertoli cells. Myoid cell nuclei (arrows) are irregular and many are triangular in

profile. The thickened boundary zone (arrowheads) has indistinct components. A large lymphatic space (L) surrounds the tubule and three blood vessels. Resin; toluidine blue; X 500.

Fig. 3 Atrophic tubule of left testis from rat showing bilateral testicular degeneration. The lumen is small and the epithelium composed only of Sertoli cells. Several myoid cell nuclei have a triangular form (arrows). A clear zone (arrowheads) between the myoid cells and the endothelium of the surrounding lymphatic spaces (L) represents the outer myoid cell basal lamina. Resin; toluidine blue; X 312.

Fig. 4 Atrophic tubule of right testis from rat showing bilateral testicular degeneration. The lumen is small and the epithelium composed only of Sertoli cells. Several myoid cell nuclei are triangular in form (arrows). A clear zone (arrowheads) separating the myoid cells from the endothelium of the surrounding lymphatic spaces (L) represents the outer myoid cell basal lamina. Resin; toluidine blue; X 312.

Fig. 5 Transmission electron micrograph (EM) of Sertoli cell and boundary zone (BZ) from the left testis of a rat showing healthy testes. The euchromatic Sertoli cell nucleus (N) has a prominent nucleolus and deep indentation. The cytoplasm shows rough endoplasmic reticulum, mitochondria and vesicles. The Sertoli cell rests on the basal lamina of the seminiferous epithelium (s). A myoid cell (M) is surrounded by its inner and outer basal laminae (i & o). Fine collagen fibers (f) lie between the basal lamina of the seminiferous epithelium and the inner basal lamina of the myoid cell. Lymphatic endothelium (E) lies peripheral to the outer myoid cell basal lamina. Bar = 2 μ m.

Fig. 6 EM of boundary zones of two adjacent degenerated seminiferous tubules from a rat showing ipsilateral testicular degeneration. Sertoli cell cytoplasm (S) and nuclei (N) lie in the tubules. Regions of myoid cells containing nuclei (arrows) have

triangular profiles. In both tubules, the basal lamina of the seminiferous epithelium and the inner basal lamina of the myoid cells show complex folding (arrowheads). The outer basal lamina of the myoid cells (o) is also folded and separated from the cells. Bar = 20 μ m.

Fig. 7 EM of boundary zone of a degenerated seminiferous tubule from the left testis of a rat with bilateral testicular degeneration. Sertoli cells (S) in the tubule and a lymphatic space (L) in the interstitium are shown. The myoid cell nucleus (M) and surrounding cytoplasm present triangular profiles. The basal lamina of the seminiferous epithelium (s) and the inner (i) and outer (o) myoid cell basal laminae are extensively folded. Fine collagen fibers (f) separate the basal lamina of the seminiferous epithelium from the inner lamina of the myoid cells. Similar material (c) lies between the outer myoid cell basal lamina and the lymphatic endothelium (E). Bar = 5 μ m.

Fig. 8 EM of boundary zone of a degenerated seminiferous tubule from the right testis of a rat showing bilateral testicular degeneration. The cytoplasm (S) of a Sertoli cell and the lumen (L) of an interstitial lymphatic space are shown. A myoid cell nucleus (M) and its surrounding cytoplasm present triangular profiles. The basal lamina of the seminiferous epithelium (s) and the inner basal lamina (i) of the myoid cells are folded and separated by collagen fibrils (f). The outer basal lamina of the myoid cell (o) and lymphatic endothelium (E) are shown. A small lymphocyte (SL) lies between the myoid cell and its inner basal lamina. Bar = 5 μ m.

Fig. 9 EM of boundary zone of left testis of a rat showing bilateral testicular degeneration. A Sertoli cell nucleus (N) is euchromatic and deeply indented. Its cytoplasm shows few organelles. The basal laminae of the seminiferous epithelium (s) and of the elongated myoid cell (M: i & o) are folded. Fine collagen fibers (f)

separate the basal lamina of the seminiferous epithelium and the inner basal lamina of the myoid cell. Lymphatic endothelium (E) lies peripheral to the outer myoid cell basal lamina. A small lymphocyte (SL) lies between the myoid cell and its outer basal lamina. Bar = 10 μ m.

Fig. 10 EM of tubular boundary zone from the degenerated adult testis of a rat treated with flutamide *in utero*. The nucleus (N) of a Sertoli cell is euchromatic and deeply indented; its cytoplasm shows few organelles. The nucleus (M) and surrounding cytoplasm of a myoid cell present triangular profiles. The basal laminae of the seminiferous epithelium (s) and the myoid cell (i & o) are folded. Collagen fibrils (f) lie between the seminiferous epithelial and inner myoid cell basal laminae. Bar = 5 μ m.

Appendix 2

Boundary changes in the seminiferous tubules of the rat following vasectomy.

CC Dobson and SW McDonald.

Several authors mention basement membrane thickening following vasectomy but few detailed investigations have been performed. Sixty young adult Albino Swiss rats underwent unilateral vasectomy or sham operation with pentobarbitone anaesthesia. Testes were collected between 6 and 18 months after operation. Thirteen of 31 vasectomized rats showed testicular atrophy. The others and all controls, had healthy testes. On light microscopy, the boundary zones of degenerated seminiferous tubules were folded and thickened compared with healthy tubules. In addition, electron micrographs showed that many epithelial cells had triangular profiles and adjacent electron lucent regions. The layer separating the myoepithelial cells from the Sertoli cells was folded and contained numerous fibrils. The layer between myoepithelium and the more peripheral lymphatic endothelium contained occasional leukocytes. While changes similar to these we report follow irradiation and chemical poisoning, their significance remains to be defined.

Presented at the British Associations of Clinical Anatomy at York in December 1993. *Clinical Anatomy* 1994; 7: 163.

Appendix 3

Comparison of boundary zone changes in atrophic rat testes following vasectomy and flutamide administration. CC Dobson, N Kassim, O Reid and SW McDonald.

In atrophic testes of vasectomized rats, we have previously reported that Sertoli cell basement membrane is folded and myoepithelial cells show triangular profiles, occasionally associated with leukocytes. This material was compared with atrophic testes from rats, of similar age, to which flutamide had been administered in *utero* and with controls. Flutamide produces mal-descent of the testes. On electron microscopy, the features noted above were also found in the flutamide treated group but not in controls. Additionally, in both experimental groups, lymphatics adjacent to seminiferous tubules frequently showed leukocytes with prominent pseudopodia. These results suggest a common response in the boundary zone of seminiferous tubules following flutamide administration and vasectomy.

Presented at the British Associations of Clinical Anatomy at Northern General Hospital, Sheffield in July 1994. *Clinical Anatomy* 1995; 8: 149.

Appendix 4

Structural alterations to Sertoli cells following vasectomy in the Albino Swiss rat. CC Dobson, O Reid and SW McDonald.

Sertoli cells create and maintain a hormonal and physiological environment essential for the production of spermatozoa. They also contribute to the basal lamina which, together with myoepithelial cells and their associated basal laminae, form the boundary zone of the seminiferous tubule. We have previously shown that a proportion of rats 6 months or more following unilateral vasectomy exhibit bilateral degeneration of seminiferous tubules which show alterations in their boundary zones. This study compares the structure of Sertoli cells from degenerated tubules following vasectomy with those of sham operated controls. Nine Albino Swiss rats underwent left unilateral vasectomy under pentobarbitone anaesthesia and 3 control animals underwent sham operation. The animals were sacrificed between 9 and 15 months following operation by overdose of pentobarbitone and perfusion-fixed using cacodylate buffer containing 3% glutaraldehyde and 1% paraformaldehyde. The testes were excised, weighed, divided into 8 portions, processed and embedded in araldite for light and electron microscopy. In controls, a typical Sertoli cell showed a basal nucleus with one or two small nuclear clefts and a prominent nucleolus amongst homogeneous nucleoplasm. The cytoplasm contained numerous mitochondria, lysosomes, lipid droplets and profiles of endoplasmic reticulum, both rough and smooth. In sharp contrast, in degenerated tubules, Sertoli cell nuclei were distributed throughout the epithelium. Nuclei showed deep intranuclear clefts and clumps of heterochromatin adjacent to the nuclear envelope. The cytoplasm appeared reduced in quantity with few organelles. These changes were most marked in highly degenerated tubules. The findings make clear that degeneration of the testis following vasectomy is associated with changes to Sertoli cells as well as spermatozoal precursors.

Presented at the joint meeting of the Anatomical Society of Great Britain and Ireland and the Anatomische Gesellschaft in Southampton December 1994. *Journal of Anatomy* 1995; 187: 238.

Appendix 5

Changes in Sertoli cells and seminiferous tubular boundary zone following vasectomy in the rat. CC Dobson and SW McDonald.

Structural changes are reported in the human testis following vasectomy. We have demonstrated that, in the vasectomized rat, mechanical damage to the seminiferous epithelium is associated with sperm granuloma formation in the epididymal head. Bilateral testicular degeneration frequently follows vasectomy on one side only and suggests the presence of autoimmune orchitis. This study compares Sertoli cells in Albino Swiss rats following unilateral vasectomy and sham operation. We found that 6 months and more after vasectomy: 1) Sertoli cells of healthy testis are similar to controls; 2) atrophic tubules of degenerated testes show Sertoli cells with large nuclear clefts and peripheral clumps of heterochromatin; 3) in both healthy and atrophic tubules, junctional complexes between Sertoli cells persist; 4) around degenerated tubules, the myoid cells change shape and the basal lamina of the Sertoli cells becomes markedly folded; 5) leukocytes are occasionally seen adjacent to the tubular boundary zone. Early results using immunocytochemical markers are suggesting that macrophages are more frequently seen in the testes of vasectomized rats but, to date, there is little evidence to confirm antigen escape from seminiferous tubules and the occurrence of autoimmune orchitis in the rat.

Presented at the joint meeting of the American and British Associations of Clinical Anatomy in the Mayo Clinic U.S.A. July 1995.

Appendix 6

Morphological integrity of Sertoli-Sertoli cell tight junctions following vasectomy in the rat. CC Dobson, O Reid and SW McDonald.

Testicular atrophy may follow vasectomy in rats. The mechanism is unclear but may involve disruption of the blood-testis barrier. The Sertoli-Sertoli cell tight junctions consist of areas of opposing cell membranes with adjacent endoplasmic reticulum separated by intermittent regions containing filamentous material. Of 7 Albino Swiss rats, 6-15 months of age after unilateral vasectomy, 3 showed bilateral and 1 ipsilateral testicular atrophy while 3 remained healthy. Three animals underwent unilateral sham operation and identical preparation to provide controls. The characteristic features of Sertoli-Sertoli cell tight junctions were identified following sham operation and vasectomy, even in severely degenerated tubules. This suggests that disruption of the blood-testis barrier is not associated with post-vasectomy degeneration.

Presented at the British Association of Clinical Anatomy at Northern General Hospital, Sheffield in July 1994. *Clinical Anatomy* 1995; 8: 149.

Appendix 7

Distribution of class I and II MHC antigens in the testis following vasectomy in the Albino Swiss rat, DOBSON CC., McDONALD SW, Laboratory of Human Anatomy, University of Glasgow, Glasgow, UK.

This study examines the distribution of class I and class II MHC antigens in the vasectomized rat testis using monoclonal antibodies OX18 and OX6 respectively (Seralab). Frozen sections were taken from 3 animals with healthy testes and 3 animals with degenerated testes following unilateral vasectomy and compared with material from 3 sham-operated controls. Animals were sacrificed 1 year following procedure using an overdose of pentobarbitone. In healthy experimental and control testes, OX18 labelling showed a similar distribution being largely restricted to the interstitium and late spermatids, with no detectable staining of Sertoli cells or early sperm precursors. In degenerated testes, healthy tubular profiles showed the same pattern while atrophic tubules exhibited marked labelling of Sertoli cells. OX6-positive cells lay scattered in the interstitium in both healthy experimental and control testes; counts per high-powered field showed no significant difference between these groups. In the degenerated testes, OX6-positive cells seemed more plentiful in the interstitium but this may have reflected tubular atrophy. In addition, occasional labelled cells were noted in the tubules. Focal accumulations of OX6 positive cells were observed in both testes of one animal with ipsilateral degeneration following vasectomy. The expression of class I MHC by Sertoli cells of degenerated tubules and the presence of occasional class II MHC invading the atrophic tubules suggests a role for the immune system in degeneration of the testes following vasectomy.

Presented at the British Neuroendocrine Group at the University of Oxford in December 1995. *Journal of Reproduction and Fertility*; abstract series 16: 31.

REFERENCES:

1. Comhaire, F.H. Male contraception: Hormonal, mechanical and other. *Human Reproduction (Oxford)* 1994; 9: 586-90.
2. Paul C, Skegg DCG, Smeijers J, Spears GFS. Contraceptive practice in New Zealand. *N Zeal Med J.* 1988; 101: 809-13.
3. Marquette CM, Koonin LM, Antarsh L, Gargiullo PM, Smith JC. Vasectomy in the United States, 1991. *Am J Pub Health* 1995; 85: 644-9.
4. Haws JM, Morgan GT, Pollack AE, Koonin LM, Magnani RJ, Gargiullo PM. Clinical aspects of vasectomies performed in the United States in 1995. *Urology* 1999; 52: 685-91.
5. Liu X, Li S. Vasal Sterilisation in China. *Contraception* 1993; 48: 255-65.
6. Blaustein D, Ablin RJ, Barthkus JM. Immunological Consequences of vasectomy and consideration of some of their implications. *Allergol et Immunopathol* 1986; 14: 95-9.
7. Giovannucci E, Tosteson TD, Speizer FE, Vessey MP, Colditz GA. A long term study of mortality in men who have undergone Vasectomy. *N Engl J Med* 1992; 21: 1392-8.
8. Massey FJ jr, Bernstein GS, O'Fallon WM, Schuman LM. Health status of American men - a study of post-vasectomy sequelae. Chapter sixteen. Discussion and Conclusions. *J Clin Epid* 1993; 46: 921-6.
9. Thon WF, Stief, C.G, Jonas U. Vasectomy: Minor surgery with a potential for grave consequences. *Urologe Ausgabe A.* 1992; 31: 55-7.
10. Miller WB, Shain RN, Pasta D J. Tubal sterilization or vasectomy: How do married couples make the choice. *Fert Steril* 1991; 56: 278-84.
11. Philp T, Guillebaud J, Budd D. Complications of Vasectomy: Review of 16000 Patients, *Brit J Urol* 1984; 56: 745-8.
12. Alderman PM. Complications in a series of 1224 Vasectomies. *J Fam Pract* 1991; 33: 579-84.
13. Holt BA, Higgins AF. Minimally invasive vasectomy. *Brit J Urol* 1996; 77: 585-6.
14. De Knijff DW, Vrijhof HJ, Arends J, Janknegt RA. Persistence or reappearance of nonmotile sperm after vasectomy: does it have clinical consequences?. *Fert Steril* 1997; 67: 332-5.

15. Black TRL, Gates DS, Lavelly K, *et al.* The percutaneous electrocoagulation vasectomy technique: A comparative trial with standard incision technique at Marie Stopes House, London (UK). *Contraception* 1989; 39: 359-68.
16. Thompson B, MacGregor JE, MacGillivray I, Garvie WHH. Experience with sperm counts following vasectomy. *Brit J Urol* 1991; 68: 230-3.
17. Smith JC, Cranston D, C'Brien T, Guillebaud J, Hindmarsh J, Turner AG. Fatherhood without apparent spermatozoa after vasectomy. *Lancet (North American Ed.)* 1994; 344: 30.
18. Dunn DC, Rawlinson N. *Surgical Diagnosis and Management*. First ed. Blackwell Scientific Publications, 1989.
19. Noldus J, Otto U, Schulze W, Salamon J, Schulze W, Klosterhalfen H. Vasovasostomy after Vasectomy. *Urologe Ausgabe A* 1992; 31: 103-5.
20. Goebel P. On the development of the desire for refertilization in vasectomized men. *Praxis der Psychotherapie und Psychosomatik* 1988; 33: 310-22.
21. Belker AM, Thomas AJR, Fuchs EF, *et al.* Results of 1469 microsurgical vasectomy reversals by the Vasovasostomy Study Group. *J Urol* 1991; 145: 505-11.
22. Humphrey M, Humphrey H. Vasectomy as a reason for donor insemination. *Social Sci Med* 1993; 37: 263-6.
23. Schmidt SS. Vasectomy: Principles and comments. *J Fam Pract* 1991; 33: 571-3.
24. Bigazzi PE. Autoimmune Orchitis and Thyroiditis. *Methods Enzymology* 1988; 162: 461-78.
25. Caldwell JC, McGadey J, Kerr R, Bennett NK, Mc Donald SW. Cell Recruitment to the Sperm Granuloma Which Follows Vasectomy in the Rat. *Clin Anat* 1996; 9: 302-8.
26. Shapiro EI, Silber SJ. Open ended vasectomy, sperm granuloma and post vasectomy orchalgia. *Fertil Steril* 1979; 32: 546-50.
27. Gade J, Brasso K. Sperm Granulomata. *Ugeskr-Laeger* 1990; 152: 2282-4.
28. McMahon AJ, Buckley J, Taylor A, Lloyd SN, Deane RF, Kirk D. Chronic testicular pain following vasectomy. *Brit J Urol* 1992; 69: 188-91.
29. Ahmed I, Rasheed S, White C, Shaikh NA. The incidence of post-vasectomy chronic testicular pain and the role of nerve stripping (denervation) of the spermatic cord in its management. *Brit J Urol* 1997; 79: 269-70.

30. Jarvis LJ, Dubbins PA. Changes in epididymus after vasectomy: sonographic findings. *Am J Roetgenology* 1989; 152: 531-4.
31. McCormack M, Lapointe S. Physiologic consequences and complications of vasectomy. *Can Med Assoc J* 1988; 138: 223-5.
32. Magnani RJ, Haws JM, Morgan GT, Gargiullo PM, Pollack AE, Koonin LM. Vasectomy in the United States, 1991 and 1995. *Am J Public Health.* 1999; 89: 92-4.
33. Selikowitz SM, Schned AR. A late post-vasectomy syndrome. *J Urol* 1985; 134: 494-7.
34. Schmidt SS, Free MJ. The bipolar needle for vasectomy 1: Experience with the first 1000 cases. *Fertil Steril* 1979; 29: 676-80.
35. Moss WM. A Comparison of Open-ended versus Closed-ended Vasectomies: a report on 6220cases. *Contraception* 1992; 46: 521-5.
36. Fox M. Vasectomy reversal: Microsurgery for best results. *Brit J Urol* 1994; 73: 449-53.
37. Sarlip ID. What is the best pregnancy rate that may be expected from vasectomy reversal? *J Urol* 1993; 149: 1469-71.
38. Jequier AM. Vasectomy related infertility: a major and costly medical problem. *Hum Reprod* 1998; 13: 1757-9.
39. Mo ZN, Huang X, Zhang SC, Yang JR. Early and late long-term effects of vasectomy on serum testosterone, dihydrotestosterone, luteinizing hormone and follicle-stimulating hormone levels. *J Urol* 1995; 154: 2065-9.
40. John EM, Whittemore AS, Wu AH, *et al.* Vasectomy and prostate cancer: results from a multiethnic case-control study. *J Nat Can Instit* 1995; 87: 662-9.
41. Rosenberg L, Palmer JR, Zauber AG, Warshauer ME, Stolley PD, Shapiro S. Vasectomy and the risk of prostatic cancer. *Am J Epidem* 1990; 132: 1051-5.
42. Giovannucci E, Tosteson TD, Speizer FE, Ascherio A, Vessey MP, Colditz GA. A retrospective cohort study of vasectomy and prostate cancer in US men. *JAMA* 1993; 269: 878-82.
43. Giovannucci E, Ascherio A, Rimm EB, Colditz GA, Stampfer MJ, Willwt WC. A prospective cohort study of vasectomy and prostate cancer in US men. *JAMA* 1993; 269: 873-77.

44. Kawachi I, Colditz GA, Hankinson S. Long-term benefits and risks of alternative methods of fertility control in the United States. *Contraception* 1994; 50: 1-16.
45. Hsing AW, Wang RT, Gu FL, *et al.* Vasectomy and prostate cancer risk in China. *Cancer Epidemiology, Biomarkers & Prevention*. 1994; 3: 285-8.
46. Nienhulus H, Goldacre M, Seagroatt V, Gill L, Vessey M. Incidence of disease after vasectomy: A record linkage retrospective cohort study. *BMJ* 1992; 304: 743-6.
47. Wei Q, Tang X, Yang Y, San Y, Yin H. Risk factors of prostate cancer sad: A matched case control study. *J West China University of Medical Sciences* 1994; 25: 87-90.
48. Zhu K, Stanford JL, Dallying JR. Vasectomy and prostate cancer: a case-control study in a health maintenance organisation. *Am J Epid* 1996; 144: 717-22.
49. Rosenberg I, Palmer JR, Zauber AG, *et al.* The relation of Vasectomy to the Risk of Cancer. *Am J Epidem* 1994; 140: 431-438.
50. Key T. Risk factors for prostate cancer. *Cancer Surveys*. 1995; 23: 63-77.
51. Giovannucci E. How is individual risk for prostate cancer assessed?. *Hematol Oncol Clin N Am* 1996; 10: 537-48.
52. Stanford JL, Wicklund KG, McKnight B, Daling JR, Brawer MK. Vasectomy and risk of prostate cancer. *Cancer Epidemiology, Biomarkers & Prevention*. 1999; 8: 881-6.
53. Bernal-Delgado E, Latour-Perez J, Pradas-Arnal F, Gomez-Lopez LI. The association between vasectomy and prostate cancer: a systematic review of the literature. *Fertil Steril* 1998; 70: 191-200.
54. Jakobsen H, Torp-Pedersen S, Juul N, Hald T. The long term influence of vasectomy on prostatic volume and morphology in man. *Prostate* 1988; 13: 57-68.
55. Thornhill JA, Conroy RM, Kelly DG, Walsh A, Fennelly JJ, Fitzpatrick JM. An evaluation of predisposing factors for testis cancer in Ireland. *Eur Urol* 1988; 14: 429-53.
56. Cale ARJ, Farouk M, Prescott RJ, Wallace IWJ. Does vasectomy accelerate testicular tumour? Importance of testicular examination before and after vasectomy. *BMJ* 1990; 300: 370.
57. Moller H, Knudsen LB, Lynge E. Risk of testicular cancer after vasectomy: cohort study of over 73 000 men. *BMJ* 1994; 309: 295-99.

58. UK Testicular Cancer Study Group. Aetiology of testicular cancer: Association with congenital abnormalities, age at puberty, infertility and exercise. *BMJ* 1994; 308: 1393-99.
59. Clarkson TB, Alexander NJ. Long-term vasectomy: effects on the occurrence and extent of atherosclerosis in the Rhesus monkey. *J Clin Invest* 1980; 40: 497-9.
60. Goldacre MJ, Holford TR, Vessey MP. Cardiovascular disease and vasectomy: findings from two epidemiological studies. *NEJM* 1983; 308: 805-8.
61. Manson JE, Ridker PM, Spelsberg A, Ajani U, Lotufo PA, Hennekens CH. Vasectomy and subsequent cardiovascular disease in US physicians. *Contraception* 1999; 59: 181-6.
62. Tang GH, Zhong YH, Ma YM, *et al.* Vasectomy and health: Cardiovascular and other diseases following vasectomy in Sichuan Province China. *Int J Epidem* 1988; 17: 608-17.
63. Crozier R, Bernstein GS. Chapter one. Historical background and objectives of study. *J Clin Epid* 1993; 46: 697-706.
64. McDonald SW. Is vasectomy harmful to health?. *Brit J GP* 1997; 47: 381-6.
65. Kronmal RA, Alderman E, Krieger JN, Killip T, Kennedy JW, Athearn MW. Vasectomy and urolithiasis. *Lancet* 1988; i: 22-3.
66. Kronmal RA, Krieger JN, Coxon V, Wortley P, Thompson L, Sherrard DJ. Vasectomy is associated with an increased risk for urolithiasis. *Am J Kid Dis* 1997; 29: 207-13.
67. Byrne PA, Evans WD, Rajan KT. Does vasectomy predispose to osteoporosis?. *Brit J Urol* 1997; 79: 599-601.
68. Shulman S, Zappi E, Ahmed U, Davis JE. Immunological consequences of vasectomy *Contraception* 1972; 5: 269-78.
69. Aitken RJ, Parslow JM, Hargreave TB, Hendry WF. Influence of antisperm antibodies on human sperm function. *Brit J Urol* 1988; 62: 367-73.
70. Broderick GA, Tom R, McClure RD. Immunological status of patients before and after vasovasostomy as determined by the immunobead antisperm antibody test. *J Urol* 1989; 142: 752-5.
71. Ahmed K, Naz RK. Effects of human antisperm antibodies on development of preimplantation embryos. *Arch Androl* 1992; 29: 9-20.

72. Newton RA. IgG antisperm antibodies attached to sperm do not correlate with infertility following vasovasostomy. *Microsurgery* 1988; 9: 278-80.
73. Naaby-Hansen S. The humoral autoimmune response to vasectomy described by immunoblotting from two-dimensional gels and demonstration of a human spermatozoal antigen immunochemically crossreactive with the D2 adhesion molecule. *J Reprod Immunol* 1990; 17: 187-206.
74. Tung KSK, Bryson RK, Han LPE, Walker LC. Circulating immune complexes in vasectomy. In: Lepow IH, Crozier R editors. *Vasectomy. Immunological and Pathophysiological effects in animals and man*. Academic Press, Inc, New York; 1979: 301-38.
75. Bigazzi PE, Alexander NJ, Silber SJ. Studies on testicular biopsies from vasectomized men. In: Lepow IH, Crozier R editors. *Vasectomy. Immunological and Pathophysiological effects in animals and man*. New York: Academic Press Inc, 1979: 459-69.
76. Maddocks S, Setchell BP. Recent evidence for immune privilege in the testis. *J Reprod Immunol* 1990; 18: 9-18.
77. Hendry WF, Parslow JM, Levison DA, Royle MG, Parkinson MC. Testicular obstruction: clinicopathological studies. *Annals Roy Col Surg Eng* 1990; 72: 396-407.
78. Mullooly JP, West WM, Alexander NJ, Greenlick MR, Fulgham DL. Vasectomy, serum assays and coronary heart disease symptoms and risk factors. *J Clin Epidem* 1993; 46: 101-9.
79. Nagarkatti PS, Rao SS. Cell mediated immunity to homologous spermatozoa following vasectomy. *Clin Exp Immunol* 1976; 26: 239-42.
80. Tung KSK, Mahi-Brown CA. Autoimmune Orchitis and Oophoritis. *Reprod Immunol* 1990; 10: 199-214.
81. Lehmann D, Temminck B, DaRugna D, Leibundgut B, Sulmoni A, Muller HJ. Role of immunological factors in male infertility: Immunohistochemical and serological evidence. *Lab Inves* 1987; 57: 21-8.
82. Salomon F, Hedinger CE. Abnormal Basement membrane structures of seminiferous tubules in infertile men. *Lab Inves* 1982; 47: 543-54
83. Salomon F, Saremaslani P, Jakob M, Hedinger CE. Immune complex orchitis in infertile men. *Lab Inves* 1982; 47: 555-67.
84. Hendry WF, Stedronska J, Parslow JM, *et al*. Immune orchitis: A rare but treatable cause of azoospermia or severe oligospermia in man. *J Androl* 1985; 6:54-P.

85. Suominen J, Soderstrom KO. Lymphocyte infiltration in human testicular biopsies. *Int J Andrology* 1982; 5: 461-66.
86. Kubota R. Electron microscopic studies of the testis after vasectomy on rats and man. *Jpn J Urol* 1969; 60: 373-97.
87. Hagedoorn JP, Davis JE. Fine structure of the seminiferous tubules after vasectomy in man. *Physiologist* 1974; 17: 236-41.
88. Mehrotra R, Nath P, Singh KM, *et al.* Changes in seminiferous tubules after vasectomy. *Ind J Path Microbiol* 1985; 28: 371-78.
89. Mehrotra R, Nath P, Tandon P, Singh KM, Kumar H. Ultrastructural appearances of interstitial tissue of testis in vasectomized individuals. *Ind J Med Res* 1983; 77: 347-52.
90. Jarow JP. Quantitative pathological changes in the human testis after vasectomy. *N Eng J Med* 1985; 313: 1252-56.
91. Jarow JP, Goluboff ET, Chang TS, Marshall FF. Relationship between antisperm antibodies and testicular histologic changes in humans after vasectomy. *Urol* 1994; 43: 521-4.
92. Derrick FC, Lloyd Glover W, Kanjuparamban Z, *et al.* Histologic changes in the seminiferous tubules after vasectomy. *Fertil Steril* 1974; 25: 649-58.
93. Hirsch IH, Sedor J, Kulp D, McCue PJ, Staas WEjr. Objective assessment of spermatogenesis in man with functional and anatomic obstruction of the genital tract. *Int J Androl* 1994; 17: 29-34.
94. DeKretser DM, Kerr JB, Paulsen CA. The Peritubular tissue in the normal and pathological human testes: an ultrastructural study. *Biol Reprod* 1975; 12: 317-24.
95. Takaba H. A morphological study of the testes in patients with idiopathic male infertility: immunohistochemical analysis of collagens and laminins in human testes. *Acta Urologica Japonica* 1990; 36: 1173-80.
96. Sarrat R, Whyte J, Torres A, Lostale F, Diaz MP. Experimental vasectomy and testicular structure. *Histol Histopath* 1996;11:1-6.
97. Tung KSK, Alexander NJ. Immunopathologic studies on vasectomized Guinea pigs. *Biol Reprod* 1977; 17: 241-54.
98. Flickinger CJ. Focal changes in the Seminiferous Tubules of Vasectomized Hamsters. *J Androl* 1981; 5: 269-77.
99. Horan AH. When and why does occlusion of the vas deferens affect the testis? *Fertil Steril* 1975; 26: 317-28.

100. Alexander NJ, Tung KSK. Immunological and morphological effects of vasectomy in the rabbit. *Anatom Rec* 1977; 188: 339-50.
101. Laumas KR, Uniyal JP. Disintegration of spermatozoa and testicular degeneration by a sialastic block of the vas deferens in rats. *Ind J Exp Biol* 1967; 5: 199-202.
102. Flickinger CJ, Herr JC. The influence of vasovasostomy on testicular alterations after vasectomy in Lewis rats. *Anat Rec* 1987; 217: 137-45.
103. Lohiya NK, Dixit VP. Biochemical studies of the testes and sex accessory organs of the desert gerbil after vasectomy. *Fertil Steril* 1974; 25: 617-20.
104. Hadley MA, Dym M. Spermatogenesis in vasectomized monkey. *Anat Rec* 1983; 205: 381-6.
105. Barrat CLR, Cohen J. Quantitation of sperm disposal and phagocytic cells in the tract of short- and long- term vasectomized mice. *J Reprod Fert* 1987; 81: 377-84.
106. Paufler SL, Foote RH. Spermatogenesis in the rabbit following ligation of the epididymus at different levels. *Anat Rec* 1969; 164: 339-48.
107. Lamano-Carvalho TL, Favaretto ALV, Ferreira AL, Antunes-Rodrigues J. Histophysiological study of vasectomized rats. *Braz J Med Biol Res* 1984; 17: 83-91.
108. Vare AM, Bansal PC. Changes in the canine testis after bilateral vasectomy-an experimental study. *Fertil Steril* 1973; 24: 793-7.
109. Chapman ES, Heidger PM, Harrison RM, Roberts JA, Domingue GJ, Schlegel JU. Vasectomy in Rhesus monkeys IV: EM studies of the seminiferous epithelium. *Anat Rec* 1978; 192: 41-54.
110. Singh P, Dominic CJ. Effects of vasectomy on the testis , epididymus and seminal vesicle of the laboratory mouse. *Eur Arch Biol* 1990; 101: 345-58.
111. Singh RP, Awasthi CH. Effect of Vasectomy on Spermatogenesis in the Albino Rat (*Mus norvegicus*). *Folia Morphologica* 1988; 36: 260-3.
112. Flickinger CJ. Fine structure of the rabbit testis after vasectomy. *Biol Reprod* 1975; 13: 61-7.
113. Alexander NJ, Tung KSK. Vasectomy in the rabbit immunological and morphological effects. In: Lepow IH, Crozier R editors. *Vasectomy. Immunological and Pathophysiological effects in animals and man*. New York: Academic Press Inc, 1979: 355-78.

114. Aitken H, Kumarakuru S, Orr R, Reid O, Bennett NK, McDonald SW. Effect of Long-term Vasectomy on Seminiferous Tubules in the Guinea Pig. *Clin Anat* 1999; 12: 250-263.
115. Muir VY, Turk JL, Hanley HG. Comparison of allergic aspermatogenesis with that induced by vasectomy in vivo: studies in the Guinea pig. *Clin Exp Immunol* 1976; 24: 72-80.
116. Tung KSK, Alexander NJ. Monocytic orchitis and aspermatogenesis in normal and vasectomized rhesus macaques (*Macaca mulatta*). *Am J Path* 1980; 101: 17-27.
117. Handley HH, Flickinger CJ, Herr JC. Biphasic production of antisperm autoantibodies follow vasectomy of the Lewis rat. *J Repro Immunol* 1990;17:53-67.
118. Flickinger CJ, Baran ML, Howards SS, Herr JC. Sperm autoantigens recognised by autoantibodies in developing rats following prepubertal obstruction of the vas deferens. *J Androl* 1996;17:433-42.
119. Herr JC, Flickinger CJ. The relationship between Antisperm Antibodies and Testicular Alterations after Vasectomy and Vasovasostomy in Lewis Rats. *Biol Repro* 1987; 37: 1297-1305.
120. McDonald SW, Spilg EG, Alexander JA, Scothorne RJ. Testicular Atrophy following vasectomy- is the position of the sperm granuloma important ? *Clin. Anat.* 1990; 3:68.
121. Smith G. The effects of ligation of the vasa efferentia and vasectomy on testicular function in adult rats. *J Edocrinol* 1962; 23: 385-400.
122. Flickinger CJ. Ultrastructure of the rat testis after vasectomy. *Anat Rec* 1972; 174: 477-93.
123. Feller JA. Comparison of the short term effects of vasoligation and open-ended vasectomy in the reproductive tracts of the male rat. *Andrologia* 1986; 18: 639-48.
124. Sackler AM, Weltman AS, Pandhi V, Schwartz R. Gonadal effects of vasectomy and vasoligation. *Science* 1973; 179: 293-5.
125. Bedford JM. Adaptations of the male reproductive tract and the fate of spermatozoa following vasectomy in the rabbit, Rhesus monkey, hamster and rat. *Biol Reprod* 1976; 14: 118-42.
126. Ishizu K, Shiraishi K, Nakane H, Naito K, Baba Y, Takihara H. The effect of unilateral vasectomy on spermatogenesis in the bilateral testes in Lewis rats. *Source Jap J of Fertil Steril* 1999; 44: 29-34.

127. Sanchez FJ, Villaplana TL, Sarti MM. Light microscopy study of rat testicle after vasectomy. *Acta Urol Espan* 1996;20:403-7.
128. Neaves WB. The effect of vasectomy on the testis of inbred Lewis rats. *J Repro Fertil* 1978; 54: 405-11.
129. Flickinger CJ, Herr JC. The influence of vasovasostomy on testicular alterations after vasectomy in Lewis rats. *Anat Rec* 1987; 217: 137-45.
130. Flickinger CJ. The effects of vasectomy on the testis. *N Eng J Med* 1985; 313: 1283-5.
131. Bigazzi PE, Kosuda LL, Harnick LL. Sperm Autoantibodies in Vasectomized Rats of Different Inbred Strains. *Science* 1977; 197: 1282-3.
132. Flickinger CJ, Howards SS, Bush LA, Baker LA, Herr JC. Antisperm autoantibody responses to vasectomy and vasovasostomy in Fischer and Lewis rats. *J Reprod Immunol* 1995;28:137-57.
133. Flickinger CJ, Howards SS, Carey PO, *et al.* Testicular alterations are linked to the presence of increased anti sperm antibodies in Sprague-Dawley rats post vasectomy and vasovasostomy. *J Urol* 1988; 140: 627-31.
134. Flickinger CJ, Howards SS, Bush LA, Baker LA, Herr JC. Temporal recognition of sperm autoantigens by IgM and IgG autoantibodies after vasectomy and vasovasostomy. *J Reprod Immunol* 1994;27:135-50.
135. McDonald, Scothorne RJ. A quantitative study of the effects of vasectomy on spermatogenesis in rats. *J Anat* 1988;159:219-25.
136. Soler C, Blazquez C, Pertusa J, Nunez M, Nunez J, Nunez A. A comparison of the effects of bilateral efferent duct ligation and of partial epididymectomy on the testis in rats. *Reprod Fertil Dev* 1990; 2: 231-6.
137. Heller GV, Rothchild I. The influence of the surgical technique used for vasectomy on the testis in rats. *J Reprod Fertil* 1974; 39: 81-4.
138. McDonald SW, Falconer JS, Al-Saffar RA, Scothorne RJ. Sperm granuloma formation in the caput epididymidis is associated with testicular degeneration in rats. *Clinical Anatomy* 1990; 3: 65.
139. McDonald SW, Lockhart A, Gormal D, Bennett NK. Changes in the Testes Following Vasectomy in the Rat. *Clin. Anat.* 1996; 9: 296-301.
140. Al-Saffar RAS. Morphological studies of the immune response to vasectomy. Ph.D. thesis, University of Glasgow , Glasgow, U.K.
141. McDonald SW, Scothorne RJ. A quantitative study of the effect of vasectomy on spermatogenesis in rats. *J Anat* 1988; 159: 219-225.

142. Lacy D, Rotblat J. Study of Normal and Irradiated Boundary Zone Tissue of the Seminiferous Tubules of the Rat. *Exp Cell Res* 1960; 21: 49-70.
143. Christl HW. The lamina propria of vertebrate seminiferous tubules: a comparative light and electron microscopic investigation. *Andrologia* 1990; 22: 85-94.
144. Dym M. Basement membrane regulation of Sertoli cells. *Endocrin Rev* 1994;15:102-116.
145. Dym M, Romrell LJ. Intra epithelial lymphocytes in the male reproductive tract of rats and Rhesus monkeys. *J Reprod Fertil* 1975; 42: 1-7.
146. Hadley MA, Dym M. Immunocytochemistry of the extracellular matrix of the lamina propria of the rat testis: electron microscopic localisation. *Biol Reprod* 1987; 37: 1283-9.
147. Damsky CH, Bernfield M. Cell-to-cell contact and extracellular matrix. *Curr Opin Cell Biol* 1991; 3: 777-8.
148. Harris JD, Lipshultz LI. The effect of vasectomy on Sertoli cell function in rats. *Invest Urol* 1981;18:305-7.
149. Dym M. The Male Reproductive System. In: Weiss L eds. *Histology; Cell and Tissue Biology*. 5th ed. New York: Elsevier, 1983: 1000-53. ISBN 0-333-35406-0.
150. Russell LD. Form, Dimensions and cytology of Mammalian Sertoli cells. In: Russell LD, Griswold MD eds. *The Sertoli Cell*. Cache River Press, 1993; Chpt 1: 1-39.
151. Jegou B. The Sertoli cell in vivo and in vitro. *Cell Biol Toxicol* 1992;8:49-54.
152. Dym M, Fawcett DW. The blood-testis barrier in the rat and the physiological compartmentation of the seminiferous epithelium. *Biol Rep* 1970;3:308-326.
153. Chakraborty J. Conditions Adversely Affecting Sertoli Cells. In: Russell LD, Griswold MD eds. *The Sertoli Cell*. Cache River Press, 1993; Chpt 28: 577-95.
154. Nistal M, De Mora JC, Paniagua R. Classification of several types of maturational arrest of spermatogonia according to Sertoli cell morphology: an approach to aetiology. *Int J Andrology* 1998; 21: 317-26.
155. Clegg EJ. Studies on artificial cryptorchidism: morphological and quantitative changes in the Sertoli cells of rats testes. *J Endocrinol* 1963; 26: 567-574.

156. Flickinger CJ, Loving CK. Fine structure of the testis and epididymus of rats treated with cyproterone acetate. *Am J Anat* 1976; 146: 359-84.
157. Lee HY. Studies on vasectomy: IV Experimental Studies on Biological and Histochemical Effects of Vasectomy. *J Korean Med Assoc* 1967; 10: 51-71.
158. Husmann DA, Boone TB, McPhaul MJ. Flutamide induced testicular undescend in the rat is associated with alteration in genitofemoral nerve morphology. *J Urol* 1994; 151: 509-13.
159. Kassim NM, McDonald SW, Reid O, Bennett NK, Gilmore DP, Payne AP. The effects of pre- and postnatal exposure to the nonsteroidal antiandrogen flutamide on testis descent and morphology in the Albino Swiss Rat. *J Anat* 1997; 190: 577-88.
160. Weakley, BS. Biological transmission electron microscopy. 2nd ed. Churchill Livingstone, 1981.
161. Nicolini C, Kendall F, Giaretti W. Objective identification of cell cycle phase and subphase by automated image analysis. *Biophysical Journal* 1977; 19: 163-76.
162. Schulze C, Holstein AF. Human Sertoli Cells Under Pathological Conditions. In: Russell LD, Griswold MD eds. *The Sertoli Cell*. Cache River Press, 1993; Chpt; 29: 597-610.
163. Saxena R, Bedwal RS, Mathur RS. Zinc toxicity and male reproduction in rats: a histological and biochemical study. *Trac Elem Med* 1989; 6: 119-33.
164. Abraham M. The male germ cell protective barrier along phylogenesis. *Int Rev Cytol* 1991;130:111-90.
165. Bustos-Obregon E. Ultrastructure and Function of the Lamina Propria of Mammalian Seminiferous Tubules. *Andrologia* 1975; 8: 179-85.
166. Russell LD, Peterson RN. Sertoli cell junctions: morphological and functional correlates. *Int Rev Cytol* 1985;94:177-211.
167. Pelletier PM, Byers SW. The Blood-Testis Barrier and Sertoli cell junctions: structural considerations. *Micros Res Tech* 1992;20:3-33.
168. Shinoda K, Okamiya H, Imazawa T, *et al*. Application of BRD U immunohistochemistry and Lanthanum tracer methods to the pathological evaluation of 1,3 dinitrobenzene testicular toxicity. (*Jap*) *Eisei Shikenjo Hokoku* 1989;107:63-7.

169. Huang HFS, Yang CS, Meyenhofer M, Gould S, Boccabella AV. Disruption of sustentacular (Sertoli) cell tight junctions and regression of spermatogenesis in vitamin A deficient rats. *Act Anat* 1988;133:10-15.
170. Cavicchia JC, Sacerdote FL. Correlation between blood-testes-barrier development and onset of the first spermatogenic wave in normal and in busulphan treated rats, a lanthanum and freeze-fracture study. *Anat Rec* 1991;230:361-68.
171. Shaklai M, Tavassoli M. Lanthanum as a Microscopic Stain. *J Histochem Cytochem* 1982;30:1325-30.
172. Neaves WB. Permeability of Sertoli cell tight junction to lanthanum after ligation of the *ductus deferens* and *ductuli efferentes*. *J Cell Biol* 1973;59:559-72.
173. Osman DI, Ploen L. The Terminal Segment of the seminiferous tubule and the blood-testis barrier before and after efferent ductule ligation in the rat. *Int J Androl* 1978;1:235-249.
174. Ross MH. Sertoli-Sertoli junctions and the Sertoli-spermatid junctions after efferent ductule ligation and Lanthanum treatment. *Am J Anat* 1977;148:49-56.
175. Ismail N, Morales, CR. Effects of Vitamin A Deficiency on the Inter Sertoli cell tight junction and on the Germ cell population. *Micro Res Tech* 1992;20:43-9.
176. Hagenas L, Ploen L, Ritzen EM, Ekwall H. Blood-testes barrier: Maintained function of inter-Sertoli cell junctions in experimental cryptorchidism in the rat, as judged by a simple lanthanum-immersion technique. *Andrologia* 1977;9:250-54.
177. Furuya S, Kumamoto Y, Ikegaki S. The Blood-Testis-Barrier in Men with Idiopathic Hypogonadotropic Eunuchoidism and Postpuberal Pituitary failure. *Arch Androl* 1980;5:361-7.
178. Castro AE, Seiguer AC. The permeability of the blood-testis barrier to lanthanum during immune induced aspermatogenesis and following vasectomy in the Guinea pig. *Virchow Arch B* 1974;16:297-309.
179. Lustig L, Lourtau L, Perez R and Doncel GF. Phenotypic characterisation of lymphocytic cell infiltrates into the testes of rats undergoing autoimmune orchitis. *Int J Androl* 1993;6:279-284.
180. El-Demiry M, Hargreave TB, Busuttill A, Elton R, James K, Chisholm GD. Immunocompetent cells in human testis in health and disease. *Fertil Steril* 1987;48:470-9.

181. Dallman MJ, Mason DW, Webb M. The role of host and donor cells in the rejection of skin allografts by Tcell-deprived rats injected with syngeneic T cells. *Eur J Immunol* 1982; 12: 511-8.
182. Woolett GR, Barclay AN, Puklavec M, Williams AF. Molecular and antigenic heterogeneity of the rat leucocyte common antigen from thymocytes and t and B lymphocytes. *Eur J Immunol* 1985; 15: 168-173.
183. Robinson AP, White TM, Mason DW. Macrophage heterogeneity as delineated by 2 monoclonal antibodies MRC OX41 and MRC OX42 the latter recognising complement receptor type 3. *Immunology* 1986; 57: 239-47.
184. Lui GY, Baker D, Fairchild S, *et al.* Complete characterisation of the expressed immune response genes in Biozzi AB/H mice; structural and functional identity between AB/H and NOD A region molecules. *Immunogenetics* 1992; 37: 296-300.
185. Fukumoto T, McMaster RW, Williams AF. Mouse monoclonal antibodies against rat MHC antigens. Two Ia antigens and expression of Ia and class I antigens in rat thymus. *Eur J Immunol*; 1982: 12; 237-43.
186. Barclay AN. The localisation of populations of lymphocytes defined by monoclonal antibodies in rat lymphoid tissue. *Immunology* 1981; 42: 593-600.
187. Barclay AN. Different reticular elements in rat lymphoid tissue identified by location of Ia, Thy1 and MRC OX2 antigen. *Immunology* 1981; 44: 727-36.
188. Doncel GF, Di Paola JA, Lustig L. Sequential study of the histopathology and cellular and humoral immune response during the development of an autoimmune orchitis in Wistar rats. *Am J Reprod Immunol* 1989; 20: 44-51.
189. Bishara A, Oksenberg JR, Frankel G, *et al.* Human leukocyte antigens (HLA) class I and classII on sperm cells studied at the serological, cellular and genomic levels. *Am J Repro Immunol* 1987; 13: 97-103.
190. Hass GG, D`Cruz OJ, De Bault LE. Distribution of Human Leukocyte Antigen-ABC and D/DR Antigens in the unfixed human testis. *Am J Repro Immunol* 1988; 18: 47-51.
191. Fiszer D, Kurpisz M. Major histocompatibility complex expression on human, male germ cells: a review. *Am J Repro Immunol* 1998; 40 :172-6.
192. Aydos K, Soygur T, Kupeli B, *et al.* Testicular effects of vasectomy in rats: an ultrastructural and immunohistochemical study. *Urol* 1998; 51: 1051-6.
193. Nistal M, Garcia-Rodeja E, Paniagua R. Granular Transformation of Sertoli cells in Testicular Disorders. *Human Path* 1991;22:131-137.

194. Wheeler JE. Histology of the Fertile and Infertile Testis. Monographs Pathol 1991; 331: 56-103.
195. Gaunt IF, Sharratt M, Grasso P, Landsdown ABG, Gangolli SD. Short term toxicity of cyclohexylamine hydrochloride in the rat. Food Cosmet Toxicol 1974; 12: 609-24.
196. Kaido M, Mori, K, Koide, O. Testicular Damage Caused by Inhalation of Ethylene Oxide in Rats: Light and Electron Microscopic Studies. Toxic Path 1992; 20: 32-43.
197. Fuse H, Iwasaki M, Katayama T. Endocrine/ histological parameters of spermatogenic damage in doxorubicin-treated rats. Adv Cont Deliv Syst 1992; 8: 33-40.
198. Collins P, Lacy D. Studies on structure and function of the mammalian testis. II Cytological and histochemical observations on the testis of the rat after a single exposure to heat applied for different lengths of time. Proc Roy Soc B 1969; 172: 17-38.
199. Lee KP, Gillies, PJ. Ultrastructural Alterations in Hexafluoracetone Induced Testicular Atrophy in the Rat. Exp Mol Path 1984; 40: 29-37.
200. Holstein AE, Roosen-Rounge EC, Schirren C eds. Illustrated pathology of human spermatogenesis. Berlin Grosse-Verlag 1988: pages 96-8.
201. Aydos K, Kupeli B, Soygur T, *et al.* Analysis of the relationship between histologic alterations and the generation of reactive oxygen species in vasectomized rat testes. Urol 1998; 51: 510-5.
202. Carr I, Clegg EJ, Meek GA. Sertoli cells as phagocytes: an EM study. J Anat 1968; 102: 501-9.
203. Housseau F Rouas-Freiss N, Roy M, Bidart JM, Guillet JG, Bellet D. Antigen-presenting function of murine gonadal epithelial cell lines. Cellular Immunology 1997; 177: 93-101.